Institute of Thermoelectricity, Academy of Sciences and Ministry of Education and Science of Ukraine

Journal of THERMOELECTRICITY

International Research

Founded in December, 1993

published 6 times a year

No. 3 *2020*

Editorial Board

International Editorial Board

Founders – National Academy of Sciences, Ukraine
Institute of Thermoelectricity of National Academy of Sciences and Ministry of Education and Science of Ukraine

Certificate of state registration № КВ 15496-4068 ПР

Approved for printing by the Academic Council of Institute of Thermoelectricity of the National Academy of Sciences and Ministry of Education and Science, Ukraine

Address of editorial office:
Ukraine, 58002, Chernivtsi, General Post Office, P.O. Box 86.
Phone: +(380-372) 90 31 65.
Fax: +(380-3722) 4 19 17.
E-mail: jt@inst.cv.ua
http://www.jt.inst.cv.ua

Signed for publication 26.07.2020. Format 70×108/16. Offset paper №1. Offset printing.
Printer's sheet 11.5. Publisher's signature 9.2. Circulation 400 copies. Order 5.

Printed from the layout original made by "Journal of Thermoelectricity" editorial board
in the printing house of "Bukrek" publishers,
10, Radischev Str., Chernivtsi, 58000, Ukraine

CONTENTS

V.A.Romaka, *doc. techn sciences, professor*[1],
Yu.V. Stadnyk, *cand. chem. of science*[2],
L.P. Romaka, *cand. chem. of science*[2],
A.M. Horyn, *cand. chem. of science*[2],
I.M. Romaniv, *cand. chem. of science*[2],
V.Z. Pashkevych, *cand. tehn. of science*[1]
A.Ya. Horpeniuk, *cand. tehn. of science*[1]

[1]National University "Lvivska Politechnika", 12, S. Bandera Str., Lviv, 79013, Ukraine,
e-mail: vromaka@polynet.lviv.ua;
[2]Ivan Franko National University of Lviv, 6, Kyryla and Mefodiya Str., Lviv, 79005, Ukraine,
e-mail: lyubov.romaka@lnu.edu.ua;

FEATURES OF STRUCTURAL, ENERGETIC, ELECTROKINETIC INVESTIGATION OF ENERGY AND ELECTROKINETIC CHARACTERISTICS OF THERMOELECTRIC MATERIAL *$TiCo_{1-x}Mn_xSb$*

The crystal and electronic structure, temperature and concentration dependences of the resistivity and the Seebeck coefficient of the thermoelectric material $TiCo_{1-x}Mn_xSb$, $x = 0.01–0.10$, in the temperature range $T = 80$-400 K have been studied. It was shown that the doping of the initial TiCoSb semiconductor by Mn atoms is accompanied by the simultaneous generation of structural defects of acceptor and donor nature and the appearance in the band gap of acceptor band ε_A (substitution of Co atoms by Mn ones) and also donor bands ε_D^1 и ε_D^2 of different nature. The concentration ratio of the ionized acceptors and donors generated in $TiCo_{1-x}Mn_xSb$ determines the position of the Fermi level ε_F and the mechanisms of electrical conductivity of the thermoelectric material. Bibl. 14, Fig. 7.
Keywords: electronic structure, electrical resistivity, *Seebeck* coefficient.

Introduction

One of the ways to obtain semiconductor thermoelectric materials with high efficiency of thermal into electrical energy conversion is doping of the base semiconductor by impurity atoms, which generate structural defects of donor and/or acceptor nature in the crystal. This allows purposeful changing the values of conductivity σ, the Seebeck coefficient α and thermal conductivity κ to obtain the maximum values of thermoelectric figure of merit Z ($Z = \alpha^2 \cdot \sigma/\kappa$) [1].

The results of studies of a new semiconductor thermoelectric material *$TiCo_{1-x}Mn_xSb$*, $x = 0.01–0.10$, obtained by doping the base semiconductor *TiCoSb* (*MgAgAs* structure type, space group $Fm\bar{4}3m$ [2]) by *Mn* atoms ($3d^5 4s^2$) by replacing of *Co* ($3d^7 4s^2$), are given below. It was expected that the substitution of *Co* atoms by *Mn* would generate structural defects of acceptor nature in the *$TiCo_{1-x}Mn_xSb$* semiconductor (the *Mn* atom has fewer 3*d*-electrons than *Co*), which would allow

us to control the position of the Fermi level ε_F and change the values of its electrokinetic characteristics.

In [3], the authors showed that the structure of the base semiconductor *TiCoSb* is defective. Thus, there are vacancies (Va) (~ 1%) in the crystallographic position 4*a* of *Ti* atoms, and additional *Co** atoms (up to ~1%) are located in the tetrahedral voids of the structure, which occupy ~24% of the unit cell volume [2]. As result, the formula of the *TiCoSb* semiconductor is transformed into $(Ti_{0.99}Va_{0.01})Co(Co^*_{0.01})Sb$. Vacancies generate structural defects of acceptor nature in position 4*a* of *Ti* atoms, and the corresponding acceptor band ε_A appears in the band gap ε_g. Additional *Co** atoms generate defects of donor nature in the tetrahedral voids of the semiconductor structure, and the donor band ε_D appears in the band gap ε_g.

All described above explains the nature of the mechanism of simultaneous "a priori" doping of the initial *TiCoSb* semiconductor by donor and acceptor impurities, which makes it heavily doped and highly compensated [4]. Taking into account that the Fermi level ε_F in *TiCoSb* lies within the band gap between the states of ionized donors and acceptors, the changes in the ratio between them caused, for example, by the modes of thermal annealing of samples and their cooling, purity of initial components, etc., will shift the position of the Fermi level ε_F relative to impurity bands and continuous energies bands. For this reason, the compound *TiCoSb* is a semiconductor of the hole-type conductivity at temperatures $T < 90$ K, which is indicated by positive values of the Seebeck coefficient α, and at higher temperatures the majority carriers are electrons. This temperature dependence of the type of the majority carriers also indicates a different depth of energy levels: the acceptor states are smaller and ionized at lower temperatures than the donor ones.

Semiconductor thermoelectric materials based on *TiCoSb* were reported in [3-9]. Thus, in $Ti_{1-x}V_xCoSb$ and $Ti_{1-x}Mo_xCoSb$ semiconductors, structural defects of acceptor nature are simultaneously generated as vacancies in the positions of *Ti* and *Co* atoms, and occupation of 4*a* positions of *Ti* atoms by *V* or *Mo* atoms generates defects of donor nature. The mechanism of simultaneous appearance of acceptors and donors provides the semiconductor properties of $Ti_{1-x}V_xCoSb$ and $Ti_{1-x}Mo_xCoSb$. Doping of *TiCoSb* by *Sc* atoms ($3d^14s^2$) introduced by substitution of *Ti* atoms ($3d^24s^2$) generates structural defects of acceptor nature in $Ti_{1-x}Sc_xCoSb$ (*Sc* atom has fewer 3*d*-electrons than *Ti*), and the ratio of defects of donor and acceptor nature determines the position of the Fermi level ε_F in the band gap ε_g and the mechanisms of electrical conductivity.

The study of the semiconductor thermoelectric material $TiCo_{1-x}Ni_xSb$ revealed a linear variation in the value of the unit cell parameter a(x), which indicates the substitution of *Co* atoms by *Ni* ones. In this case, donors are generated in the crystal, because the *Co* atom ($3d^74s^2$) has a smaller number of 3*d*-electrons than the *Ni* atom ($3d^84s^2$). The thermoelectric material $TiCo_{1-x}Cu_xSb$ has a different behaviour of structural parameters depending on the impurity concentration.

The presented results of studying the electrokinetic and energy characteristics of the semiconductor solid solution $TiCo_{1-x}Mn_xSb$, $x = 0.01–0.10$, as well as their comparison with the results of modeling the electronic structure, will help to identify the mechanisms of electrical conductivity in order to determine the conditions of synthesis of thermoelectric materials with maximum efficiency of thermal energy into electrical energy conversion.

Investigation procedures

$TiCo_{1-x}Mn_xSb$ samples were synthesized by arc-melting the charge of the constituent components (the content of the main component not less than 99.9 wt.%) in an electric arc furnace in

an inert atmosphere followed by homogenizing annealing for 720 h at 1073 K. Excess 1–3 wt. % *Sb* was used to compensate for losses during the electric arc-melting procedure. The chemical and phase compositions of the samples were examined by X-ray phase (DRON-4.0 diffractometer, *Fe*Kα radiation) and metallographic analyses (TESKAN VEGA 3 LMU electron microscope equipped with an X-ray analyzer with energy dispersion spectroscopy (EDRS)). The structural parameters of the solid solution $TiCo_{1-x}Mn_xSb$ samples were calculated using the Fullprof Suite program [10]. Modeling of the electronic structure of $TiCo_{1-x}Mn_xSb$ was performed by the KKR method (Corringa-Kohn-Rostoker method) in the approximation of the coherent potential CPA and local density LDA [11]. Licensed software AkaiKKR and SPR-KKR in the LDA approximation for the exchange-correlation potential with Moruzzi-Janak-Williams (MJW) parameterization were used for KKR calculations [12]. The Brillouin zone was divided into 1000 *k*-points, which were used to model energy characteristics by calculating DOS. The width of the energy window was 22 eV and was chosen to capture all semi-core states of p-elements. The full potential FP in the representation of plane waves was used in the calculations by the linear MT orbital method. The LDA approximation with MJW parameterization was used as the exchange-correlation potential. The accuracy of calculating the position of the Fermi level is ± 4 meV. Temperature and concentration dependences of electric resistivity (ρ) and the Seebeck coefficient (α) relative to copper of $TiCo_{1-x}Mn_xSb$ were measured in the ranges: T = 80–400 K, x = 0.01–0.10.

Research on structural characteristics of $TiCo_{1-x}Mn_xSb$

Microprobe analysis of the concentration of atoms on the surface of $TiCo_{1-x}Mn_xSb$ samples established their correspondence to the initial compositions of the charge (Fig. 1), and X-ray phase and structural analyses showed that the powder patterns of samples, including the composition x=0–0.10, are indexed in the *MgAgAs* structure type and contain no traces of other phases. (Fig. 2a).

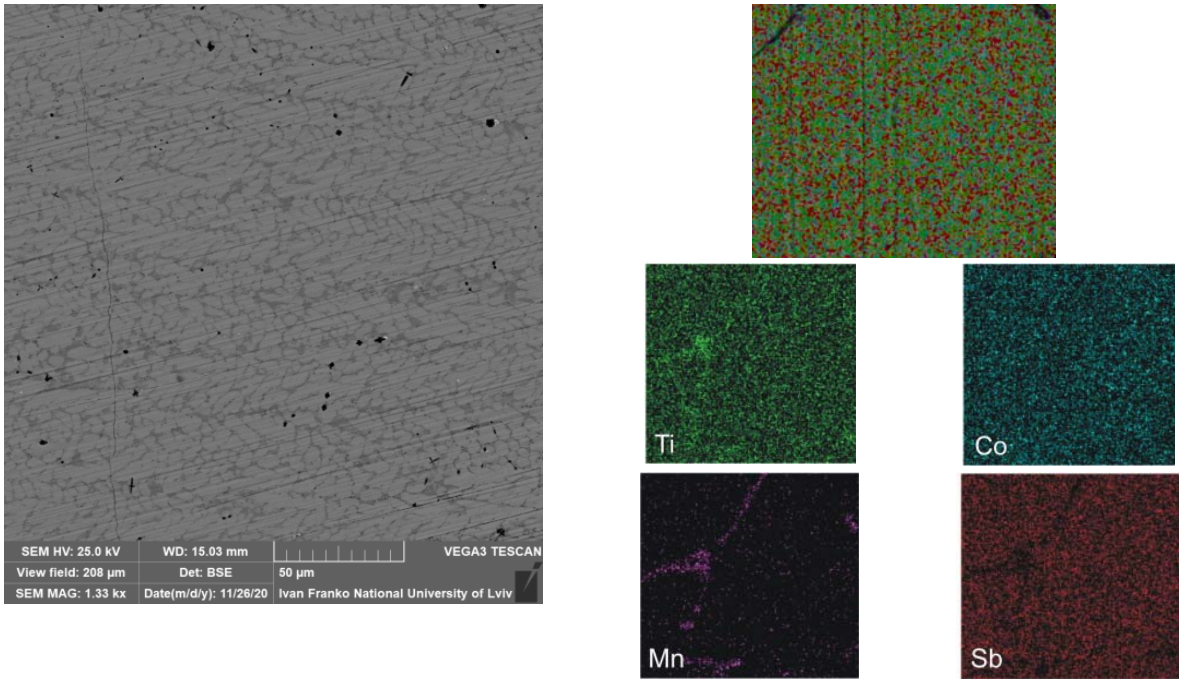

a) *b)*

Fig. 1. Photograph of the surface (a) and distribution of elements (b) in the sample $TiCo_{0.95}Mn_{0.05}Sb$

Structural studies of $TiCo_{1-x}Mn_xSb$ solid solution revealed the complex character of the inclusion of impurity *Mn* atoms into the semiconductor structure matrix. Since the atomic radius of *Mn* ($r_{Mn} = 0.130$ nm) is larger than that of *Co* atom ($r_{Co} = 0.125$ nm), then the increase of the unit cell parameter a(x) of $TiCo_{1-x}Mn_xSb$ in the concentration range $x = 0$–0.05 is logical (Fig. 2b). Such behavior of the parameter a(x) should indicate the realization of $TiCo_{1-x}Mn_xSb$ substitutional solid solution, where structural defects of acceptor nature are generated in the crystallographic site 4*c* of *Co* atoms. In this case, an impurity acceptor band ε_A^{Mn} should be formed in the band gap ε_g of the semiconductor.

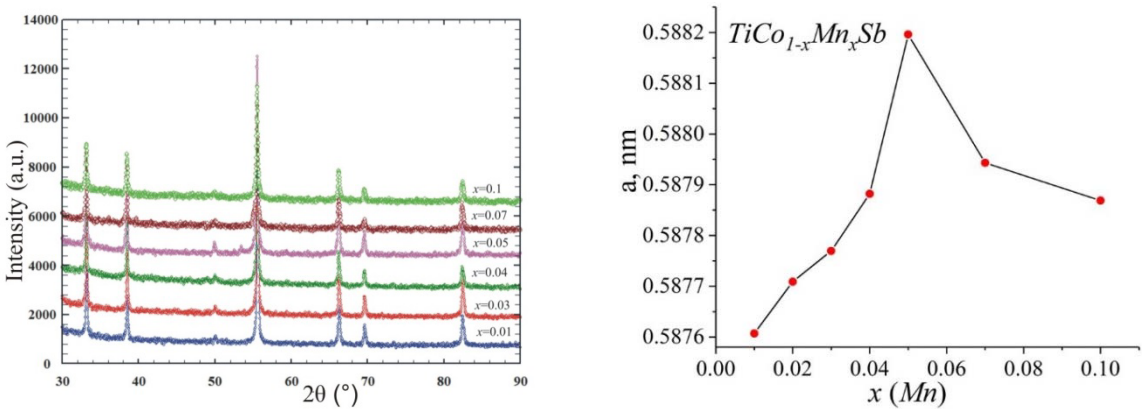

a) *b)*

*Fig. 2. X-ray powder diffraction patterns of samples (**a**) and variation of the unit cell parameter a(x) (**b**) for $TiCo_{1-x}Mn_xSb$*

However, the appearance of an extremum on the dependence a(x) of $TiCo_{1-x}Mn_xSb$ at $x = 0.05$, followed by a decrease of the unit cell parameter a(x) at $x > 0.05$ do not fit into the logic of forming a substitutional solid solution when *Co* atoms are replaced by *Mn* atoms. Thus, if the concentration of impurity *Mn* atoms at $x = 0.05$ would be the limit of the existence of solid substitution (the limit of solubility of these atoms in the semiconductor structure matrix), then the value of the unit cell parameter a(x) of $TiCo_{1-x}Mn_xSb$ should not change significantly. At the same time, the decrease in the values of a(x) of $TiCo_{1-x}Mn_xSb$ at $x > 0.05$ indicates the existence of a substitutional solid solution, but now the impurity *Mn* atoms occupy a different crystallographic position. In this connection, it is worth reminding the study of $Ti_{1-x}V_xCoSb$ semiconductor [8], where the authors found the fact of simultaneous occupation of *V* ($3d^34s^2$) impurity atoms both in the 4*a* crystallographic position of *Ti* atoms, which generated structural defects of donor nature (*V* atom contains more electrons than *Ti* atom) and in the 4*c* position of *Co* atoms, which generated defects of acceptor nature (*V* has fewer 3*d*-electrons than *Co*).

The most probable in $TiCo_{1-x}Mn_xSb$ at $x > 0.05$ is the occupation by the *Mn* atoms of the crystallographic position 4*a* of the *Ti* atoms. Indeed, since the atomic radius of the *Mn* atom is smaller than that of *Ti* ($r_{Ti} = 0.146$ nm), the decrease of the unit cell parameter a(x) for $TiCo_{1-x}Mn_xSb$ at $x > 0.05$ (Fig. 2b) becomes clear. In this case, structural defects of donor nature will be generated in crystallographic position 4*a* (*Mn* atoms have a larger number of 3*d*-electrons than *Ti*), and the impurity donor band ε_D^{Mn} should be formed in the band gap ε_g of the $TiCo_{1-x}Mn_xSb$ semiconductor.

We can assume that in a real $TiCo_{1-x}Mn_xSb$ crystal these processes occur simultaneously, but the rate of substitution of certain atoms depends on the concentration of impurity *Mn* atoms. At lower concentrations of *Mn* atoms ($x \le 0.05$) they replace *Co* atoms to a greater extent, and at $x > 0.05$ – *Ti*

atoms. Herewith, donors and acceptors are generated simultaneously at different rates in $TiCo_{1-x}Mn_xSb$, and the semiconductor becomes heavily doped and highly compensated (HDHCS) [13].

However, taking into account the small number of impurity *Mn* atoms dissolved in the structure matrix of the initial semiconductor, as well as the poor accuracy of the X-ray method of studying the structure, we failed to record any other structural changes.

Thus, structural studies of the semiconductor thermoelectric material $TiCo_{1-x}Mn_xSb$ showed a complex mechanism of impurity inclusion into the semiconductor matrix. The results of experimental investigations of electrokinetic properties for $TiCo_{1-x}Mn_xSb$ will show the correspondence of the conclusions to the real processes in the crystal.

Investigation of the electronic structure of $TiCo_{1-x}Mn_xSb$

To predict the behavior of the Fermi level ε_F, the band gap ε_g, and the electrokinetic characteristics of the $TiCo_{1-x}Mn_xSb$ semiconductor, the distribution of density of electronic states (DOS) was calculated (Fig. 3) for an ordered variant of the structure when *Ti* atoms are substituted by *Mn* atoms in the crystallographic position 4*a*. From Fig. 3 we can see that in the base *TiCoSb* semiconductor the Fermi level ε_F lies near the middle of the band gap ε_g, but closer to the edge of the conduction band ε_C. Since the substitution of *Co* atoms by *Mn* ones generates structural defects of acceptor nature, already at the concentration of $TiCo_{0.99}Mn_{0.01}Sb$ the Fermi level ε_F will drift from the conduction band ε_C and will be located in the middle of the band gap ε_g. At higher concentrations of the acceptor impurity, the concentration of acceptors will increase, and the Fermi level ε_F will approach, and then will cross the percolation level of the valence band ε_V of $TiCo_{1-x}Mn_xSb$, and the dielectric-metal conduction transition will occur [14].

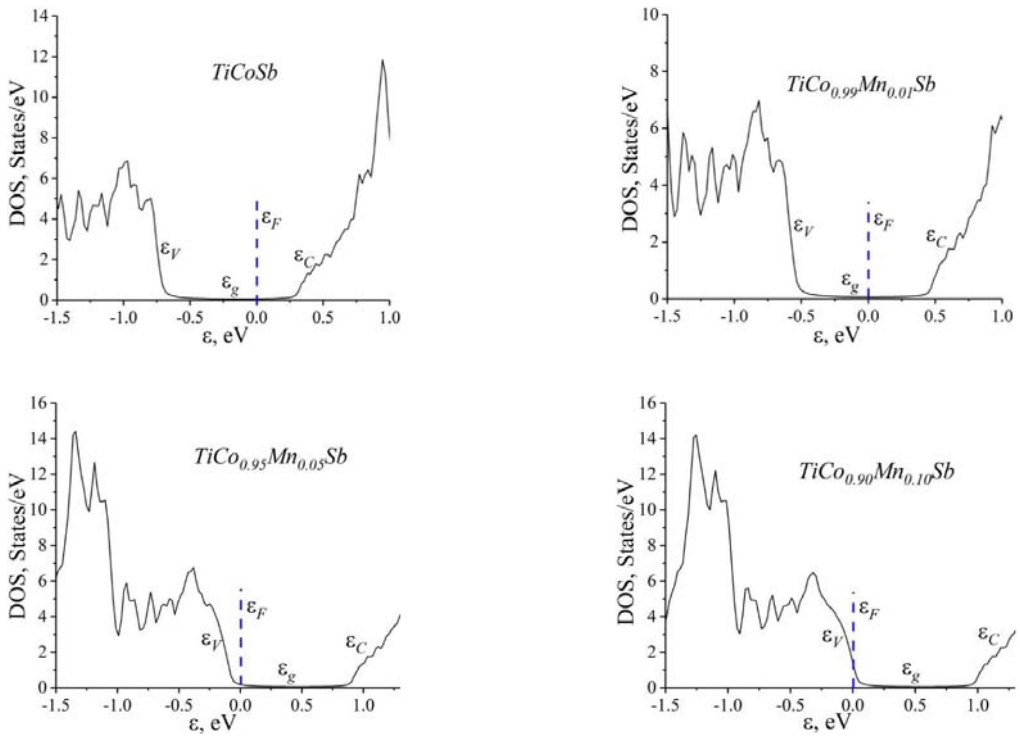

Fig. 3. Distribution of density of electronic states DOS for an ordered variant of the $TiCo_{1-x}Mn_xSb$ structure

Approaching the Fermi level ε_F to the percolation level of the valence band ε_V will lead to the sign inversion of the Seebeck coefficient α(*T*, *x*) from negative to positive, and the Fermi level ε_F crossing the percolation level of the valence band ε_V will change the conduction of the $TiCo_{1-x}Mn_xSb$ semiconductor from activation to metal type [4, 13]. That is, in the experiment the activation parts will disappear on the dependences ln(ρ(1/*T*)), and the values of the resistivity ρ will increase with temperature.

The calculation of distribution of the density of electronic states DOS for the ordered variant of the crystal structure of the thermoelectric material $TiCo_{1-x}Mn_xSb$ allows modeling the behavior of electrokinetic characteristics (Fig. 4). In Fig. 4*a*, as an example, the results of variation of the Seebeck coefficient α(*x*,*T*) are shown at different impurity concentrations and temperatures. As expected, the values α(*x*,*T*) are positive at all concentrations and temperatures, and the maximum values α(*x*,*T*) are reached at concentration $x \approx 0.08$. At the concentrations of *Mn* atoms, $x \approx 0.08–0.10$, the values of the thermoelectric power factor $Z^*_{calc.}$ increase rapidly (Fig. 4b).

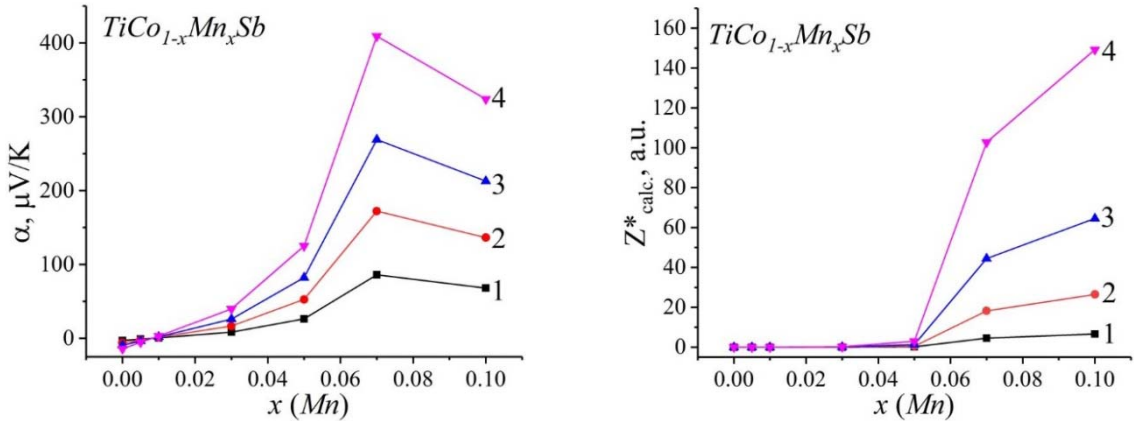

a) *b)*

Fig. 4. Modeling of variation of the Seebeck *coefficient α (**a**) and the thermoelectric power factor $Z^*_{calc.}$ (**b**) for an ordered variant of the $TiCo_{1-x}Mn_xSb$ structure at temperatures: 1 – 80 K; 2 – 160 K; 3 – 250 K; 4 – 380 K*

Investigation of the electrokinetic and energy characteristics of $TiCo_{1-x}Mn_xSb$

Temperature and concentration dependences of electrical resistivity ρ and the Seebeck coefficient α for $TiCo_{1-x}Mn_xSb$ are given in Figs. 5–7.

The temperature dependence of the electrical resistivity ln(ρ(1/*T*)) for *TiCoSb* (Fig. 5) is typical for doped and compensated semiconductors and is described by known relation [13]:

$$\rho^{-1}(T) = \rho_1^{-1} \exp\left(-\frac{\varepsilon_1^{\rho}}{k_B T}\right) + \rho_3^{-1} \exp\left(-\frac{\varepsilon_3^{\rho}}{k_B T}\right), \qquad (1)$$

where the first high-temperature term describes the activation of current carriers ε_1^{ρ} = 100.6 meV from the Fermi level ε_F to the percolation level of the conduction band ε_C, and the second term, at low temperatures, – the hopping conduction with energy ε_3^{ρ} = 5.1 meV at donors impurity states. As seen from Fig. 5, for $TiCo_{1-x}Mn_xSb$ samples, except for the sample at x=0.05, the dependences ln(ρ(1/*T*)) are also described by relation (1).

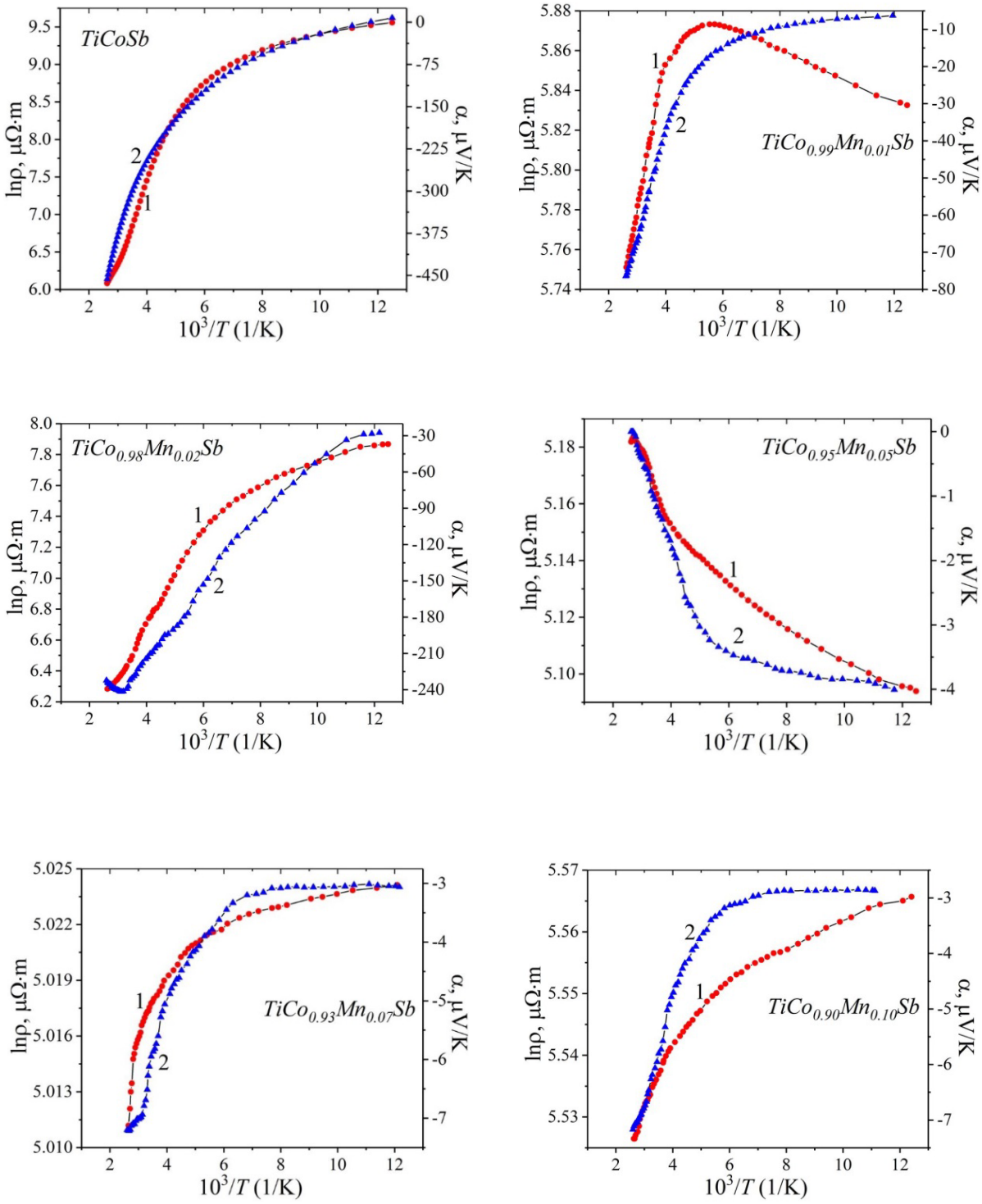

Fig. 5. Temperature dependences of electrical resistivity ln(ρ(1/T)) and the Seebeck coefficient α(1/T) of thermoelectric material $TiCo_{1-x}Mn_xSb$

The variation of the Seebeck coefficient values α(1/*T*) for $TiCo_{1-x}Mn_xSb$ (Fig. 5) is also a classic for doped and compensated semiconductors and is described by the relation [14]:

$$\alpha = \frac{k_B}{e}\left(\frac{\varepsilon_i^{\alpha}}{k_B T} - \gamma + 1\right), \qquad (2)$$

where γ is a parameter that depends on the nature of scattering. From the temperature dependence of α(1/*T*) of *TiCoSb* at high temperatures, the value of activation energy ε_1^{α} = 214.1 meV is calculated, which is proportional to the amplitude of large-scale fluctuations of the continuous energies bands of heavily doped and highly compensated semiconductor [4, 13]. In turn, from the low-temperature dependence α(1/*T*) at low temperatures, the value of activation energy ε_3^{α} = 10.2 meV is determined, which is proportional to the amplitude of modulation of small-scale fluctuation of HDHCS [4, 13].

The results of measuring the electrokinetic characteristics for the initial *TiCoSb* semiconductor are fully consistent with those previously obtained in Refs. [3–9]. The high compensation of *TiCoSb* (closeness of concentrations of ionized acceptors and donors) is evidenced by the character of the variation of the Seebeck coefficient α (Figs. 5, 6). Indeed, *TiCoSb* is a semiconductor of the hole-type conduction at temperatures *T* = 80–90 K, as indicated by the positive values of the Seebeck coefficient: $\alpha_{80\ K}$ = 7.75 μV/K and $\alpha_{90\ K}$ = 0.71 μV/K. However, at higher temperatures, the sign of the Seebeck coefficient α of *TiCoSb* becomes negative ($\alpha_{95\ K}$ = -6.33 μV/K), indicating electrons as the majority charge carriers.

Doping the initial semiconductor *TiCoSb* by the lowest concentration of impurity *Mn* atoms, *x* = 0.01, leads to substantial changes in the temperature dependence ln(ρ(1/*T*)) (see Fig. 5). The presence of a high-temperature activation part on the ln(ρ(1/*T*)) dependence for $TiCo_{0,99}Mn_{0,01}Sb$ is evidence of the location of the Fermi level ε_F within the band gap ε_g, and the negative values of the Seebeck coefficient α(*T*,*x*) (Figs. 5, 6) specify its position which is at a distance of ~6 meV from the percolation level of the conduction band ε_C (Fig. 7). In this case, the electrons are the majority carriers of the semiconductor.

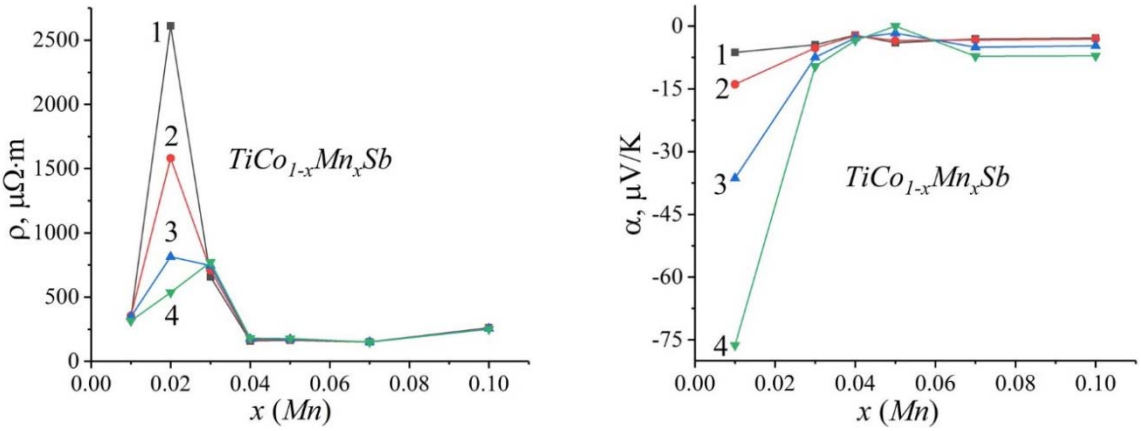

a) *b)*

*Fig. 6. Variation of electrical resistivity ρ(x,T) (**a**) and the Seebeck coefficient α(x,T) (**b**) for $TiCo_{1-x}Mn_xSb$ at different temperatures: 1 – 80 K, 2 – 160 K, 3 – 250 K, 4 – 380 K*

The fact that there is no mechanism of hopping conduction ε_3^{ρ} at low temperatures in $TiCo_{0,99}Mn_{0,01}Sb$ (low-temperature activation part is absent on the dependence ln(ρ(1/*T*))) indicates a significant number of donors, which exceeds the concentration of introduced acceptors. There is an overlap of the wave functions of the electrons of impurity states near the Fermi level ε_F, which makes the mechanism of hopping conduction needless [13].

Negative values of the Seebeck coefficient $\alpha(T,x)$ for $TiCo_{0,99}Mn_{0,01}Sb$ in the temperature range 80–400 K (Figs. 5, 6), when the concentrations of acceptors and donors are close according to DOS calculations (Fig. 3), can be explained by a slightly higher concentration of uncontrolled donors over acceptors. But even at higher impurity *Mn* concentration, in $TiCo_{0,98}Mn_{0,02}Sb$, the sign of the Seebeck coefficient $\alpha(T,x)$ is negative. An increase in the value of resistivity $\rho(x,T)$ was observed, for example, at temperature $T = 80$ K from $\rho(x = 0.01) \approx 341$ μΩ·m to $\rho(x=0.02) \approx 2612$ μΩ·m (Fig. 6a). This increase in the values of $\rho(x,T)$ is evidence of an increase in the compensation degree of the semiconductor, which will lead to the appearance of the hopping conduction mechanism ε_3^{ρ} at low temperatures (low-temperature activation part appears on the dependence $\ln(\rho(1/T))$).

The change of the position of the Fermi level ε_F in the sample $TiCo_{0,98}Mn_{0,02}Sb$, which has shifted from the percolation level of the conduction band ε_C at the distance of ~30 meV (Fig. 7), is evidence of an increase of the compensation degree of semiconductor (reduction of the difference between ionized donors and acceptors). Therefore, the increase in the values of the resistivity $\rho(x,T)$ of $TiCo_{1-x}Mn_xSb$ in the concentration range $x = 0.01$–0.02 is a direct proof of the generation of acceptors in the crystal when the *Co* atoms are substituted by *Mn* atoms. This generation of acceptors leads to the capture of free electrons, which reduces their concentration and causes an increase of the resistivity values $\rho(x,T)$. On the other hand, the negative values of the Seebeck coefficient $\alpha(x,T)$ are also experimental evidence that the $TiCo_{1-x}Mn_xSb$ semiconductor has a significant concentration of donors that is greater than the number of introduced acceptors ($x = 0.02$), or in the crystal acceptors and donors are generated simultaneously by different mechanisms.

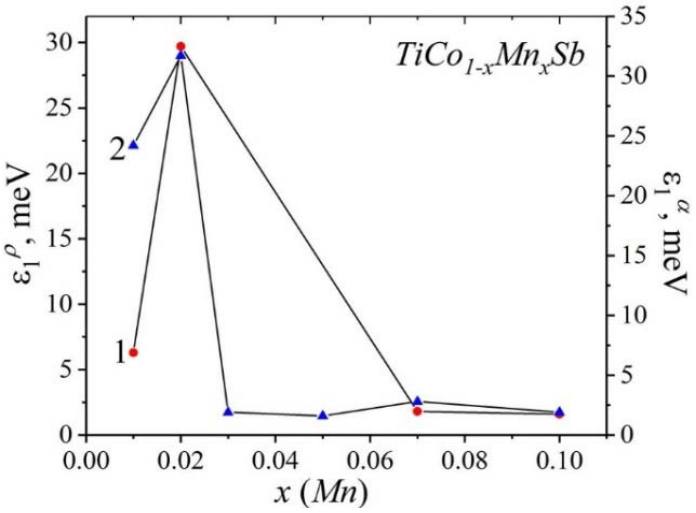

Fig. 7. Variations of the activation energies values ε_1^{ρ} *(1) and* ε_1^{α} *(2) for* $TiCo_{1-x}Mn_xSb$

The appearance of the maximum on the dependence of the resistivity $\rho(x, T)$ of $TiCo_{1-x}Mn_xSb$ (Fig. 6*a*) is an argument that the generation rates of acceptors and donors in the semiconductor are different. At the point of maximum of dependence $\rho(x, T)$ for $TiCo_{1-x}Mn_xSb$, these rates are balanced. However, the number of acceptors is slightly less than the number of free electrons. This is indicated by the negative values of the Seebeck coefficient $\alpha(x, T)$ (Fig. 6*b*). Thus, at $T = 80$ K, to balance the ionized acceptors and donors, it is necessary to introduce a concentration of *Mn* atoms ($x = 0.02$) that generates acceptors so that the concentrations of holes and electrons are close. At higher temperatures, ionization of deep donor states takes place, which increases the concentration of electrons, and

therefore it is necessary to introduce a higher concentration of impurity *Mn* atoms into the crystal ($x = 0.03$). It is logical that the maximum on the dependence $\rho(x,T)$ appears at $x = 0.03$ (Fig. 6*a*). The fact of shifting the maximum on the dependence $\rho(x,T)$ with increasing temperature is evidence of the existence of several mechanisms for generating donors of different nature (origin), which generate in the band gap ε_g donor bands ε_D^1 and ε_D^2 of different nature with different depths of their location relative to the percolation level of the conduction band ε_C.

The experimental result described above does not correspond to the conclusions made in the calculations of the electronic structure of the $TiCo_{1-x}Mn_xSb$ semiconductor for the ordered variant of its crystal structure (Fig. 3). When *Co* ($3d^74s^2$) atoms are substituted by *Mn* ($3d^54s^2$) atoms in $TiCo_{1-x}Mn_xSb$, acceptors should be generated in the semiconductor, which will capture all free electrons at concentration $x \approx 0.02$. This process must not be accompanied by inversion of the sign of the Seebeck coefficient α, and free holes will remain the majority charge carriers of the semiconductor (Fig. 4*a*). We can assume that more complex structural changes occur in $TiCo_{1-x}Mn_xSb$ than the substitution of *Co* atoms by *Mn*. At the same time, structural defects of acceptor and donor nature are generated in the crystal by different mechanisms, but the concentration of donors exceeds the concentration of acceptors.

Calculations of the location depth of the Fermi level ε_F relative to the percolation level of the conduction band ε_C of $TiCo_{1-x}Mn_xSb$ at a higher concentration of impurity *Mn* atoms ($x \geq 0.07$) (the sign of the Seebeck coefficient $\alpha(T,x)$ is negative) showed that the Fermi level ε_F very closely approached the percolation level: $\varepsilon_F(x = 0.07) = 1.8$ meV and $\varepsilon_F(x = 0.10) = 1.6$ meV (Fig. 7). The presence of high- and low-temperature activation parts on the $\ln(\rho(1/T))$ dependences of $TiCo_{1-x}Mn_xSb$ at $x \geq 0.07$ is possible provided semiconductor compensation (simultaneous existence of ionized donors and acceptors). However, the fact that the Fermi level ε_F lies within the band gap ε_g near the percolation level of the conduction band indicates a weak compensation of the semiconductor, when the concentration of free electrons is much higher than the concentration of holes.

What is the reason for such, at first glance, illogical behavior of electrokinetic and energy characteristics in the semiconductor thermoelectric material $TiCo_{1-x}Mn_xSb$?

If we remind that in the structure of the base semiconductor *TiCoSb* there are simultaneously ~1% of vacancies in position 4*a* of the *Ti* atoms that generate acceptors, and in the tetrahedral voids of the structure there are ~1% of additional *Co** atoms that generate donors [3], the situation becomes clearer. In turn, structural studies of $TiCo_{1-x}Mn_xSb$ showed that the introduction of impurity *Mn* atoms into the disordered structure of the base semiconductor *TiCoSb* is accompanied by its ordering. This means that the vacancies in position 4*a* of the *Ti* atoms, and also the corresponding acceptor band ε_A disappear. Instead, the *Ti* atoms occupying the vacancies in position 4*a* are a source of electrons that generates the donor band ε_D^1. Partial occupation of tetrahedral voids of the structure by impurity *Mn* atoms is a mechanism of the formation of another donor band ε_D^2.

Conclusions

The result of a complex investigation of the crystal and electronic structures, electrokinetic and energy characteristics of the thermoelectric material $TiCo_{1-x}Mn_xSb$ is the establishment of the nature of structural defects of donor and acceptor nature. It was shown that doping of the base semiconductor *TiCoSb* by *Mn* atoms simultaneously generates the acceptor band ε_A (substitution of *Co* atoms by *Mn*) and the donor bands ε_D^1 and ε_D^2 of different nature. The ratio of the concentrations of ionized acceptors and donors generated in $TiCo_{1-x}Mn_xSb$ determines the position of the Fermi level ε_F and the

mechanisms of electrical conduction. However, this issue requires additional research, in particular, modeling the electronic structure of thermoelectric material under different conditions of introduction into the structure and concentrations of impurity *Mn* atoms. The investigated $TiCo_{1-x}Mn_xSb$ solid solution is a promising thermoelectric material.

References

1. Anatychuk L.I. (1979). *Termoelementy i termoelectricheskiie ustroistva. Spravochnik.* [*Thermoelements and thermoelectric devices*. *Reference book]*. Kyiv: Naukova dumka [in Russian].
2. Romaka V.V., Romaka L.P., Krayovskyy V.Ya., Stadnyk Yu.V. (2015). *Stanidy ridkisnozemelnykh ta perekhidnykh metaliv* [*Stannides of rare earth and transition metals]* Lviv: Lvivska Polytechnika [in Ukrainian].
3. Romaka L.P., Shelyapina M.G., Stadnyk Yu.V., Fruchart D., Hlil E.K., Romaka V.A. (2006). Peculiarity of metal–insulator transition due to composition change in semiconducting $TiCo_{1-x}Ni_xSb$ solid solution. I. Electronic structure calculations, *J. Alloys Compd.*, 414, 46–50.
4. Romaka V.A., Stadnyk Yu.V., Krayovskyy V.Ya., Romaka L.P., Guk O.P., Romaka V.V., Mykyuchuk M.M., Horyn A.M. (2020). *Novitni termochutlyvi materialy ta peretvoriuvachi temperatury* [*New thermosensitive materials and temperature converters*]. Lviv, Lvivska Polytechnika [in Ukrainian].
5. Stadnyk Yu.V., Romaka V.A., Shelyapina M.G., Gorelenko Yu.K., Romaka L.P., Fruchart D., Tkachuk A.V., Chekurin V.F. (2006). Impurity band effect on $TiCo_{1-x}Ni_xSb$ conduction. Donor impurities. *J. Alloys Compd.*, 421, 19–23.
6. Romaka V.A., Stadnyk Yu.V., Fruchart D., Tobola J., Gorelenko Yu.K., Romaka L.P., Chekurin V.F., Horyn A.M. (2007). Features of doping the *p-TiCoSb* intermetallic semiconductor with a *Cu* donor impurity. 1. Calculation of electron structure. *Ukr. J. Phys*., 52(5), 453–457.
7. Romaka V.A., Stadnyk Yu.V., Fruchart D., Tobola J., Gorelenko Yu.K., Romaka L.P., Chekurin V.F., Horyn A.M. (2007). Specific features of doping the *p-TiCoSb* intermetallic semiconductor with a *Cu* donor impurity. 2. Experimental Studies. *Ukr. J. Phys*., 52(7), 650–656.
8. Romaka V.A., Stadnyk Yu.V., Akselrud L.G., Romaka V.V., Frushart D., Rogl P., Davydov V.N., Gorelenko Yu.K. (2008). Mechanism of local amorphization of a heavily doped $Ti_{1-x}V_xCoSb$ intermetallic semiconductor. *Semiconductors*, 42(7), 753–760.
9. Romaka V.A., Stadnyk Yu.V., Romaka L.P., Krayovskyy V.Ya., Romaka V.V., Horyn A.M., Konyk M.B., Romaniv I.M., Rokomaniuk M.V. (2019). Features of structural, energetic and magnetic characteristics of thermoelectric material $Ti_{1-x}Sc_xCoSb$. *J. Thermoelectricity*, 1, 25–41.
10. Roisnel T., Rodriguez-Carvajal J. (2001). WinPLOTR: a windows tool for powder diffraction patterns analysis. *Mater. Sci. Forum*, Proc. EPDIC7 378–381, 118–123.
11. Schruter M., Ebert H., Akai H., Entel P., Hoffmann E., Reddy G.G. (1995). First-principles investigations of atomic disorder effects on magnetic and structural instabilities in transition-metal alloys. *Phys. Rev*. B 52, 188–209.
12. Moruzzi V.L., Janak J.F., Williams A.R. (1978). *Calculated electronic properties of metals.* NY: Pergamon Press.
13. Shklovskii B.I. and Efros A.L. (1984). *Electronic properties of doped semiconductors* NY: Springer; (1979) Moscow: Nauka.
14. Mott N.F., Davis E.A. (1979). *Electron processes in non-crystalline materials*. Oxford: Clarendon Press.

Submitted 30.06.2020

Ромака В.А., *док. тех. наук*, *професор*[1]
Стадник Ю.В., *канд. хім. наук*[2]
Ромака Л.П., *канд. хім. наук*[2]
Горинь А.М., *канд. хім. наук*[2]
Романів І.М., *канд. хім. наук*[2],
Пашкевич В.З., *канд. техн. наук*[1]
Гопернюк А.Я., *канд. техн. наук*[1]

[1]Національний університет "Львівська політехніка"
вул. С. Бандери, 12, Львів, 79013, Україна,
e-mail: vromaka@polynet.lviv.ua;
[2]Львівський національний університет ім. І. Франка
вул. Кирила і Мефодія, 6, Львів, 79005, Україна;
e-mail: lyubov.romaka@lnu.edu.ua

ДОСЛІДЖЕННЯ ЕНЕРГЕТИЧНИХ ТА КІНЕТИЧНИХ ХАРАКТЕРИСТИК ТЕРМОЕЛЕКТРИЧНОГО МАТЕРІАЛУ $TiCo_{1-x}Mn_xSb$

Досліджено кристалічну та електронну структури, температурні і концентраційні залежності питомого електроопору та коефіцієнта термо-ерс термоелектричного матеріалу $TiCo_{1-x}Mn_xSb$, x = 0.01–0.10, у діапазоні температур T = 80–400 K. Показано, що легування базового напівпровідника TiCoSb атомами Mn супроводжується одночасним генеруванням структурних дефектів акцепторної та донорної природи та появою в забороненій зоні акцепторної ε_A (заміщення атомів Co на Mn) і донорних зон ε_D^1 та ε_D^2 різної природи. Співвідношення генерованих у $TiCo_{1-x}Mn_xSb$ концентрацій іонізованих акцепторів і донорів визначає положення рівня Фермі ε_F та механізми електропровідності термоелектричного матеріалу. Бібл. 14, рис. 7.
Ключові слова: електронна структура, електроопір, коефіцієнт термоЕРС.

Ромака В.А., *док. тех. наук*, *профессор*[1]
Стаднык Ю.В., *канд. хим. наук*[2]
Ромака Л.П., *канд. хим. наук*[2]
Горынь А.М., *канд. хим. наук*[2]
Романив И.М., *канд. хим. наук*[2],
Пашкевич В.З., *канд. техн. наук*[1]
Гопернюк А.Я., *канд. техн. наук*[1]

[1]Национальный университет "Львовская политехника",
ул. С. Бандеры, 12, Львов, 79013, Украина,
e-mail: vromaka@polynet.lviv.ua;
[2]Львовский национальный университет имени Ивана Франко,
ул. Кирилла и Мефодия, 6, Львов, 79005, Украина,
e-mail: lyubov.romaka@lnu.edu.ua;

ИССЛЕДОВАНИЕ ЭНЕРГЕТИЧЕСКИХ И КИНЕТИЧЕСКИХ ХАРАКТЕРИСТИК ТЕРМОЭЛЕКТРИЧЕСКИХ МАТЕРИАЛОВ $TiCo_{1-x}Mn_xSb$

Исследованы кристаллическая и электронная структуры, температурные и концентрационные зависимости удельного электросопротивления и коэффициента термоЭДС термоэлектрического материала $TiCo_{1-x}Mn_xSb$, x = 0.01 – 0.10, в диапазоне температур T = 80 – 400 K. Показано, что легирования базового полупроводника TiCoSb атомами Mn сопровождается одновременным генерированием структурных дефектов акцепторной и донорной природы и появлением в запрещенной зоне акцепторной ε_A (замещение атомов Co на Mn) и донорных зон ε_D^1, ε_D^2 различной природы. Соотношение генерируемых в $TiCo_{1-x}Mn_xSb$ концентраций ионизированных акцепторов и доноров определяет положение уровня Ферми ε_F и механизмы электропроводности термоэлектрического материала. Библ. 14, рис. 7.

Ключевые слова: Электронная структура, электросопротивление, коэффициент термоЭДС

References

1. Anatychuk L.I. (1979). *Termoelementy i termoelectricheskiie ustroistva. Spravochnik.* [*Thermoelements and thermoelectric devices*. *Reference book]*. Kyiv: Naukova dumka [in Russian].
2. Romaka V.V., Romaka L.P., Krayovskyy V.Ya., Stadnyk Yu.V. (2015). *Stanidy ridkisnozemelnykh ta perekhidnykh metaliv* [*Stannides of rare earth and transition metals]* Lviv: Lvivska Polytechnika [in Ukrainian].
3. Romaka L.P., Shelyapina M.G., Stadnyk Yu.V., Fruchart D., Hlil E.K., Romaka V.A. (2006). Peculiarity of metal–insulator transition due to composition change in semiconducting $TiCo_{1-x}Ni_xSb$ solid solution. I. Electronic structure calculations, *J. Alloys Compd.*, 414, 46–50.
4. Romaka V.A., Stadnyk Yu.V., Krayovskyy V.Ya., Romaka L.P., Guk O.P., Romaka V.V., Mykyuchuk M.M., Horyn A.M. (2020). *Novitni termochutlyvi materialy ta peretvoriuvachi temperatury* [*New thermosensitive materials and temperature converters*]. Lviv, Lvivska Polytechnika [in Ukrainian].
5. Stadnyk Yu.V., Romaka V.A., Shelyapina M.G., Gorelenko Yu.K., Romaka L.P., Fruchart D., Tkachuk A.V., Chekurin V.F. (2006). Impurity band effect on $TiCo_{1-x}Ni_xSb$ conduction. Donor impurities. *J. Alloys Compd.*, 421, 19–23.
6. Romaka V.A., Stadnyk Yu.V., Fruchart D., Tobola J., Gorelenko Yu.K., Romaka L.P., Chekurin V.F., Horyn A.M. (2007). Features of doping the *p-TiCoSb* intermetallic semiconductor with a *Cu* donor impurity. 1. Calculation of electron structure. *Ukr. J. Phys*., 52(5), 453–457.
7. Romaka V.A., Stadnyk Yu.V., Fruchart D., Tobola J., Gorelenko Yu.K., Romaka L.P., Chekurin V.F., Horyn A.M. (2007). Specific features of doping the *p-TiCoSb* intermetallic semiconductor

with a *Cu* donor impurity. 2. Experimental Studies. *Ukr. J. Phys*., 52(7), 650–656.

8. Romaka V.A., Stadnyk Yu.V., Akselrud L.G., Romaka V.V., Frushart D., Rogl P., Davydov V.N., Gorelenko Yu.K. (2008). Mechanism of local amorphization of a heavily doped $Ti_{1-x}V_xCoSb$ intermetallic semiconductor. *Semiconductors*, 42(7), 753–760.
9. Romaka V.A., Stadnyk Yu.V., Romaka L.P., Krayovskyy V.Ya., Romaka V.V., Horyn A.M., Konyk M.B., Romaniv I.M., Rokomaniuk M.V. (2019). Features of structural, energetic and magnetic characteristics of thermoelectric material $Ti_{1-x}Sc_xCoSb$. *J. Thermoelectricity*, 1, 25–41.
10. Roisnel T., Rodriguez-Carvajal J. (2001). WinPLOTR: a windows tool for powder diffraction patterns analysis. *Mater. Sci. Forum*, Proc. EPDIC7 378–381, 118–123.
11. Schruter M., Ebert H., Akai H., Entel P., Hoffmann E., Reddy G.G. (1995). First-principles investigations of atomic disorder effects on magnetic and structural instabilities in transition-metal alloys. *Phys. Rev*. B 52, 188–209.
12. Moruzzi V.L., Janak J.F., Williams A.R. (1978). *Calculated electronic properties of metals.* NY: Pergamon Press.
13. Shklovskii B.I. and Efros A.L. (1984). *Electronic properties of doped semiconductors* NY: Springer; (1979) Moscow: Nauka.
14. Mott N.F., Davis E.A. (1979). *Electron processes in non-crystalline materials*. Oxford: Clarendon Press.

Submitted 30.06.2020

S.I. Menshikova *cand. phys. - math. sciences*
E.I. Rogacheva *doc. phys. - math. sciences*

National Technical University "Kharkiv Polytechnic Institute", 2, Kyrpychova Str., Kharkiv, 61002, Ukraine

S.I. Menshikova

E.I. Rogacheva

EFFECT OF DEVIATION FROM STOICHIOMETRY ON THERMAL CONDUCTIVITY OF Bi_2Se_3 POLYCRYSTALS

The dependences of electronic and lattice thermal conductivity on the composition (59.9 - 60.0) at. % Se of Bi_2Se_3 polycrystals subjected to a long-term annealing at 650 K. A non-monotonic behavior of these concentration dependences, associated with a change in the phase composition and defect structure under the deviation from stoichiometry, was observed. The boundaries of the Bi_2Se_3 homogeneity region were estimated. The results of the present work confirm those obtained earlier in our study of the effect of deviation from stoichiometry (59.9 - 60.0 at.% Se) on the electrical conductivity, Hall coefficient, Seebeck coefficient and microhardness of Bi_2Se_3 polycrystals after a similar preparation technology. Bibl. 33. Fig. 3.
Keywords: *bismuth selenide, stoichiometry, concentration, defect structure, thermal conductivity*

Introduction

Solid solutions based on the bismuth selenide are the well-known *n*-type thermoelectric (TE) materials for cooling devices [1]. Bi_2Se_3 belongs to a narrow-gap semiconductor group and demonstrates the unique properties of topological insulator (material which is dielectric in the bulk with a metallic layer on the surface) [2]. The efficiency of a TE energy convertor depends on the value of TE figure of merit Z of a TE material ($Z = S^2 \cdot \sigma/\lambda$, where σ and λ are the electrical and thermal conductivities, respectively, S is the Seebeck coefficient).

Bi_2Se_3 is a bertollide [3-5] with the homogeneity region (HR) shifted to the Bi-rich side at $T >$ 675 K [6]. Bi_2Se_3 melts congruently with an open maximum at 979 K [3,7,8], which is deviated from stoichiometry and located at (59.98 ± 0.01) at. % Se [3-6,9].

Bi_2Se_3 always exhibits *n*-type conductivity which is commonly associated with the presence of a large number of Se vacancies (V_{Se1}) [5,6,10-21] acting as donors. The existence of V_{Se1} was confirmed by a number of authors [6,12,15-18,22-24] with the help of different experimental and theoretical methods (scanning tunneling microscopy, measurements of the Hall coefficient in the temperature range 80-330 K, calculation of the formation energies of various types of defects etc.). Later [24-26], the coexistence of V_{Se1} and antisite defects (AD) – bismuth atoms that occupy positions of selenium ones (Bi_{Se}), in the *n*-Bi_2Se_3 was suggested.

The deviation from stoichiometry in chemical compound leads to the appearance of intrinsic defects, the concentration of which varies within the HR of the compound which determines the properties of the TE material. Analysis of the literature showed, that the HR boundaries of the Bi_2Se_3 were determined just for temperatures above 675 K [6], and the boundaries of the maximal HR are (59.984 - 59.997) at.% Se at 900 K. Despite the fact that Bi_2Se_3 is used for TE applications at

temperatures close to room temperature, the investigation of the HR boundaries at these temperatures are not available in the literature. In our previous work [27], based on the study of the electrical conductivity, Hall coefficient, Seebeck coefficient and microhardness of Bi_2Se_3 polycrystals with deviation from stoichiometry to the Bi-rich side after a long-term annealing at 670 K with subsequent cooling to the room temperature, the HR boundaries were estimated. The investigation of the thermal properties of such crystals could expand the range of research, supplement and/or confirm the results of [27]. As far as we know, no study of the thermal properties of Bi_2Se_3 polycrystals under the deviation from stoichiometry has been performed yet.

The typical values of λ for Bi_2Se_3 single crystals lie within 2.5-3.1 $W \cdot m^{-1} \cdot K^{-1}$ [12,28,29] and for pressed polycrystals – within 1.0-1.3 $W \cdot m^{-1} \cdot K^{-1}$ [30-32]. It is also known, that usually electronic component of thermal conductivity is comparable to the lattice one in single [28] and pressed [33] crystals. The values of $Z = 5 \cdot 10^{-4}$ K^{-1} [29] and $Z = 1.6 \cdot 10^{-4}$ K^{-1} [33] at a room temperature are typical for single and polycrystals Bi_2Se_3, respectively.

The purpose of the work was to study the effect of deviation from stoichiometry on the thermal conductivity and TE figure of merit of Bi_2Se_3 polycrystals at a room temperature.

Experimental

Bi-Se polycrystals with different Se concentrations (59.9 - 60.0) at. % were prepared by fusing high-purity (99.999 at. % of the main component) Bi and Se in evacuated quartz ampoules at a temperature of T = (980 ± 10) K. The melt was kept at this temperature for 3 h with vibrational stirring. After that the alloys were annealed for 200 h at T = 820 K with subsequent cooling to room temperature in the turned-off furnace. The synthesized alloys were used for subsequent preparing of powders for pressing with particle size of 200 μm. Pressed samples were prepared by cold-pressed method at a fixed load of 400 MPa for 60 s with subsequent homogenizing annealing in evacuated quartz ampoules at 650 K for 250 h with subsequent cooling to room temperature.

The thermal conductivity λ was measured by the dynamic λ-calorimeter method in monotonic heating regime with help of IT-λ-400 experimental facility. The errors of λ measurement did not exceed ± 5 %. The measurements were carried out at a room temperature.

The determination of the lattice component λ_{ph} of thermal conductivity was determined by subtracting the electronic component λ_{el} from the total thermal conductivity. The λ_{el} values were calculated with the help of the Wiedemann-Franz law:

$$\lambda_{el} = L\sigma T,$$

where L is the Lorenz number ($L = 2.44 \cdot 10^{-8}$ V^2/K^2 for degenerate statistics), T is the temperature. The values of σ obtained in our previous work [27] for Bi_2Se_3 polycrystals with a deviation towards the excess of Bi after a similar preparation technology were used for calculation of λ_{el}.

Experimental results and discussion

The investigated polycrystals were homogeneous in its chemical composition and properties [27].

The obtained room-temperature dependence of λ on the composition of the Bi-Se pressed crystals is shown in Fig. 1.

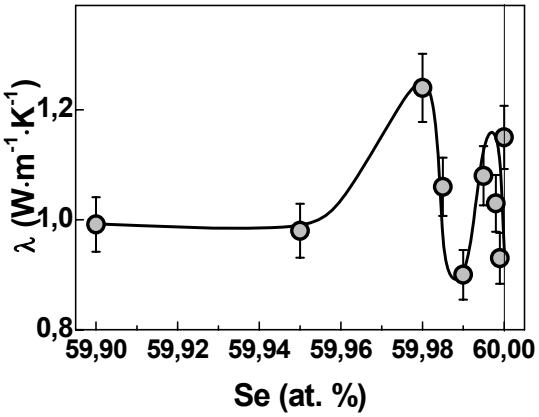

Fig. 1. Room-temperature dependence of thermal conductivity λ on Se content in Bi-Se polycrystals

The results of calculation of λ_{el} and λ_{ph} for Bi-Se polycrystals with different composition are shown in Fig. 2.

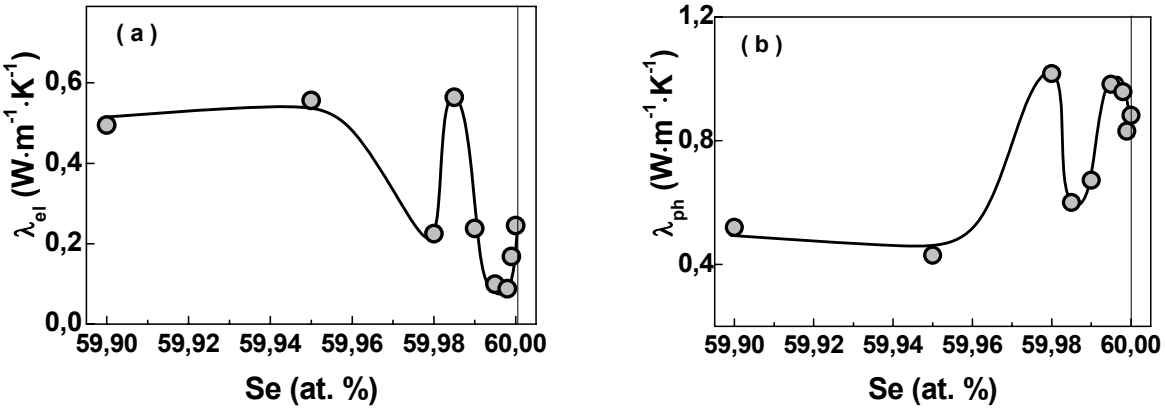

Fig. 2. The dependences of electronic λ_{el} (a) and lattice thermal conductivity λ_{ph} (b) on Se content in Bi-Se polycrystals

The calculation of the value of the TE figure of merit of Bi_2Se_3 crystals with an excess of Bi for different composition was made using the values of σ and S, obtained in our previous work [27], and λ, obtained in the present work (Fig. 3).

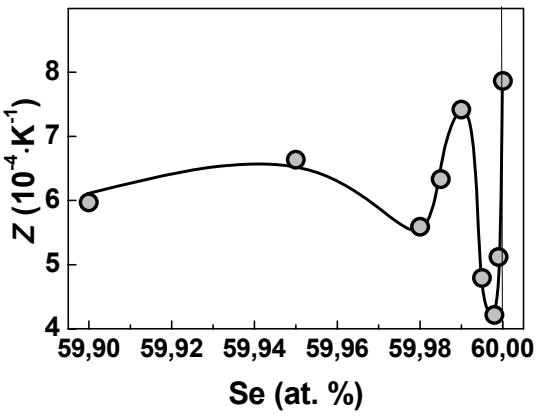

Fig. 3. The dependence of the TE figure of merit Z on Se content in Bi-Se polycrystals

As can be seen from Fig. 1 and Fig. 2, under the deviation from the stoichiometry of Bi_2Se_3 to the Bi-rich side, general trends of increasing in λ_{el} and decreasing in λ and λ_{ph} are observed. Starting from ~ 59.95 at.% Se, the values of λ_{el}, λ and λ_{ph} practically do not change. In the composition range (59.95–60 at.% Se) the concentration dependences of the thermal conductivity and its components are non-monotonic and exhibit an oscillating behavior. From Fig. 1 and Fig. 2 one can identify five regions with different dependence behaviors of properties on Se content:

1) 60.0 - 59.998 at.% Se, where λ_{el} tends to decrease, and λ and λ_{ph} tend to increase;

2) 59.998- 59.985 at.% Se, where λ_{el} increases, λ and λ_{ph} decrease;

3) 59.985- 59.98 at.% Se, where λ_{el} decreases, λ and λ_{ph} increase again;

4) 59.98 - 59.95 at.% Se, where increase in λ_{el} and decrease in λ and λ_{ph} are observed;

5) 59.95 - 59.90 at.% Se, where λ_{el}, λ and λ_{ph} do not change.

It should be noted that behavior of σ (see [27]) and λ_{el} (Fig. 2) on concentration coincide. This is logical, because λ_{el} is determined by the values of σ. The dependences of λ_{el} and λ_{ph} on the composition have an opposite character: the positions of observed maxima of the λ_{el} correspond to the positions of the minima of λ_{ph}.

A complicated behavior of the concentration dependences of compound properties under the deviation from stoichiometry indicates the crossing of the phase boundary. But within the HR, which is a single-phase region, such a behavior can indicate the self-organization processes in the compound and be determined by the redistribution of atoms and non-stoichiometric defects. Taking into account the long-term isothermal annealing at 650 K carried out for Bi-Se polycrystals after its pressing, one can assume that a phase state close to the equilibrium state at 650 K was reached and the subsequent cooling in the turned-off furnace to room temperature does not change this state.

According to the phase diagram of Bi-Se [3,4,6], a two-phase region (Bi_2Se_3 + Se) under the deviation from stoichiometry to the Bi-rich side should exist at a temperature $T > 675$ K. At temperature decrease below 675 K, the phase boundary may be shifted. Taking into account the trend of the boundary shifting with temperature decrease from 900 K to 675 K [3,6], the shift of phase boundary is most likely to occur at a lower Se concentration. So, it assumed that the first concentration range 60.0–59.998 at.% Se corresponds to the two-phase region (Bi_2Se_3 + Se), which is in the state of decomposition of the solid solution. In this region, many different factors affect the character of the composition dependences of properties (for example, the number and size of precipitated particles, cooling rate, etc.).

In the second region (59.998 - 59.985 at.% Se) we could expect the reaching of the HR boundary of Bi_2Se_3 from the Se-rich side. We can assume that subsequent deviation from stoichiometry towards the Bi excess in this region leads to V_{Se1} increase, which are electrically active defects and cause an increase in electron concentration (λ_{el} increases) and creates additional centers of phonon scattering in the lattice (λ_{ph} decreases).

The further deviation from stoichiometry (region 59.985 - 59.980 at.% Se) should result in further increase in the concentration of non-stoichiometric defects. It can be assumed, that the formation of an another type of non-stoichiometric defects – acceptor type AD (Bi_{Se}) [18,24] – becomes thermodynamically favorable. The appearance of Bi atoms at Se positions can lead to an increase in λ_{ph}. Taking into account that Bi_{Se} defects provide acceptor effect [18,23,24], these defects can partially compensate the donor action of V_{Se1} and lead to the decrease in λ_{el} in this region.

The next concentration region 59.98 - 59.95 at. % Se (λ_{el} increases, λ and λ_{ph} decrease) presumably corresponds to the reaching of the boundary of the Bi_2Se_3 HR from the Bi-rich side.

Further practically unvaried values of thermal properties of crystals in the range 59.95 - 59.90 at.% Se, most probably, indicate the precipitation of a second phase BiSe [3] upon crossing the solidus line.

Thus, based on the analysis of the obtained experimental data (Fig. 1, Fig. 2) we assumed that the boundary of the Bi_2Se_3 HR on the Bi-rich side lies in the range 59.98 - 59.95 at.% Se, and on the Se-rich side corresponds to ~ 59.998 at% Se. It should be noted that the HR boundaries of the Bi_2Se_3 and the character of change in the defect structure, experimentally determined in the present work, coincide and add further confirmation of the results of our earlier work [27].

Analysis of calculated electronic and lattice components of λ shows that the contribution of electronic component for all investigated samples is close to the lattice one. It should be also noted that under the deviation from stoichiometry to the Bi-rich side the contribution of λ_{ph} to the total thermal conductivity becomes smaller (see Fig. 2b). It is logical to associate this tendency with creation of different types of crystal defects. The latter indicates that phonons scatter strongly on defects (presumably, Bi_{Se} and V_{Se1}).

It should be noted that the value of λ_{ph} for the stoichiometric crystal (λ_{ph} = 0.85 $W \cdot m^{-1} \cdot K^{-1}$) was slightly lower than the data available in the literature (λ_{ph} = 1.07 $W \cdot m^{-1} \cdot K^{-1}$ [32]) for pressed crystals. This difference in the values of λ_{ph} could be explained by a different method of preparing samples (spark-plasma sintering at a temperature of 593 K for 5 min at a uniaxial pressure of 40 MPa was used in [32]).

As can be seen from Fig. 3, the value of Z also exhibits a non-monotonic type of dependence on the Se content in Bi-Se polycrystals. It can be seen that the largest value of $Z = 8 \cdot 10^{-4}$ K^{-1} is inherent in a crystal with the stoichiometric composition, and even under a slight deviation from the stoichiometry towards the Bi excess (59,998 at.% Se), the value of Z drops sharply ($Z = 4.2 \cdot 10^{-4}$ K^{-1}), which is important from a practical point of view. It should be noted that the values of Z obtained here for Bi-Se crystals at a room temperature were slightly higher than those known in the literature for pressed stoichiometric Bi_2Se_3 [29,33]. This gain in the value of Z is a consequence of the lower value of λ and the higher value of S [27] of the crystal, which was subjected to a long-term annealing at 650 K with subsequent cooling to room temperature in the turned-off furnace in the present work, compared with the literature data [29,33] for the pressed crystals.

Conclusions

The effect of the deviation from stoichiometry to the Bi-rich side (59.9–60.0) at. % Se on the electronic and lattice components of thermal conductivity of the Bi_2Se_3 polycrystals was studied. The boundaries of the Bi_2Se_3 homogeneity region (on the Se-rich side – 59.998 at. % Se, and on the Bi-rich side – in the interval of 59.98–59.95 at. % Se) after a long-term annealing at 650 K with subsequent cooling to the room temperature were estimated.

The estimated HR boundaries of Bi_2Se_3 confirm the previous results [27] in the analysis of the concentration dependences of the electrical conductivity, Hall coefficient, Seebeck coefficient and microhardness.

The non-monotonic behavior of the concentration dependences of the electronic and phonon thermal conductivities at a room temperature attributed to a change in the phase composition and defect structure under the deviation from stoichiometry of Bi_2Se_3 was observed. It is supposed that within the homogeneity region with the dominant type of non-stoichiometric defects (selenium vacancies) the formation of antisite defects Bi_{Se} occurs.

This work was supported by the Ministry of Education and Science of Ukraine (Project No. M0625).

References

1. Rowe D.M. (1995). *CRC Handbook of Thermoelectrics*. Boca Raton, London, New York, Washington: CRC Press.
2. Xia Y., Qian D., Hsien D., Wray L., Pai A., Bansil A., Grauer D., Hor Y.S., Cava R.J., Hasan M.Z.(2009). Observation of a large-gap topological-insulator class with a single Dirac cone on the surface. *Nature Physics*, 5, 398 – 402.
3. Chizhevskaya S.N., Shelimova L.E., Zaitseva I.A. (1994). Critical evaluation and coordination of Bi-Se phase diagram data. *Inorg. Mater*, 30, 1289-1387.
4. Poretskaya L.V., Anukhin A.I., Korzhuev M.A. (1991). Phase diagram of Bi-Se system in region of Bi_2Se_3 compound. *Izv. Academy of Sciences of the USSR. Inorg. Mater,* 27, 1190-1193.
5. Abrikosov N.Kh, Bankina V.F., Poretskaya L.V., Skudnova E.V., Shelimova L.E. (1967). *Semiconductor compounds, their preparation and properties*. Moscow: Nauka [in Russian].
6. Dumon A., Lichanot A., Gromb S. (1973). Properties electroniques du seleniure de bismuth Bi_2Se_3 fritte: domaine d'existence, *J. Chim. Phys. et Phys.-Chim. Biol*., 70 (10), 1546-1554.
7. Abrikosov N.Kh., Bankina V.F., Kharitonovich K.F. (1960). Investigation of the phase diagram of Bi-Se. Russ. *J. Inorg. Chem*. 5, 2011-2016 [in Russian].
8. Sher A.A., Odin I.N., Novoselova A.V. (1986). Study of phases in the Bi-Se system. *Russ. J. Inorg. Chem*. 31, 764-767 [in Russian].
9. Okamoto H. (1994). The Bi-Se (Bismuth-Selenium) system. *J. Phase Equlibria*, 15 (2), 195-201.
10. Zhang J.-M., Ming W., Huang Z., Liu G.-B., Kou X., Fan Y., Wang K.L., Yao Y. (2013). Stability, electronic, and magnetic properties of the magnetically doped topological insulators Bi_2Se_3, Bi_2Te_3, and Sb_2Te_3. *Phys. Rev. B*, 88, 235131-1-9.
11. Hsieh D., Xia Y., Qian D., Wray L., Dil J.H., Meier F., Osterwalder J., Patthey L., Checkelsky J.G., Ong N.P., Fedorov A.V., Lin H., Bansil A., Grauer D., Hor Y.S., Cava R.J., Hasan M.Z. (2009). A tunable topological insulator in the spin helical Dirac transport regime. *Nature*, 460, 1101-1105.
12. Hor Y.S., Richardella A., Roushan P., Xia Y., Checkelsky J.G., Yazdami A., Hasan M.Z., Ong N.P., Cava R.J. (2009). *p*-type Bi_2Se_3 for topological insulator and low-temperature thermoelectric applications. *Phys. Rev. B*, 79, 195208-1-5.
13. Wang Z., Lin T., Wei P., Liu X., Dumas R., Liu K., Shi J. (2010). Tuning carrier type and density in Bi_2Se_3 by Ca-doping. *Appl. Phys. Lett*., 97, 042112-1-3.
14. Urazhdin S., Bilc D., Mahanti S.D., Tessmer S.H., Kyratsi T., Kanatzidis M.G. (2004). Surface effects in layered semiconductors Bi_2Se_3 and Bi_2Te_3. *Phys. Rev. B*, 69, 085313-1-7.
15. Gobrecht H., Boeters K.E., Pantzer G. (1964). Über Kristallstruktur und elektrische Eigenschaften der Wismutselenide Bi_2Se_2 und Bi_2Se_3. *Z. Phys*. 177 (1), 68-83.
16. Hyde G.R., Beale H.A., Spain I.L., Woollam J.A. (1974). Electronic properties of Bi_2Se_3 crystals. *J. Phys. Chem. Solids*, 35, 1719-1728.
17. Navratil J., Horak J., Plechacek T., Kamba S., Lostak P., Dyck J.S., Chen W., Uher C. (2004). Conduction band splitting and transport properties of Bi_2Se_3. *J. Solid State Chem*., 177, 1704-1712.
18. Zhang H., Liu C.-X., Qi X.-L., Dai X., Fang Z., Zhang S.-C. (2009). Topological insulators in Bi_2Se_3, Bi_2Te_3 and Sb_2Te_3 with a single Dirac cone on the surface. *Nature Physics*, 5, 438-442.
19. Oleshko E.V., Korolyshin V.N. (1985). Quasi-relativistic band spectrum of bismuth selenide. *Sov. Phys. Semicond*., 19 (10), 1839-1841 [in Russian].
20. Kulbachinskii V.A., Miura N., H. Nakagawa, Arimoto H., Ikaida T., Lostak P., Drasar C.(1999).

Conduction-band structure of $Bi_{2-x}Sb_xSe_3$ mixed crystals by Shubnikov–de Haas and cyclotron resonance measurements in high magnetic fields. *Phys. Rev. B*, 59 (24), 15733-15739.

21. Kulbachinskii V.A., Miura N., Arimoto H., Ikaida T., Lostak P., Horak H., Drasar C. (1999). Cyclotron resonance in high magnetic fields in Bi_2Se_3, Bi_2Te_3 and Sb_2Te_3 based crystals. *J. Phys. Soc. Jpn*., 68, 3328-3333.
22. Bogatyrev I.F., Vasko A., Tichy L., Horak J. (1974). Bi_2Se_3 crystals doped with halogen. *Phys. Stat. Sol. A*, 22, K63.
23. Wu K.K., Ramachandran B., Kuo Y.K., Sankar R., Chou F.C. (2016). Influence of induced defects on transport properties of the Bridgman grown Bi_2Se_3-based single crystals. *Journal of Alloys and Compounds*, 682, 225-231.
24. West D., Sun Y.Y., Wang H., Bang J., Zhang S.B. (2012). Native defects in second-generation topological insulators: effect of spin-orbit interaction on Bi_2Se_3. *Phys. Rev. B*, 86, 121201-1-4.
25. Horak J., Stary Z., Lostak P., Pancir J. (1990). Anti-site defects in *n*-Bi_2Se_3 crystals. *J. Phys. Chem. Solids*, 51, 12, 1353-1360.
26. Sklenar A., Drasar C., Krejcova A., Lostak P. (2000). Optical properties of $Bi_2Se_{3-x}As_x$ single crystals. *Cryst. Res. Technol*., 35, 1069.
27. Menshikova S.I., Rogacheva E.I. (2020). Effect of deviation from stoichiometry on transport and mechanical properties of Bi_2Se_3 polycrystals. *Low Temperature Physics* (accepted).
28. Navratil J., Plechacek T., Horak J., Karamazov S., Lostak P., Dyck J.S., W Chen., Uher C.(2001). Transport properties of $Bi_{2-x}In_xSe_3$ single crystals. *Journal of Solid State Chemistry*, 160, 474-481.
29. Kulbachinskii V.A., Kytin V.G., Kudryashov A.A., Tarasov P.M. (2012). Thermoelectric properties of Bi_2Te_3, Sb_2Te_3 and Bi_2Se_3 single crystals with magnetic impurities. *J. Solid State Chem*., 193, 47–52.
30. Wang S., Sun Y., Yang J., Duan B., Wu L., Zhang W., Yang J. (2016). High thermoelectric performance in Te-free $(Bi,Sb)_2Se_3$ by structural transition induced band convergence and chemical bond softening. *Energy & Environmental Science*, 00, 1-3.
31. Kang Y., Zhang Q., Fan C., Hu W., Chen C., Zhang L., Yu F., Tian Y., Xu B. (2017). High pressure synthesis and thermoelectric properties of polycrystalline Bi_2Se_3. *Journal of Alloys and Compounds*, 700, 223-227.
32. Liu R., Tan X., Ren G., Liu Y., Zhou Z., Liu C., Lin Y., Nan C. (2017). Enhanced thermoelectric performance of Te-doped $Bi_2Se_{3-x}Te_x$ bulks by self- propagating high-temperature synthesis. *Crystals*, 7, 257-1-8.
33. Liu W., Lukas K.C., McEnaney K., Lee S., Zhang Q., Opeil C.P., Chen G., Z. Ren (2013). Studies on the Bi_2Te_3–Bi_2Se_3–Bi_2S_3 system for mid-temperature thermoelectric energy conversion. *Energy Environ. Sci.*, 6, 552-560.

Submitted 07.07.2020

Меньшикова С.І., *канд. фіз.-мат. наук*
Рогачова Е.І., *докт. фіз.-мат. наук, професор*

Національний Технічний університет
"Харківський Політехнічний Інститут"
вул. Кирпичова, 2, м. Харків, 61002, Україна

ВПЛИВ ВІДХИЛЕННЯ ВІД СТЕХІОМЕТРІЇ НА ТЕПЛОПРОВІДНІСТЬ ПОЛІКРИСТАЛІВ Bi_2Se_3

Отримано залежності електронної та граткової теплопровідності від складу (59.9 - 60.0 ат. % Se) полікристалів Bi_2Se_3 після довготривалого відпалу за температури 650 К. Виявлено немонотонний характер цих залежностей, який пояснюється зміною у фазовому складі та дефектній структурі при відхиленні від стехіометрії. Зроблено оцінку меж області гомогенності Bi_2Se_3. Результати даної роботи підтверджують результати, які були отримані нами раніше при дослідженні впливу відхилення від стехіометрії (59.9 - 60.0 at. % Se) на електропровідність, коефіцієнт Холла, коефіцієнт Зеєбека та мікротвердість полікристалів Bi_2Se_3 після аналогічної технології приготування. Бібл. 33, рис. 3.
Ключові слова: селенід вісмуту, стехіометрія, концентрація, дефектна структура, теплопровідність

Меньшикова С.И., *канд. физ.-мат. наук*
Рогачова Е.И., *докт. физ.-мат. наук, професор*

Национальный технический университет
"Харьковский политехнический институт"
ул. Кирпичева, 2, г. Харьков, 61002, Украина

ВЛИЯНИЕ ОТКЛОНЕНИЯ ОТ СТЕХИОМЕТРИИ НА ТЕПЛОПРОВОДНОСТЬ ПОЛИКРИСТАЛЛОВ Bi_2Se_3

Получены зависимости электронной и решеточной теплопроводности от состава (59.9 - 60.0 ат.% Se) поликристаллов Bi_2Se_3 после длительного отжига при температуре 650 К. Обнаружен немонотонный характер этих зависимостей, который объясняется изменением в фазовом составе и дефектной структуре при отклонении от стехиометрии. Произведена оценка границ области гомогенности Bi_2Se_3. Результаты данной работы подтверждают результаты, полученные нами ранее при исследовании влияния отклонения от стехиометрии (59.9 - 60.0 at.% Se) на электропроводность, коэффициент Холла, коэффициент Зеебека и микротвердость поликристаллов Bi_2Se_3, изготовленных по аналогичной технологии. Библ. 33, рис. 3.
Ключевые слова: селенид висмута, стехиометрия, концентрация, дефектная структура, теплопроводность

References

1. Rowe D.M. (1995). *CRC Handbook of Thermoelectrics*. Boca Raton, London, New York, Washington: CRC Press.
2. Xia Y., Qian D., Hsien D., Wray L., Pai A., Bansil A., Grauer D., Hor Y.S., Cava R.J., Hasan M.Z.(2009). Observation of a large-gap topological-insulator class with a single Dirac cone on the surface. *Nature Physics*, 5, 398 – 402.
3. Chizhevskaya S.N., Shelimova L.E., Zaitseva I.A. (1994). Critical evaluation and coordination of Bi-Se phase diagram data. *Inorg. Mater*, 30, 1289-1387.
4. Poretskaya L.V., Anukhin A.I., Korzhuev M.A. (1991). Phase diagram of Bi-Se system in region of Bi_2Se_3 compound. *Izv. Academy of Sciences of the USSR*. *Inorg. Mater,* 27, 1190-1193.
5. Abrikosov N.Kh, Bankina V.F., Poretskaya L.V., Skudnova E.V., Shelimova L.E. (1967). *Semiconductor compounds, their preparation and properties*. Moscow: Nauka [in Russian].
6. Dumon A., Lichanot A., Gromb S. (1973). Properties electroniques du seleniure de bismuth Bi_2Se_3 fritte: domaine d'existence, *J. Chim. Phys. et Phys.-Chim. Biol*., 70 (10), 1546-1554.
7. Abrikosov N.Kh., Bankina V.F., Kharitonovich K.F. (1960). Investigation of the phase diagram of Bi-Se. Russ. *J. Inorg. Chem*. 5, 2011-2016 [in Russian].
8. Sher A.A., Odin I.N., Novoselova A.V. (1986). Study of phases in the Bi-Se system. *Russ. J. Inorg. Chem*. 31, 764-767 [in Russian].
9. Okamoto H. (1994). The Bi-Se (Bismuth-Selenium) system. *J. Phase Equlibria*, 15 (2), 195-201.
10. Zhang J.-M., Ming W., Huang Z., Liu G.-B., Kou X., Fan Y., Wang K.L., Yao Y. (2013). Stability, electronic, and magnetic properties of the magnetically doped topological insulators Bi_2Se_3, Bi_2Te_3, and Sb_2Te_3. *Phys. Rev. B*, 88, 235131-1-9.
11. Hsieh D., Xia Y., Qian D., Wray L., Dil J.H., Meier F., Osterwalder J., Patthey L., Checkelsky J.G., Ong N.P., Fedorov A.V., Lin H., Bansil A., Grauer D., Hor Y.S., Cava R.J., Hasan M.Z. (2009). A tunable topological insulator in the spin helical Dirac transport regime. *Nature*, 460, 1101-1105.
12. Hor Y.S., Richardella A., Roushan P., Xia Y., Checkelsky J.G., Yazdami A., Hasan M.Z., Ong N.P., Cava R.J. (2009). *p*-type Bi_2Se_3 for topological insulator and low-temperature thermoelectric applications. *Phys. Rev. B*, 79, 195208-1-5.
13. Wang Z., Lin T., Wei P., Liu X., Dumas R., Liu K., Shi J. (2010). Tuning carrier type and density in Bi_2Se_3 by Ca-doping. *Appl. Phys. Lett*., 97, 042112-1-3.
14. Urazhdin S., Bilc D., Mahanti S.D., Tessmer S.H., Kyratsi T., Kanatzidis M.G. (2004). Surface effects in layered semiconductors Bi_2Se_3 and Bi_2Te_3. *Phys. Rev. B*, 69, 085313-1-7.
15. Gobrecht H., Boeters K.E., Pantzer G. (1964). Über Kristallstruktur und elektrische Eigenschaften der Wismutselenide Bi_2Se_2 und Bi_2Se_3. *Z. Phys*. 177 (1), 68-83.
16. Hyde G.R., Beale H.A., Spain I.L., Woollam J.A. (1974). Electronic properties of Bi_2Se_3 crystals. *J. Phys. Chem. Solids*, 35, 1719-1728.
17. Navratil J., Horak J., Plechacek T., Kamba S., Lostak P., Dyck J.S., Chen W., Uher C. (2004). Conduction band splitting and transport properties of Bi_2Se_3. *J. Solid State Chem*., 177, 1704-1712.
18. Zhang H., Liu C.-X., Qi X.-L., Dai X., Fang Z., Zhang S.-C. (2009). Topological insulators in Bi_2Se_3, Bi_2Te_3 and Sb_2Te_3 with a single Dirac cone on the surface. *Nature Physics*, 5, 438-442.
19. Oleshko E.V., Korolyshin V.N. (1985). Quasi-relativistic band spectrum of bismuth selenide. *Sov. Phys. Semicond*., 19 (10), 1839-1841 [in Russian].
20. Kulbachinskii V.A., Miura N., H. Nakagawa, Arimoto H., Ikaida T., Lostak P., Drasar C.(1999).

Conduction-band structure of $Bi_{2-x}Sb_xSe_3$ mixed crystals by Shubnikov–de Haas and cyclotron resonance measurements in high magnetic fields. *Phys. Rev. B*, 59 (24), 15733-15739.

21. Kulbachinskii V.A., Miura N., Arimoto H., Ikaida T., Lostak P., Horak H., Drasar C. (1999). Cyclotron resonance in high magnetic fields in Bi_2Se_3, Bi_2Te_3 and Sb_2Te_3 based crystals. *J. Phys. Soc. Jpn*., 68, 3328-3333.
22. Bogatyrev I.F., Vasko A., Tichy L., Horak J. (1974). Bi_2Se_3 crystals doped with halogen. *Phys. Stat. Sol. A*, 22, K63.
23. Wu K.K., Ramachandran B., Kuo Y.K., Sankar R., Chou F.C. (2016). Influence of induced defects on transport properties of the Bridgman grown Bi_2Se_3-based single crystals. *Journal of Alloys and Compounds*, 682, 225-231.
24. West D., Sun Y.Y., Wang H., Bang J., Zhang S.B. (2012). Native defects in second-generation topological insulators: effect of spin-orbit interaction on Bi_2Se_3. *Phys. Rev. B*, 86, 121201-1-4.
25. Horak J., Stary Z., Lostak P., Pancir J. (1990). Anti-site defects in *n*-Bi_2Se_3 crystals. *J. Phys. Chem. Solids*, 51, 12, 1353-1360.
26. Sklenar A., Drasar C., Krejcova A., Lostak P. (2000). Optical properties of $Bi_2Se_{3-x}As_x$ single crystals. *Cryst. Res. Technol*., 35, 1069.
27. Menshikova S.I., Rogacheva E.I. (2020). Effect of deviation from stoichiometry on transport and mechanical properties of Bi_2Se_3 polycrystals. *Low Temperature Physics* (accepted).
28. Navratil J., Plechacek T., Horak J., Karamazov S., Lostak P., Dyck J.S., W Chen., Uher C.(2001). Transport properties of $Bi_{2-x}In_xSe_3$ single crystals. *Journal of Solid State Chemistry*, 160, 474-481.
29. Kulbachinskii V.A., Kytin V.G., Kudryashov A.A., Tarasov P.M. (2012). Thermoelectric properties of Bi_2Te_3, Sb_2Te_3 and Bi_2Se_3 single crystals with magnetic impurities. *J. Solid State Chem*., 193, 47–52.
30. Wang S., Sun Y., Yang J., Duan B., Wu L., Zhang W., Yang J. (2016). High thermoelectric performance in Te-free $(Bi,Sb)_2Se_3$ by structural transition induced band convergence and chemical bond softening. *Energy & Environmental Science*, 00, 1-3.
31. Kang Y., Zhang Q., Fan C., Hu W., Chen C., Zhang L., Yu F., Tian Y., Xu B. (2017). High pressure synthesis and thermoelectric properties of polycrystalline Bi_2Se_3. *Journal of Alloys and Compounds*, 700, 223-227.
32. Liu R., Tan X., Ren G., Liu Y., Zhou Z., Liu C., Lin Y., Nan C. (2017). Enhanced thermoelectric performance of Te-doped $Bi_2Se_{3-x}Te_x$ bulks by self- propagating high-temperature synthesis. *Crystals*, 7, 257-1-8.
33. Liu W., Lukas K.C., McEnaney K., Lee S., Zhang Q., Opeil C.P., Chen G., Z. Ren (2013). Studies on the Bi_2Te_3–Bi_2Se_3–Bi_2S_3 system for mid-temperature thermoelectric energy conversion. *Energy Environ. Sci.*, 6, 552-560.

Submitted 07.07.2020

Anatychuk L.I. *acad. NAN Ucraine*[1,2]
Kobylianskyi R.R. *cand. phys.– math sciences*[1,2]
Fedoriv R.V.[1,2]

[1]Institute of Thermoelectricity of the NAS and MES
of Ukraine, Chernivtsi, Ukraine
[2]Yuriy Fedkovych Chernivtsi National
University, Chernivtsi, Ukraine

COMPUTER SIMULATIONOF CYCLIC TEMPERATURE EFFECT ON THE ONCOLOGICAL NEOPLASM OF THE HUMAN SKIN

The paper presents the results of computer simulation of the temperature effect on the tumor of the human skin in a dynamic mode. The physical, mathematical and computer models of the human skin with oncological neoplasm (melanoma) were built with regard to thermophysical processes, blood circulation, heat exchange, metabolic processes and phase transition. As an example, the case is considered when a work tool is located on the tumor surface, the temperature of which changes cyclically according to a predetermined law in the temperature range [-50 ÷ +50] °C. Temperature distributions in the tumor and various layers of human skin in the cooling and heating modes have been determined. The results obtained make it possible to predict the depth of freezing and heating of biological tissue, in particular a tumor, at a given temperature effect. Bibl. 59, Fig. 6, Tabl. 2.

Keywords: temperature effect, human skin, tumor, melanoma, dynamic mode, computer simulation.

Introduction

Cryodestruction [4 5, 8 27] and hyperthermia [28 32] of biological tissue are increasingly used to neutralize malignant and benign oncological neoplasms of the human skin [1 7]. When performing such procedures, it is important to control the temperature in the tumor, but there are still no tools to determine the temperature in the tumor during cryodestruction and hyperthermia. Thus, during the above procedures, the temperature in the tumor remains unknown, and, therefore, the destruction of oncological neoplasm remains an open question.

One of the methods for determining the temperature in a tumor with a given cyclic change in the temperature of the work tool is computer simulation [33 – 35]. However, in the computer models used so far, blood circulation, heat exchange, metabolic processes and other thermophysical processes are taken into account, but the phase transition in biological tissue is disregarded [36 38].

Therefore, *the purpose of this work* is computer simulation to determine the temperature in the tumor, taking into account the phase transitions.

Physical model

A physical model (Fig. 1) of the area of biological tissue of human skin is a structure of three skin layers (epidermis 1, dermis 2, subcutaneous layer 3), inner biological tissue 4 and tumor 5 which is characterized by thermophysical properties [33-35, 39-43], such as thermal conductivity κ_i, specific

heat C_i, density ρ_i, blood perfusion rate ω_{bi}, blood density ρ_b, blood temperature T_b, blood heat capacity C_b and specific heat release Q_{meti} due to metabolic processes and latent heat of phase transition L. The thermophysical properties of biological tissue of the skin and tumor in the normal [44-49] and frozen states [50, 51] are given in Tables 1, 2. In this paper, we use a 2D model with axial symmetry, because the proposed physical model is symmetric about the y-axis. Also, such a model allows increasing the speed of calculations without loss of accuracy [33-35, 39 – 43].

The corresponding layers of biological tissue 1-5 are considered as bulk heat sources q_i, where:

$$q_i = Q_{met\,i} + \rho_b \cdot C_b \cdot \omega_{bi} \cdot (T_b - T), \quad i = 1..5\,. \tag{1}$$

The geometric dimensions of each skin layer 1-4 are a_i, b_i, and of tumor (melanoma) are as follows: thickness b_5 and radius n. The skin surface accommodates a work tool 6 with thickness d and radius c. The temperatures at the boundaries of respective layers 1-5 and work tool 6 are T_1, T_2, T_3, T_4, T_5, T_6, T_7. The temperature inside biological tissue is T_1. The ambient temperature is T_9. The surface of the human skin with temperature T_5 is in the state of heat exchange with the environment (heat transfer coefficient α and radiation coefficient ε) at temperature T_9. The lateral surface of the skin is adiabatically insulated.

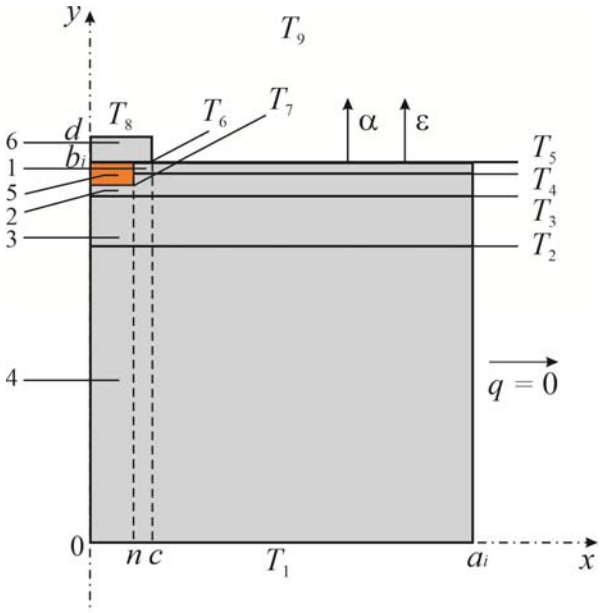

Fig.1. Physical 2D model of the human skin with a tumor: 1 – epidermis, 2 – dermis, 3 – subcutaneous layer, 4 – inner biological tissue, 5 – tumor (melanoma), 6 – work tool

Mathematical description

In the general form, the equation of heat exchange in biological tissue is as follows [52]:

$$C_i \cdot \frac{\partial T}{\partial t} = \nabla \cdot (\kappa_i \cdot \nabla T) + \rho_b \cdot C_b \cdot \omega_{bi} \cdot (T_b - T) + Q_{meti}, \quad i = 1..5\,, \tag{2}$$

where C_i, κ_i is specific heat and thermal conductivity of the respective skin layers and tumor, ρ_b is blood density, C_b is blood specific heat, ω_{bi} is blood perfusion of respective layers, T_b is blood temperature, T is temperature of biological tissue; Q_{meti} is heat released due to metabolic

processes in each layer.

The term on the left side of equation (2) is the rate of change of thermal energy contained in a unit volume of biological tissue. The three terms on the right part of this equation represent, respectively, the rate of change of thermal energy due to thermal conductivity, blood perfusion and metabolic heat.

Heat transfer equation in biological tissue (2) is solved with the corresponding boundary conditions. The temperature on the surface of work tool changes by the given dependence in the temperature range $T_8 = [-50 \div +50]$ °C. The temperature inside biological tissue is $T_1 = +37$°C. The lateral surfaces of biological tissue are adiabatically insulated (q = 0), and the upper surface of the skin is in a state of heat exchange (heat transfer coefficient α and radiation coefficient ε) with the environment at temperature T_9.

$$q_i(x,y,t)\Big|_{\substack{c\le x\le a\\ y=h_i}} = \alpha\cdot(T_9 - T_5) + \varepsilon\cdot\sigma\cdot(T_9^4 - T_5^4)\,, \tag{3}$$

where $q_i(x,y,t)$ is heat flux density of the i-th layer of the skin and tumor, α is coefficient of convective heat exchange of the skin surface with the environment, ε is radiation coefficient, σ is the Boltzmann constant, T_5 is surface temperature of the human skin, T_9 is ambient temperature (T_9=+22 °C).

At the initial moment of time t = 0 s, it is considered that the temperature in the entire volume of the skin is $T = T_b = +37$°C, that is, the initial conditions for solving equation (2) are as follows:

$$T_i(x,y,0) = T, \qquad i = 1..5. \tag{4}$$

As a result of solving the initial boundary value problem (2) - (4), the distributions of temperature $T_i(x,y,t)$ and heat fluxes $q_i(x,y,t)$ in the corresponding layers of the skin and tumor at any time are determined.

During the freezing process, a phase change will occur in the cells at the freezing point, while there will be a loss of phase transition heat (L) and the temperature in these cells will not change. The phase transition in biological cells occurs in the temperature range (-1 ÷ -8) ° C. In the temperature range (-1 ÷ -8) ° C, when the cells are frozen, the heat of the phase transition is absorbed which in this work is simulated by adding the corresponding value of L to the heat capacity C [50, 51].

Freezing of the human skin causes vasoconstriction and freezing of blood, therefore the value of blood perfusion ω_{bi} tends to zero. In addition, cells will not be able to generate metabolic heat when frozen, and metabolic heat Q_{meti} will be zero at temperatures below zero.

In the frozen state, the properties of biological tissue of the skin will have the following values (5)-(8), where i = 1..4:

$$C_i = \begin{cases} C_{i(1)} & T \ge -1°C \\ \dfrac{L}{-1-(-8)} + \dfrac{C_{i(1)} + C_{i(2)}}{2} & -8°C \le T \le -1°C\,, \\ C_{i(2)} & T \le -8°C \end{cases} \tag{5}$$

$$\kappa_i = \begin{cases} \kappa_{i(1)} & T \ge -1°C \\ \dfrac{\kappa_{i(1)} + \kappa_{i(2)}}{2} & -8°C \le T \le -1°C\,, \\ \kappa_{i(2)} & T \le -8°C \end{cases} \tag{6}$$

$$Q_{met_i} = \begin{cases} Q_{met(i)} & T \geq -1°C \\ 0 & -8°C \leq T \leq -1°C \\ 0 & T \leq -8°C \end{cases}, \quad (7)$$

$$\omega_{b_i} = \begin{cases} \omega_{b(i)} & T \geq -1°C \\ 0 & -8°C \leq T \leq -1°C \\ 0 & T \leq -8°C \end{cases}. \quad (8)$$

Accordingly, the properties of tumor in the frozen state will have the following values (9)-(12):

$$C_5 = \begin{cases} C_{5(1)} & T \geq -1°C \\ \dfrac{L}{-1-(-8)} + \dfrac{C_{5(1)} + C_{5(2)}}{2} & -8°C \leq T \leq -1°C \\ C_{5(2)} & T \leq -8°C \end{cases}, \quad (9)$$

$$\kappa_5 = \begin{cases} \kappa_{5(1)} & T \geq -1°C \\ \dfrac{\kappa_{5(1)} + \kappa_{5(2)}}{2} & -8°C \leq T \leq -1°C \\ \kappa_{5(2)} & T \leq -8°C \end{cases}, \quad (10)$$

$$Q_{met_5} = \begin{cases} Q_{met(5)} & T \geq -1°C \\ 0 & -8°C \leq T \leq -1°C \\ 0 & T \leq -8°C \end{cases}, \quad (11)$$

$$\omega_{b_5} = \begin{cases} \omega_{b(5)} & T \geq -1°C \\ 0 & -8°C \leq T \leq -1°C \\ 0 & T \leq -8°C \end{cases}. \quad (12)$$

Computer simulation example

To create a computer model, as an example, we used the following geometric dimensions of the skin – the thickness of epidermis b_1=0.08 mm, dermis b_2=2 mm, subcutaneous layer b_3=10 mm, inner tissue b_4=30 mm, radius a_i=20 mm (i=1..4) and tumor (melanoma) – thickness b_5 = 1 mm and radius n = 2 mm [53, 54]. The surface of the skin accommodates a work tool 6, which is a copper probe in the form of a round disc. Its geometrical dimensions are as follows: thickness d = 1 mm and radius c = 3 mm. This model does not take into account the thermal contact resistance between the work tool and the human skin, since it is estimated to be insignificant and makes $R_c = 2 \cdot 10^{-3}$ m^2·K/W [55]. The temperature inside the biological tissue is T_1 = +37°C. The ambient temperature is T_9 = +22 °C. As an example, this paper considers the case when the temperature of the work tool varies according to a given dependence in the temperature range of T_8 = [-50 ÷ +50] °C. However, it is noteworthy that the developed computer model makes it possible to consider the cases when the temperature of work tool $T_f(t)$ varies in any temperature range or according to any predetermined function. The thermophysical properties of biological tissue of the human skin and tissue in the normal and frozen states are given in Tables 1, 2 [44 – 49].

Table 1.

Thermophysical properties of biological tissue of the human skin and tumor in the normal state [44 – 49]

Layers of biological tissue	Epidermis	Dermis	Subcutaneous layer	Internal tissue	Tumor (melanoma)
Specific heat, C ($J \cdot kg^{-1} \cdot K^{-1}$)	3590	3300	2500	4000	3852
Thermal conductivity, κ ($W \cdot m^{-1} \cdot K^{-1}$)	0.24	0.45	0.19	0.5	0.558
Density, ρ ($kg \cdot m^{-3}$)	1200	1200	1000	1000	1030
Metabolism, Q_{met} (W/m^3)	368	368	368	368	3680
Blood perfusion rate, ω_b ($ml/s \cdot ml$)	0	0.0005	0.0005	0.0005	0.0063
Blood density, ρ_b ($kg \cdot m^{-3}$)	1060	1060	1060	1060	1060
Blood heat capacity, C_b ($J \cdot kg^{-1} \cdot K^{-1}$)	3770	3770	3770	3770	3770

Table 2

Thermophysical properties of biological tissue of the human skin in the frozen state [50, 51]

Thermophysical properties of biological tissue	Value	Measurement units
Heat capacity of frozen biological tissue (C_2)	1800	J/m^3 °C
Thermal conductivity of frozen biological tissue (κ_2)	2	Wт/m °C
Latent heat of phase transition (L)	$250 \cdot 10^3$	J/m^3
Upper temperature of phase transition (T_1)	-1	°C
Lower temperature of phase transition (T_2)	-8	°C

Thus, a three-dimensional computer model of the human skin with oncological neoplasms (melanoma) was created. To construct a computer model, the Comsol Multiphysics software package was used [56], which makes it possible to simulate thermophysical processes in biological tissue, taking into account blood circulation, heat exchange, metabolic processes and phase transition.

The distribution of temperatures and heat flux densities in biological tissue was calculated by the finite element method, the essence of which is that the object under study is divided into a large number of finite elements and in each of them a function value is sought for that satisfies given second-order differential equations with the corresponding boundary conditions. The accuracy of solving the formulated problem depends on the level of partitioning and is ensured by the use of a large number of finite elements [56] and is T=±0.1 °C.

Computer simulation results

According to the known methods of cryodestruction and hyperthermia of biological tissue [11, 31, 57-59], the cooling rate should be at least (40-50) °C/min, and the heating rate (20-25) °C/min. Therefore, in this paper, as an example, we consider the case in which the temperature of the work tool $T_f(t)$ varies in the range [-50 ÷ +50] ° C as follows (Fig. 2, graph 1). First, cryodestruction of the tumor is carried out with a cooled work tool at a temperature of T=*-50°C* for t=30 s, then the temperature of the work tool changes from *-50°C* to *+50°C* for the next 240 s (note that in this case when the temperature changes, the freezing of the tumor continues to grow for a few more seconds), following which a heated work tool is used to conduct tumor hyperthermia at a temperature of T=*+50°C* for t=30 s. The subsequent decrease in temperature to T = - 50 °C occurs within 120 s, and then this temperature effect is repeated cyclically to achieve tumor destruction.

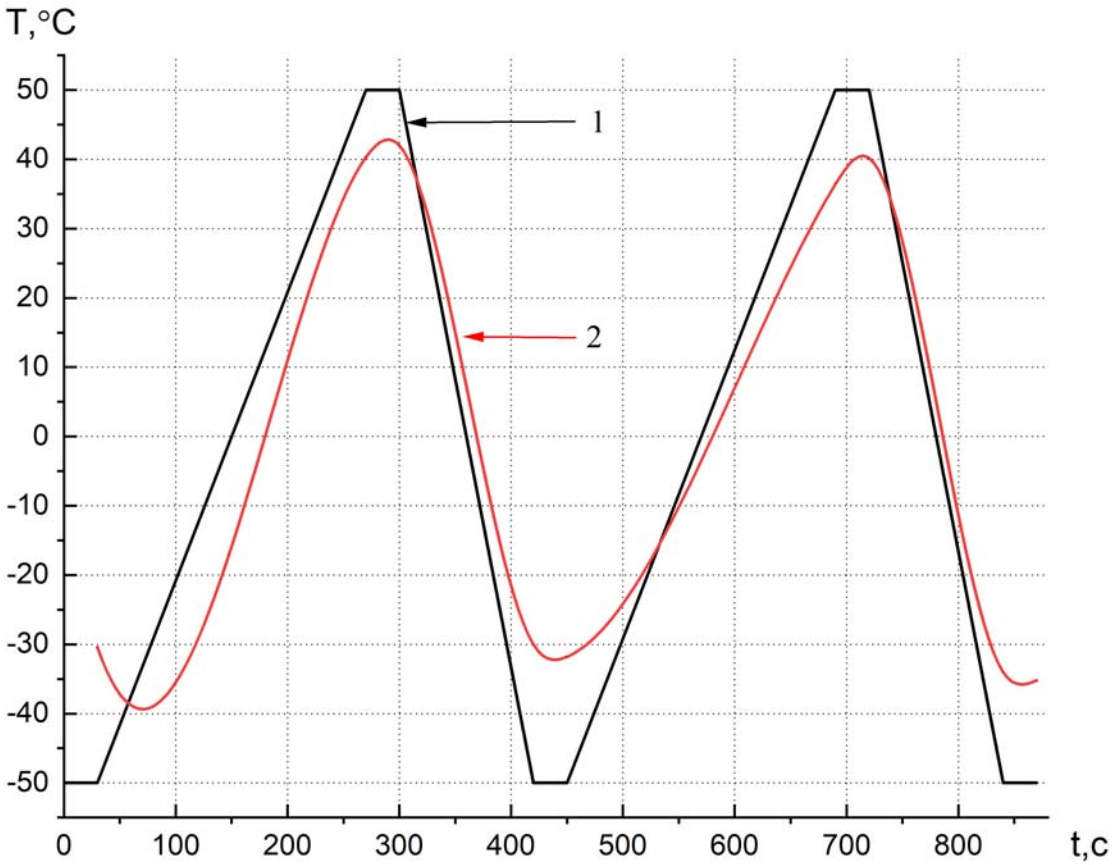

Fig.2. The plots of work tool temperature (1) and tumor temperature (2) versus time. The tumor temperature was taken at the depth of 1 mm from the skin surface along the Oy axis.

With the help of computer simulation, the temperature distribution in the tumor was determined at different points in time with the corresponding specified cyclic change in the temperature of the work tool. The results of computer simulation, namely the temperature in the tumor at a depth of 1 mm from the skin surface on the Oy axis, are shown in plot 2, Fig.2.

Figs.3-6 show the temperature distributions in the cross-section of the skin with the tumor the surface of which accommodates a work tool the temperature of which changes cyclically according to the above dependence in the temperature range of [-50 ÷ +50]°C.

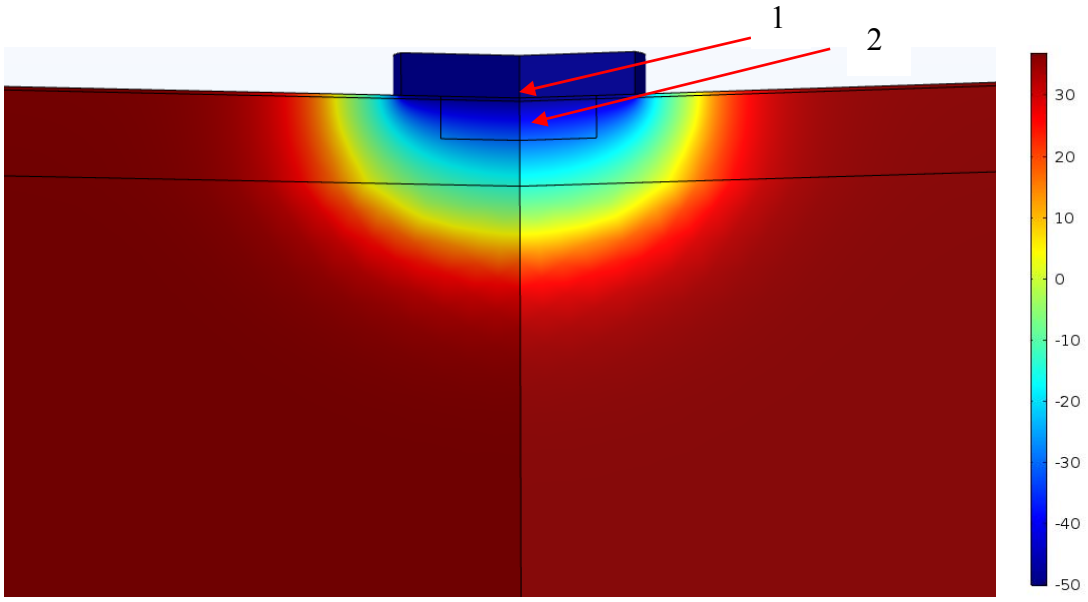

Fig.3. Distribution of temperature in the cross-section of the skin with a tumor the surface of which accommodates a work tool at a temperature of T=50°C at point of time t=30 s

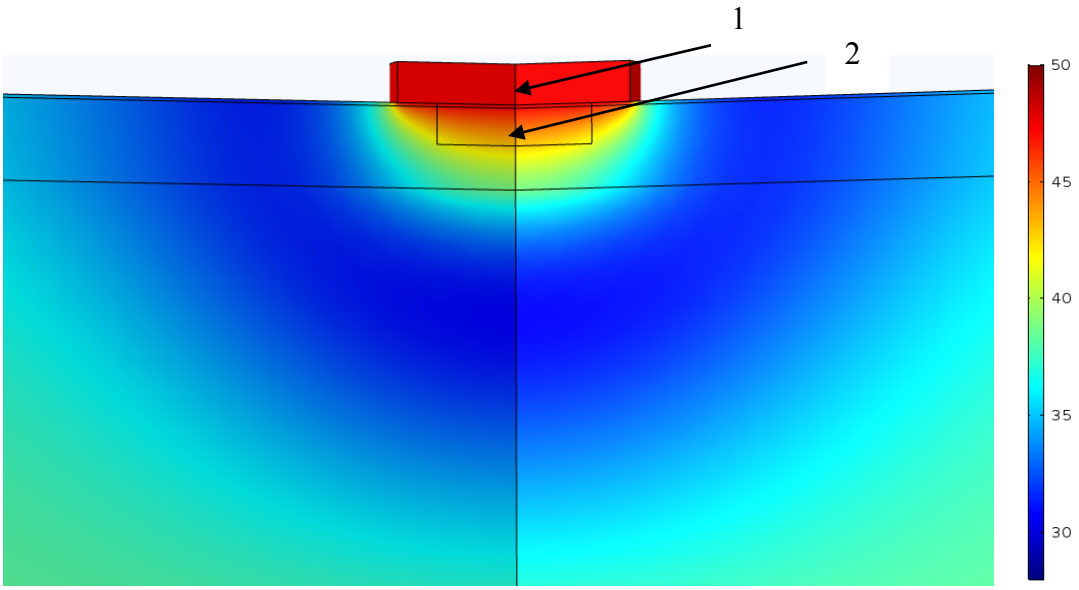

Fig.4. Distribution of temperature in the cross-section of the skin with a tumor the surface of which accomodates a work tool at a temperature of T=+50°C at point of time t=300 s

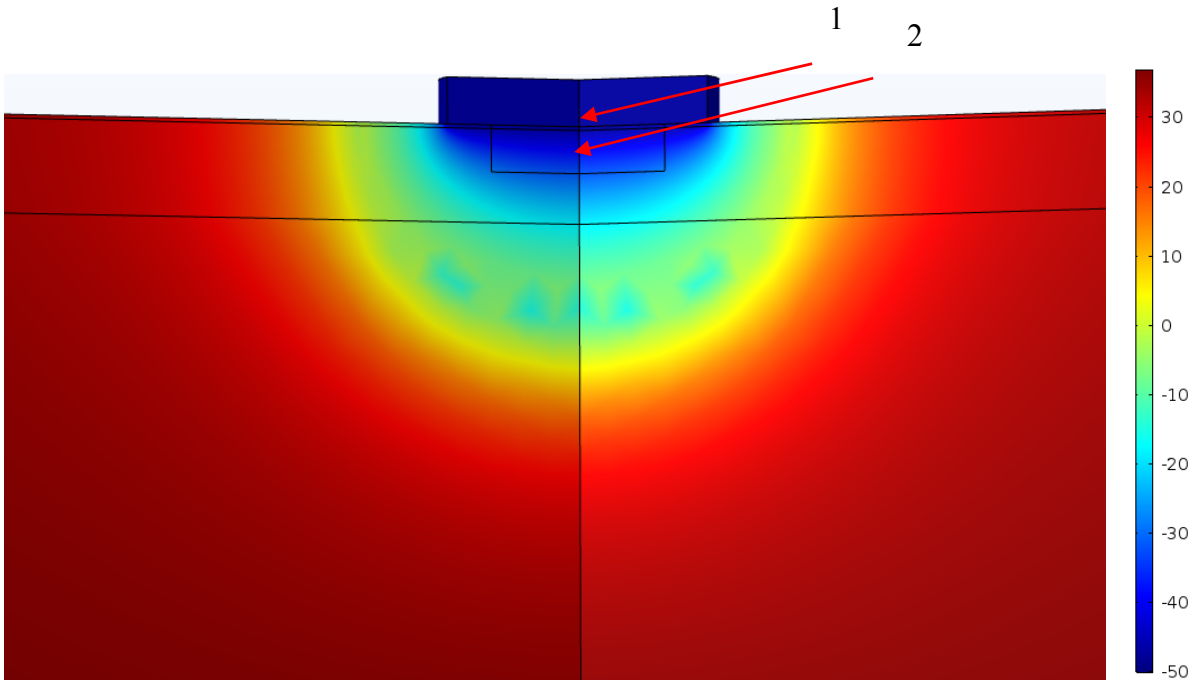

Fig.5. Distribution of temperature in the cross-section of the skin with a tumor the surface of which accommodates a work tool at a temperature of T=-50°C at point of time t=450 s

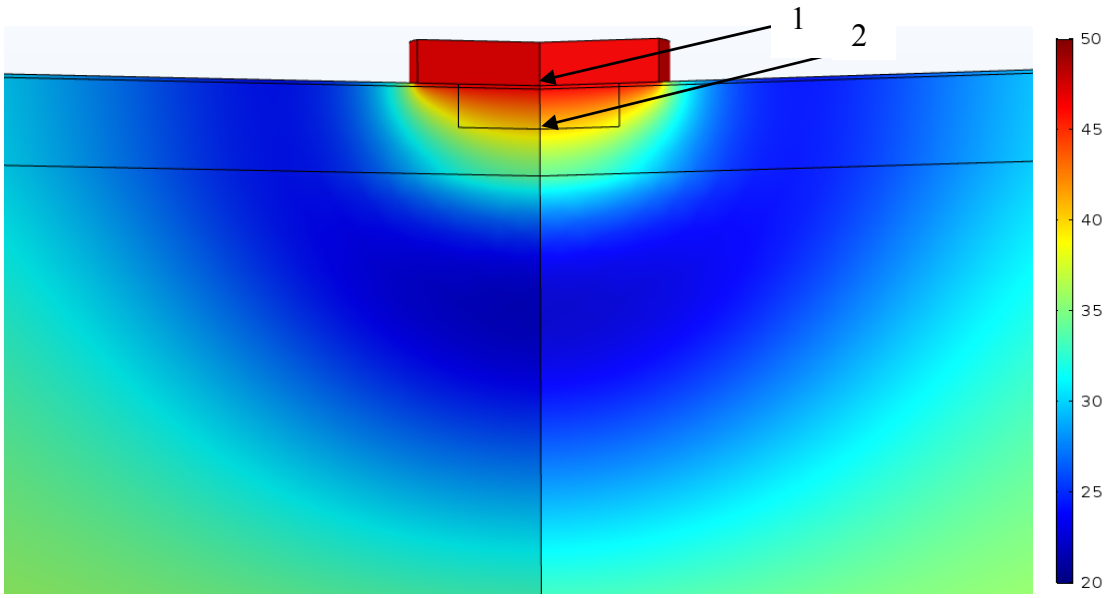

Fig.6. Distribution of temperature in the cross-section of the skin with a tumor the surface of which accommodates a work tool at a temperature of T=+50°C at point of time t=720 s

From Fig .3, 4 it is seen that at t = 30 s the skin tumor (melanoma) is cooled at point 1 to a temperature of -48.8 ° C, and at point 2 to -30.5 ° C (it should be noted that when changing temperature from -50 ° C to + 50 ° C freezing of the tumor at point 2 continues to increase to a temperature of T = -31.3 ° C for t = 4 s). And at t = 300 s the temperature at point 1 of the tumor rises to + 49.9 ° C, and at point 2 of the tumor the temperature is + 42.8 ° C. Since the tumor is in direct contact with the work tool, the

temperature at point 1 of the tumor will be close to the temperature of the work tool.

Subsequently, with repeated cyclic temperature exposure (Figs. 5, 6), it is observed that at t = 450 s after cooling, the temperature at point 1 of the tumor reaches 49.4 ° C, at point 2 of the tumor the temperature is -32.3 ° C. At t = 720 s, the temperature at point 1 of the tumor rises to + 48.6 ° C, and at point 2 of the tumor the temperature is + 40.1 ° C.

It is established that taking into account the phase transition increases the accuracy of determining the temperature in the tumor at ΔT = 6 ° C and the depth of freezing (heating) by Δh = 0.8 mm.

The obtained results make it possible to determine the depth of freezing and heating of the skin layers, in particular the tumor, at a given cyclic temperature effect to achieve maximum efficiency during cryodestruction and hyperthermia. The developed computer model in dynamic mode allows determining at any time the temperature distributions in different layers of the skin and tumor with a predetermined arbitrary function of temperature change of the work tool with time $T_f(t)$.

Conclusions

1. A computer model was developed to determine the temperature in the tumor, taking into account the phase transitions in the dynamic mode for any given cyclic change in the temperature of the work tool.
2. Using computer simulations, it was found that taking into account the phase transitions increases the accuracy of determining the temperature in the tumor by ΔT = 6 ° C and the depth of freezing (heating) by Δh = 0.8 mm.

References

1. Anatychuk L.I., Denisenko O.I., Kobylianskyi R.R., Kadeniuk T.Ya., Perepichka M.P. (2017). Suchasni metody krioterapii v dermatologichnii praktytsi [Modern cryotherapy methods in dermatological practice]. *Klinichna ta Eksperymentalna Patologiia*, XVI, 1(59), 150-156 [in Ukrainian].
2. Anatychuk L.I., Denisenko O.I., Kobylianskyi R.R., Kadenyuk T.Ya. (2015). On the use of thermoelectric cooling in dermatology and cosmetology. *J.Thermoelectricity*, 3, 57-71.
3. Kobylianskyi R.R., Kadenyuk T.Ya. (2016). Pro perspektyvy vykorystannia termoelektryky dlia likuvannia zakhvoriuvan' shkiry kholodom [On the prospects of using thermoelectricity for treatment of skin diseases with cold]. *Naukovy visnyk Chernivetskogo universitetu: zbirnyk naukovykh ptrats. Fizyka. Elektronika - Scientific Bulletin of Chernivtsi University: Collection of Scientific Papers. Physics. Electronics,* 5, 1, 67 – 72 [in Ukrainian].
4. Moskalyk I.A., Manyk O.M. (2013). On the use of thermoelectric cooling in cryodestruction practice. *J.Thermoelectricity*, 6, 84-92.
5. Moskalyk I.A. (2015) Pro vykorystannia termoelektrychnykh pryladiv u kriokhirurgii [On the use of thermoelectric devices in cryosurgery]. *Fizyka i khimiia tverdogo tila – Physics and Chemistry of Solid State*, 4, 742-746 [in Ukrainian].
6. Kobylianskyi R.R., Bezpalchuk O.O., Vyhonnyi V.Yu. (2018). Pro zastosuvannia termoelektrychnoho okholodzhennia u kosmetolohii [On the use of thermoelectric cooling in cosmetology]. *Fizyka i khimiia tverdogo tila – Physics and Chemistry of Solid State*, 19 (4), 340-344 (DOI: 10.15330/pcss.19.4.340-344).
7. Kobylianskyi R.R., Manyk O.M., Vyhonnyi V.Yu. (2018). On the use of thermoelectric cooling for cryodestruction in dermatology. *J.Thermoelectricity*, 6, 36-46.

8. Shakhov V.Yu., Kochenov V.I. et al. (1983). O naibolee ratsionalnykh metodikakh kriodestruktsii zlokachestvennykh novoobrazovanii [On the most rational methods for cryodestruction of malignant neoplasms]. *Voprosy onkologii- Problems in Oncology*, 9, 31-37 [in Russian].
9. Maruyama S., Nakagawa K., Takeda H. (2008). The flexible cryoprobe using Peltier effect for heat transfer control. *Journal of Biomechanical Science and Engineering*, 138-150.
10. Kochenov V.I. (2000). *Kriokhirurgicheskaia profilakticheskaia onkologiia [Cryosurgical preventive oncology]*. Niznii Novgorod [in Russian].
11. Kochenov V.I. (2003). *Kriologicheskaia profilakticheskaia onkologiia: kratkoie uchebnoie i metodicheskoie posobiie dlia vrachei i studentov [Cryological preventive oncology: a short educational and methodological guide for doctors and students]*. Organization Nizhnii Novgorod Regional Oncological Association of Disabled People (Ed). 2nd revised ed. Nizhnii Novgorod [in Russian].
12. Kochenov V.I., Korolev Yu.V. (2003). Prosteishiie krioinstrumenty dlia ambulatornoi praktiki vracha-kriologa [The simplest cryo-instruments for the outpatient practice of a cryologist]. *Meditsinskaia kriologiia – Medical Cryology*, 4, 157-160. Nizgnii Novgorod [in Russian].
13. Kochenov V.I. (1982). Adhesive effect in cryosurgery. *Abstract in the International Abstract Journal*, IV, 8.
14. Yiu W., Basco M.T., Aruny J.E., Sumpio B.E. (2007). Cryosurgery: A review. *Int. J. Angiol,* 16 (1),1-6.
15. Paches A.I., Shental V.V., Ptukha T.P., et al. (1978). *Kriogennyi metod lecheniia opukholei golovy i shei [Cryogenic treatment of head and neck tumors]*. Moscow: 1978 [in Russian].
16. Potapov I.I., et al. (1975). Kriokhirurgiia v otorinolaringologii [Cryosurgery in othorinolaryngology]. Moscow [in Russian].
17. Dragomiretskii V.D. (1987). Kriokhirurgicheskiie metody lecheniia zabolevanii ukha, gorla i nosa [Cryosurgical methods for the treatment of the diseases of ear, throat and nose]. *Prakticheskaia kriomeditsina [Practical cryomedicine]*. V.I.Grishchenko and B.P.Sandomirskii (Ed.). Kyiv: Zdorovia [in Russian].
18. Nikolaev N.I., Kochenov V.I., Tsybusov S.N., et al.(2003). Primenenie regenerativnykh effektov kriovozdeistviia v khirurgii i pri plastike barabannoi pereponki [Application of regenerative effects of cryotherapy in surgery and in the plastic of the tympanic membrane]. *Meditsinskaia kriologiia – Medical Cryology*, 4, 176-188. Nizgnii Novgorod [in Russian].
19. Alperovich B.I., Paramonova L.M., Merzlikin N.V. (1985). *Kriokhirurgiia pecheni i podzheludochnoi zhelezy [Cryosurgery of the liver and pancreas]*. Tomsk [in Russian].
20. Verkin B.I., Grishchenko V.I., Murinets-Markevich B.N., et al. (1978). Kriogennaia tekhnika v ginekologicheskoi practike [Cryogenic technique in gynecological practice]. *Meditsinskaia tekhnika – Biomedical Engineering*, 2, 28-32 [in Russian].
21. Grishchenko V.I. (1974). *Gipotermiia i kriokhirurgiia v akushersnve i ginekologii [Gipothermia and cryosurgery in obstetrics and gynecology]*. Moscow: Meditsina [in Russian].
22. Anatychuk L.I. (1979). *Termoelementy i termoelektricheskiie ustroistva: spravochnik [Thermoelements and thermoelectric devices: reference book]*. Kyiv: Naukova dumka [in Russian].
23. Kolenko E.A. (1967). *Termoelektricheskiie okhlazhdaiushchiie pribory [Thermoelectric cooling devices]*. 2nd ed. Leningrad: Nauka [in Russian].
24. Ismailov T.A. Sostoianiie i perspektivy razvitiia termoelektricheskogo priborostroieniia [The state and prospects of development of thermoelectric instrument making]. *Proc. of III All-Russian Scientific and Technical Conference* [in Russian].
25. Budrik V.V. (2010). *Physical fundamentals of cryomethods in medicine. Training Manual*. F.Lugnani (Ed.). L.N. Semenova (Russian transl.)
26. Cooper S.M. (2001). The history of cryosurgery. *J. R. Soc. Med*., 94, 196-201.

27. Whittaker D.K. (1984). Mechanisms of tissue destruction following cryosurgery. *Annals of the Royal College of Surgeons of England*, 66, 313-318.
28. Hypothermia — one of the promising cancer treatment technologies (2012). [Electronic resource]. Doctor.kz. Retrieved from: *http://www.doctor.kz/health/news/2012/03/21/13006.*
29. How can temperature help fight cancer [Electronic resource]. Oncology clinic "K-test". Retrieved from: *https://www.k-test.ru/index.php?rid=4.*
30. Perez C.A., Emami B.N., Nussbaum G. and Sapareto S. (1989). *Hyperthermia. Principles and practice of radiation oncology*.
31. Kandel E.I. (1974). *Kriokhirurgia [Cryosurgery*]. Moscow: Meditsina [in Russian].
32. Xu K.C., Korpar Nikolai, Niu L.Z. (2012). *Modern cryosurgery for cancer*. World Scientific Publisher.
33. Anatychuk L.I., Kobylianskyi R.R., Fedoriv R.V. (2019). Method for taking into account the phase transition in biological tissue during computer-aided simulation of cryodestruction process. *J.Thermoelectricity*, 1, 46-58.
34. Anatychuk L.I., Kobylianskyi R.R., Fedoriv R.V. (2019). Computer simulation of human skin cryodestruction process during thermoelectric cooling. *J.Thermoelectricity*, 2, 21-35.
35. Anatychuk L.I., Kobylianskyi R.R., Fedoriv R.V. (2020). Computer simulation of cyclic temperature effect on the human skin. *J. Thermoelectricity*, 3.
36. Andreozzi Assunta, Brunese Luca, Iasiello Marcello, Tucci Claudio, Vanoli Giuseppe Peter (2019). Modeling heat transfer in tumors: A review of thermal therapies. *Annals of Biomedical Engineering*, 47(3), 676–693. https://doi.org/10.1007/s10439-018-02177-x.
37. Bhowmik Arka, Repaka Ramjee (2016). Estimation of growth features and thermophysical properties of melanoma within 3-D human skin using genetic algorithm and simulated annealing. *International Journal of Heat and Mass Transfer, 98, 81-95. http://dx.doi.org/10.1016/j.ijheatmasstransfer.2016.03.020*.
38. Horsfield Michael, Sarkar Ritvik, Reffsin Sam, Seog Woo Jin (2015). A computer model for evaluating the efficiency of cryosurgery for prostate cancer.
39. Anatychuk L.I., Vikhor L.M., Kotsur M.P., Kobylianskyi R.R., Kadeniuk T.Ya. (2016). Optimal control of time dependence of cooling temperature in thermoelectric devices. *J.Thermoelectricity*, 5, 5-11.
40. Anatychuk L.I., Kobylianskyi R.R., Kadeniuk T.Ya. (2017). Computer simulation of local thermal effect on human skin. *J.Thermoelectricity*, 1, 69-79.
41. Anatychuk L.I., Vikhor L.M., Kobylianskyi R.R., Kadeniuk T.Ya. (2017). Computer simulation and optimization of the dynamic operating modes of thermoelectric device for treatment of skin diseases. *J.Thermoelectricity*, 2, 44-57.
42. Anatychuk L.I., Vikhor L.M., Kobylianskyi R.R., Kadeniuk T.Ya., Zvarych O.V. (2017). Computer simulation and optimization of the dynamic operating modes of thermoelctric reflexotherapy device. *J.Thermoelectricity*, 3, 68-78.
43. Anatychuk L., Vikhor L., Kotsur M., Kobylianskyi R., Kadeniuk T. (2018). Optimal control of time dependence of temperature in thermoelectric devices for medical purposes. *International Journal of Thermophysics*, 39, 108. https://doi.org/10.1007/s10765-018-2430-z.
44. Jiang S.C., Ma N., Li H.J., Zhang X.X. (2002). Effects of thermal properties and geometrical dimensions on skin burn injuries. *Burns*, 28, 713-717.
45. Cetingul M.P., Herman C. (2008). Identification of skin lesions from the transient thermal response using infrared imaging technique. *IEEE*, 1219-1222.
46. Ciesielski M., Mochnacki B., Szopa R. (2011). Numerical modeling of biological tissue heating. Admissible thermal dose. *Scientific Research of the Institute of Mathematics and Computer Science*,

1(10), 11-20.
47. Filipoiu Florin, Bogdan Andrei Ioan Bogdan, Carstea Iulia Maria. (2010). Computer-aided analysis of the heat transfer in skin tissue. *Proceedings of the 3rd WSEAS Int. Conference on Finite Differences - Finite Elements - Finite Volumes - Boundary Elements*, 53-59.
48. Carstea Daniela, Carstea Ion, Carstea Iulia Maria (2011). Interdisciplinarity in computer-aided analysis of thermal therapies. *WSEAS Transactions on Systems and Control*, 6(4), 115-124.
49. Cetingül M.Pirtini, Herman C. (2011). Quantification of the thermal signature of a melanoma lesion. *International Journal of Thermal Sciences*, 50, 421e431. doi:10.1016/j.ijthermalsci.2010.10.019.
50. Deng Z.S., Liu J. (2005). Numerical simulation of selective freezing of target biological tissues following injection of solutions with specific thermal properties. *Cryobiology*, 50, 183-192.
51. Lim Han Liang, Gunasekaran Venmathi (2011). *Mathematical modeling of heat distribution during cryosurgery*. https://isn.ucsd.edu/last/courses/beng221/problems/2011/project10.pdf.
52. Pennes H.H. (1948). Analysis of tissue and arterial blood temperatures in the resting forearm. *J. Appl. Physiol*., 1 (2), 93 – 122.
53. Gershenwald Jeffrey E., et. al. (2017). Melanoma staging: evidence-based changes in the American Joint Committee on Cancer Eighth Edition Cancer Staging Manual. *CA Cancer J. Clin*, 67(6), 472–492. doi:10.3322/caac.21409.
54. Dinnes J, Deeks J.J., Grainge M.J., Chuchu N, Ferrante di Ruffano L, Matin R.N., et al. (2018). Visual inspection for diagnosing cutaneous melanoma in adults. The Cochrane Database of Systematic Reviews, 12(12): CD013194. doi:10.1002/14651858.CD013194. PMC 6492463. PMID 30521684.
55. Rykaczewski Konrad (2019). Modeling thermal contact resistance at the finger-object interface. *Temperature*, 6 (1), 85-95.
56. *COMSOL Multiphysics User's Guide* (2010). COMSOLAB.
57. Zinkin A.N., Zingilevskaia N.G., Muselian B.B. (1997). *Kriovozdeistvie v otorinolaringologii: metodicheskiie rekomendatsii [Cryotherapy in otorhinolaryngology: guidelines]*. Krasnodar [in Russian].
58. Mazur P. (1968). Physical-chemical factors underlying cell injury in cryosurgical freezing. In: Cryosurgery ed. by R. W. Rand, A. P. Rinfret, H. Leden - Springfield, Illinois, U.S.A., 32-51.
59. Shafranov V.V., Borkhunova E.N., Kostylev V.A. (2012). Mekhanizm razrusheniia biologicheskikh tkanei vo vremia lokalnoi kriodestruktsii [Mechanism of destruction of biological tissues during local cryodestruction]. *Vestnik rossiiskoi akademii yestestvennykh nauk - Bulletin of the Russian Academy of Natural Sciences*, 1, 68 – 77 [in Russian].

Submitted 16.07.2020

Анатичук Л.І. *акад. НАН України*[1,2]
Кобилянський Р.Р. *канд. фіз.-мат. наук* [1,2]
Федорів Р.В.[1,2]

[1]Інститут термоелектрики НАН та МОН України,
вул. Науки 1, Чернівці, 58029, Україна
e–mail: anatych@gmail.com;
[2]Чернівецький національний університет ім.
Ю. Федьковича, Чернівці, Україна

КОМП'ЮТЕРНЕ МОДЕЛЮВАННЯ ЦИКЛІЧНОГО ТЕМПЕРАТУРНОГО ВПЛИВУ НА ОНКОЛОГІЧНЕ НОВОУТВОРЕННЯ ШКІРИ ЛЮДИНИ

У роботі наведено результати комп'ютерного моделювання температурного впливу на пухлину шкіри у динамічному режимі. Побудовано фізичну, математичну і комп'ютерну моделі шкіри з онкологічним новоутворенням (меланомою) із врахуванням теплофізичних процесів, кровообігу, теплообміну, процесів метаболізму та фазового переходу. Як приклад, розглянуто випадок, коли на поверхні пухлини знаходиться робочий інструмент, температура якого змінюється циклічно за наперед заданою залежністю у діапазоні температур [-50 ÷ +50] °C. Визначено розподіли температури у пухлині та у різних шарах шкіри в режимах охолодження і нагріву. Отримані результати дають можливість визначати глибину промерзання і прогріву біологічної тканини, зокрема пухлини, при заданому температурному впливі. Бібл.59, рис. 6, табл. 2.

Ключові слова: температурний вплив, шкіра людини, пухлина, меланома, динамічний режим, комп'ютерне моделювання.

Анатычук Л.И., *акад. НАН Украины*[1,2]
Кобылянский Р.Р., *канд. физ.-мат. наук* [1,2]
Федорив Р.В.[1,2]

[1]Институт термоэлектричества НАН и МОН Украины,
ул. Науки, 1, Черновцы, 58029, Украина,
e–mail: anatych@gmail.com;
[2]Черновицкий национальный университет
им. Юрия Федьковича, ул. Коцюбинского, 2,
Черновцы, 58012, Украина

КОМПЬЮТЕРНОЕ МОДЕЛИРОВАНИЕ ЦИКЛИЧЕСКОГО ТЕМПЕРАТУРНОГО ВОЗДЕЙСТВИЯ НА ОНКОЛОГИЧЕСКИЕ НОВООБРАЗОВАНИЯ КОЖИ ЧЕЛОВЕКА

В работе приведены результаты компьютерного моделирования температурного воздействия на опухоль кожи в динамическом режиме. Построены физическая, математическая и компьютерная модели кожи с онкологическим новообразованием (меланомой) с учетом теплофизических процессов, кровообращения, теплообмена, процессов метаболизма и фазового перехода. В качестве примера, рассмотрен случай, когда на поверхности опухоли находится рабочий инструмент, температура которого изменяется циклически по заранее заданной зависимости в диапазоне температур [-50 ÷ +50] °C. Определены распределения температуры в опухоли и в различных слоях кожи в режимах охлаждения и нагрева. Полученные результаты дают возможность определять глубину промерзания и прогрева биологической ткани, в частности опухоли, при заданном температурном воздействии. Библ. 59, рис. 6, табл. 2.

Ключевые слова: температурное воздействие, кожа человека, опухоль, меланома, динамический режим, компьютерное моделирование.

References

1. Anatychuk L.I., Denisenko O.I., Kobylianskyi R.R., Kadeniuk T.Ya., Perepichka M.P. (2017). Suchasni metody krioterapii v dermatologichnii praktytsi [Modern cryotherapy methods in dermatological practice]. *Klinichna ta Eksperymentalna Patologiia*, XVI, 1(59), 150-156 [in Ukrainian].
2. Anatychuk L.I., Denisenko O.I., Kobylianskyi R.R., Kadenyuk T.Ya. (2015). On the use of thermoelectric cooling in dermatology and cosmetology. *J.Thermoelectricity*, 3, 57-71.
3. Kobylianskyi R.R., Kadenyuk T.Ya. (2016). Pro perspektyvy vykorystannia termoelektryky dlia likuvannia zakhvoriuvan' shkiry kholodom [On the prospects of using thermoelectricity for treatment of skin diseases with cold]. *Naukovy visnyk Chernivetskogo universitetu: zbirnyk naukovykh ptrats. Fizyka. Elektronika - Scientific Bulletin of Chernivtsi University: Collection of Scientific Papers. Physics. Electronics,* 5, 1, 67 – 72 [in Ukrainian].
4. Moskalyk I.A., Manyk O.M. (2013). On the use of thermoelectric cooling in cryodestruction practice. *J.Thermoelectricity*, 6, 84-92.
5. Moskalyk I.A. (2015) Pro vykorystannia termoelektrychnykh pryladiv u kriokhirurgii [On the use of thermoelectric devices in cryosurgery]. *Fizyka i khimiia tverdogo tila – Physics and Chemistry of Solid State*, 4, 742-746 [in Ukrainian].
6. Kobylianskyi R.R., Bezpalchuk O.O., Vyhonnyi V.Yu. (2018). Pro zastosuvannia termoelektrychnoho okholodzhennia u kosmetolohii [On the use of thermoelectric cooling in cosmetology]. *Fizyka i khimiia tverdogo tila – Physics and Chemistry of Solid State*, 19 (4), 340-344 (DOI: 10.15330/pcss.19.4.340-344).
7. Kobylianskyi R.R., Manyk O.M., Vyhonnyi V.Yu. (2018). On the use of thermoelectric cooling for cryodestruction in dermatology. *J.Thermoelectricity*, 6, 36-46.
8. Shakhov V.Yu., Kochenov V.I. et al. (1983). O naibolee ratsionalnykh metodikakh kriodestruktsii zlokachestvennykh novoobrazovanii [On the most rational methods for cryodestruction of malignant neoplasms]. *Voprosy onkologii- Problems in Oncology*, 9, 31-37 [in Russian].
9. Maruyama S., Nakagawa K., Takeda H. (2008). The flexible cryoprobe using Peltier effect for heat transfer control. *Journal of Biomechanical Science and Engineering*, 138-150.
10. Kochenov V.I. (2000). *Kriokhirurgicheskaia profilakticheskaia onkologiia [Cryosurgical preventive oncology]*. Niznii Novgorod [in Russian].
11. Kochenov V.I. (2003). *Kriologicheskaia profilakticheskaia onkologiia: kratkoie uchebnoie i metodicheskoie posobiie dlia vrachei i studentov [Cryological preventive oncology: a short educational and methodological guide for doctors and students]*. Organization Nizhnii Novgorod Regional Oncological Association of Disabled People (Ed). 2nd revised ed. Nizhnii Novgorod [in Russian].
12. Kochenov V.I., Korolev Yu.V. (2003). Prosteishiie krioinstrumenty dlia ambulatornoi praktiki vracha-kriologa [The simplest cryo-instruments for the outpatient practice of a cryologist]. *Meditsinskaia kriologiia – Medical Cryology*, 4, 157-160. Nizgnii Novgorod [in Russian].
13. Kochenov V.I. (1982). Adhesive effect in cryosurgery. *Abstract in the International Abstract Journal*, IV, 8.
14. Yiu W., Basco M.T., Aruny J.E., Sumpio B.E. (2007). Cryosurgery: A review. *Int. J. Angiol,* 16 (1),1-6.
15. Paches A.I., Shental V.V., Ptukha T.P., et al. (1978). *Kriogennyi metod lecheniia opukholei golovy i shei [Cryogenic treatment of head and neck tumors]*. Moscow: 1978 [in Russian].
16. Potapov I.I., et al. (1975). Kriokhirurgiia v otorinolaringologii [Cryosurgery in othorinolaryngology]. Moscow [in Russian].
17. Dragomiretskii V.D. (1987). Kriokhirurgicheskiie metody lecheniia zabolevanii ukha, gorla i nosa [Cryosurgical methods for the treatment of the diseases of ear, throat and nose]. *Prakticheskaia*

kriomeditsina [Practical cryomedicine]. V.I.Grishchenko and B.P.Sandomirskii (Ed.). Kyiv: Zdorovia [in Russian].

18. Nikolaev N.I., Kochenov V.I., Tsybusov S.N., et al.(2003). Primenenie regenerativnykh effektov kriovozdeistviia v khirurgii i pri plastike barabannoi pereponki [Application of regenerative effects of cryotherapy in surgery and in the plastic of the tympanic membrane]. *Meditsinskaia kriologiia – Medical Cryology*, 4, 176-188. Nizgnii Novgorod [in Russian].
19. Alperovich B.I., Paramonova L.M., Merzlikin N.V. (1985). *Kriokhirurgiia pecheni i podzheludochnoi zhelezy [Cryosurgery of the liver and pancreas]*. Tomsk [in Russian].
20. Verkin B.I., Grishchenko V.I., Murinets-Markevich B.N., et al. (1978). Kriogennaia tekhnika v ginekologicheskoi practike [Cryogenic technique in gynecological practice]. *Meditsinskaia tekhnika – Biomedical Engineering*, 2, 28-32 [in Russian].
21. Grishchenko V.I. (1974). *Gipotermiia i kriokhirurgiia v akushersnve i ginekologii [Gipothermia and cryosurgery in obstetrics and gynecology]*. Moscow: Meditsina [in Russian].
22. Anatychuk L.I. (1979). *Termoelementy i termoelektricheskiie ustroistva: spravochnik [Thermoelements and thermoelectric devices: reference book]*. Kyiv: Naukova dumka [in Russian].
23. Kolenko E.A. (1967). *Termoelektricheskiie okhlazhdaiushchiie pribory [Thermoelectric cooling devices]*. 2nd ed. Leningrad: Nauka [in Russian].
24. Ismailov T.A. Sostoianiie i perspektivy razvitiia termoelektricheskogo priborostroieniia [The state and prospects of development of thermoelectric instrument making]. *Proc. of III All-Russian Scientific and Technical Conference* [in Russian].
25. Budrik V.V. (2010). *Physical fundamentals of cryomethods in medicine. Training Manual*. F.Lugnani (Ed.). L.N. Semenova (Russian transl.)
26. Cooper S.M. (2001). The history of cryosurgery. *J. R. Soc. Med*., 94, 196-201.
27. Whittaker D.K. (1984). Mechanisms of tissue destruction following cryosurgery. *Annals of the Royal College of Surgeons of England*, 66, 313-318.
28. Hypothermia — one of the promising cancer treatment technologies (2012). [Electronic resource]. Doctor.kz. Retrieved from: *http://www.doctor.kz/health/news/2012/03/21/13006.*
29. How can temperature help fight cancer [Electronic resource]. Oncology clinic "K-test". Retrieved from: *https://www.k-test.ru/index.php?rid=4.*
30. Perez C.A., Emami B.N., Nussbaum G. and Sapareto S. (1989). *Hyperthermia. Principles and practice of radiation oncology*.
31. Kandel E.I. (1974). *Kriokhirurgia [Cryosurgery*]. Moscow: Meditsina [in Russian].
32. Xu K.C., Korpar Nikolai, Niu L.Z. (2012). *Modern cryosurgery for cancer*. World Scientific Publisher.
33. Anatychuk L.I., Kobylianskyi R.R., Fedoriv R.V. (2019). Method for taking into account the phase transition in biological tissue during computer-aided simulation of cryodestruction process. *J.Thermoelectricity*, 1, 46-58.
34. Anatychuk L.I., Kobylianskyi R.R., Fedoriv R.V. (2019). Computer simulation of human skin cryodestruction process during thermoelectric cooling. *J.Thermoelectricity*, 2, 21-35.
35. Anatychuk L.I., Kobylianskyi R.R., Fedoriv R.V. (2020). Computer simulation of cyclic temperature effect on the human skin. *J. Thermoelectricity*, 3.
36. Andreozzi Assunta, Brunese Luca, Iasiello Marcello, Tucci Claudio, Vanoli Giuseppe Peter (2019). Modeling heat transfer in tumors: A review of thermal therapies. *Annals of Biomedical Engineering*, 47(3), 676–693. https://doi.org/10.1007/s10439-018-02177-x.
37. Bhowmik Arka, Repaka Ramjee (2016). Estimation of growth features and thermophysical properties of

melanoma within 3-D human skin using genetic algorithm and simulated annealing. *International Journal of Heat and Mass Transfer, 98, 81-95.* http://dx.doi.org/10.1016/j.ijheatmasstransfer.2016.03.020.

38. Horsfield Michael, Sarkar Ritvik, Reffsin Sam, Seog Woo Jin (2015). A computer model for evaluating the efficiency of cryosurgery for prostate cancer.
39. Anatychuk L.I., Vikhor L.M., Kotsur M.P., Kobylianskyi R.R., Kadeniuk T.Ya. (2016). Optimal control of time dependence of cooling temperature in thermoelectric devices. *J.Thermoelectricity*, 5, 5-11.
40. Anatychuk L.I., Kobylianskyi R.R., Kadeniuk T.Ya. (2017). Computer simulation of local thermal effect on human skin. *J.Thermoelectricity*, 1, 69-79.
41. Anatychuk L.I., Vikhor L.M., Kobylianskyi R.R., Kadeniuk T.Ya. (2017). Computer simulation and optimization of the dynamic operating modes of thermoelectric device for treatment of skin diseases. *J.Thermoelectricity*, 2, 44-57.
42. Anatychuk L.I., Vikhor L.M., Kobylianskyi R.R., Kadeniuk T.Ya., Zvarych O.V. (2017). Computer simulation and optimization of the dynamic operating modes of thermoelctric reflexotherapy device. *J.Thermoelectricity*, 3, 68-78.
43. Anatychuk L., Vikhor L., Kotsur M., Kobylianskyi R., Kadeniuk T. (2018). Optimal control of time dependence of temperature in thermoelectric devices for medical purposes. *International Journal of Thermophysics*, 39, 108. https://doi.org/10.1007/s10765-018-2430-z.
44. Jiang S.C., Ma N., Li H.J., Zhang X.X. (2002). Effects of thermal properties and geometrical dimensions on skin burn injuries. *Burns*, 28, 713-717.
45. Cetingul M.P., Herman C. (2008). Identification of skin lesions from the transient thermal response using infrared imaging technique. *IEEE*, 1219-1222.
46. Ciesielski M., Mochnacki B., Szopa R. (2011). Numerical modeling of biological tissue heating. Admissible thermal dose. *Scientific Research of the Institute of Mathematics and Computer Science*, 1(10), 11-20.
47. Filipoiu Florin, Bogdan Andrei Ioan Bogdan, Carstea Iulia Maria. (2010). Computer-aided analysis of the heat transfer in skin tissue. *Proceedings of the 3rd WSEAS Int. Conference on Finite Differences - Finite Elements - Finite Volumes - Boundary Elements*, 53-59.
48. Carstea Daniela, Carstea Ion, Carstea Iulia Maria (2011). Interdisciplinarity in computer-aided analysis of thermal therapies. *WSEAS Transactions on Systems and Control*, 6(4), 115-124.
49. Cetingül M.Pirtini, Herman C. (2011). Quantification of the thermal signature of a melanoma lesion. *International Journal of Thermal Sciences*, 50, 421e431. doi:10.1016/j.ijthermalsci.2010.10.019.
50. Deng Z.S., Liu J. (2005). Numerical simulation of selective freezing of target biological tissues following injection of solutions with specific thermal properties. *Cryobiology*, 50, 183-192.
51. Lim Han Liang, Gunasekaran Venmathi (2011). *Mathematical modeling of heat distribution during cryosurgery*. https://isn.ucsd.edu/last/courses/beng221/problems/2011/project10.pdf.
52. Pennes H.H. (1948). Analysis of tissue and arterial blood temperatures in the resting forearm. *J. Appl. Physiol*., 1 (2), 93 – 122.
53. Gershenwald Jeffrey E., et. al. (2017). Melanoma staging: evidence-based changes in the American Joint Committee on Cancer Eighth Edition Cancer Staging Manual. *CA Cancer J. Clin*, 67(6), 472–492. doi:10.3322/caac.21409.
54. Dinnes J, Deeks J.J., Grainge M.J., Chuchu N, Ferrante di Ruffano L, Matin R.N., et al. (2018). Visual inspection for diagnosing cutaneous melanoma in adults. The Cochrane Database of Systematic Reviews, 12(12): CD013194. doi:10.1002/14651858.CD013194. PMC 6492463. PMID 30521684.
55. Rykaczewski Konrad (2019). Modeling thermal contact resistance at the finger-object interface. *Temperature*, 6 (1), 85-95.

56. *COMSOL Multiphysics User's Guide* (2010). COMSOLAB.
57. Zinkin A.N., Zingilevskaia N.G., Muselian B.B. (1997). *Kriovozdeistvie v otorinolaringologii: metodicheskiie rekomendatsii [Cryotherapy in otorhinolaryngology: guidelines]*. Krasnodar [in Russian].
58. Mazur P. (1968). Physical-chemical factors underlying cell injury in cryosurgical freezing. In: Cryosurgery ed. by R. W. Rand, A. P. Rinfret, H. Leden - Springfield, Illinois, U.S.A., 32-51.
59. Shafranov V.V., Borkhunova E.N., Kostylev V.A. (2012). Mekhanizm razrusheniia biologicheskikh tkanei vo vremia lokalnoi kriodestruktsii [Mechanism of destruction of biological tissues during local cryodestruction]. *Vestnik rossiiskoi akademii yestestvennykh nauk - Bulletin of the Russian Academy of Natural Sciences*, 1, 68 – 77 [in Russian].

Submitted 16.07.2020

Rozver Yu.Yu.[1], Tinko E.V.[2]

[1]Institute of Thermoelectricity of the NAS
and MES of Ukraine,
1 Nauky str., Chernivtsi, 58029, Ukraine;
e–mail: anatych@gmail.com
[2] Yu.Fedkovych Chernivtsi National University

THERMOELECTRIC GENERATOR WITH A PORTABLE STOVE

The paper presents the results of the development and experimental research of a thermoelectric generator, which consists of a thermoelectric unit based on an army pot and a portable stove of widespread use. The obtained results confirm the possibility of using a thermoelectric generator to power mobile phone batteries and various gadgets. The achieved energy parameters significantly outperform the closest existing analogues. The expediency of constructive revision of the selected portable stove in terms of providing the possibility of using an open flame has been established. The economical calculations of the device have determined the average cost of the TEG at $ 170. Bibl.7, Fig. 7, Tabl. 2.

Key words: thermoelectric generator, physical model, portable stove.

Introduction

Portable power sources are now in active demand in places where there is no centralized grid. Interest in such sources has grown in recent years due to the need to charge the electric batteries of modern laptops and gadgets. Ukrainian soldiers in Eastern Ukraine are particularly interested in such devices. Thermoelectric generators (TEGs) on solid fuel have serious advantages over generators whose operation is based on other physical principles: photovoltaic, wind. They are more reliable, easy to maintain, not afraid of shocks and vibrations, easily disguised in the field. With the help of such devices, one can not only get electricity, but also cook and heat food, heat in winter.

The purpose of this work was to create and study a highly efficient portable thermoelectric generator characterized by low weight and size parameters and economically accessible to a wide range of consumers.

A brief overview of portable TEGs with solid fuel heat sources with analysis of the achieved parameters and characteristics.

Scientists and engineers from many countries are actively working to create more efficient thermoelectric portable generators, which would be characterized by lower weight and size parameters, high enough efficiency and modern design.

The **Biolite Basecamp** [1] device can use fallen branches, dry wood chips, cones or other wood as fuel.

The power output to the USB port of this device is 5 W, the voltage is 5V. The weight of the device is 8.16 kg. The cooking surface area is 50.5 cm^2, the diameter of the device is 33 cm. The cost of the generator is 301 US dollars.

The disadvantage of this design is the significant weight and low efficiency of thermoelectric conversion. The ratio of electric power to the weight of the generator with the stove is 0.6.

The thermoelectric generator **FireBee Power Tower** [2] converts heat from any portable stove into electricity for charging smartphones, tablets and other electronic gadgets.

The device can be used with various heat sources, it can achieve an electrical power of 10 W at a voltage of 5V, but its disadvantage is that in addition to the heat of the stove, for its operation it needs a regular replacement of the heated water with cool water. This creates an inconvenience in the field and makes it much more difficult to use this device.

The thermoelectric generator [3] comprises thermoelectric generator modules, "hot" heat exchangers, "cold" heat exchangers. “Hot" heat exchangers are immersed in the reservoir of a hot geyser, and "cold" heat exchangers are buried in the "permafrost" or immersed in a cold reservoir. The thermoelectric generator works as follows. Hot "heat exchangers" are heated from the hot reservoir of the geyser and supply heat to the thermoelectric generator modules, while "cold" heat exchangers remove heat from the thermoelectric generator modules and are cooled in "permafrost" or in a cold reservoir. Due to the temperature difference created by "hot" and "cold" heat exchangers, thermoelectric modules generate electricity. Thus, for the operation of a thermoelectric generator, natural sources of heating and cooling are used. This design solution in the actual operation of the device requires the presence of natural sources of heat and cold. This fact makes impossible wide application of such a device.

The tourist generator PowerSpot Mini Thermixc [4] realizes a stable output power of 7 W and allows charging electronic devices in the appropriate time:
Mobile phone (1500 mAh) - 1 h 30 min
Smartphone (3000 mAh) - 3 h
iPhone 6 (1800 mAh) - 1 h 45 min
iPhone 7 (1969 mAh) - 2 h
iPhone 7 plus (2900 mAh) - 2 h 50 min
iPad / tablet (6500 mAh) - 6 h 30 min
GoPro HER04 (1160 mAh) - 1 h 10 min

The developers declare a service life of 50.000 hours at operating temperatures of 150 ºC - 400 ºC. For operation, the device consumes about 50 g of liquefied gas. This circumstance makes regular use of the generator in the field practically impossible.

The purpose of this work is to create and study a highly efficient portable thermoelectric generator, which would have low weight and size and would be economically available to a wide range of consumers.

Physical model of a TEG with a heat source

Fig. 1 shows a physical model of thermoelectric generator unit comprising a thermopile, heat spreaders for heat supply and removal from the thermopile, a device for intensive heat removal and a heat source – flat-parallel surface uniformly heated with flame.

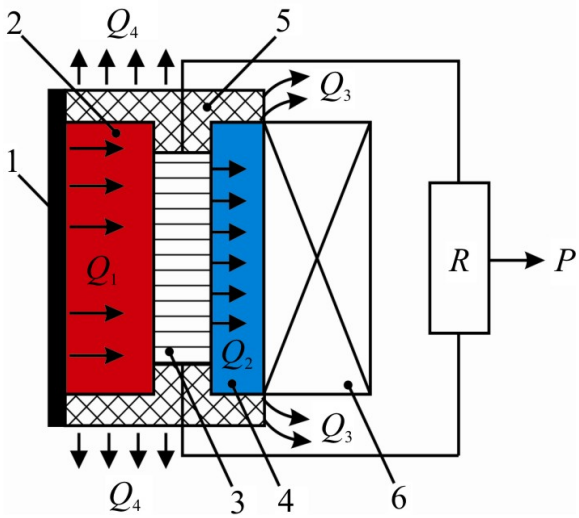

Fig. 1. Physical model of thermoelectric generator unit:
1 – heated surface; 2 – hot heat spreader;
3 – thermopile; 4 – cold heat spreader;
5 – housing; 6 – thermopile cooling block.

Since the generator is built into a heated surface, the processes of heat exchange between a real source of fuel combustion and this surface are not considered. The temperature of the heated surface is assumed to be equal to the temperature of the hot TEG heat exchanger.

Thus, heat supply from the heated surface to the hot side of the thermopile and heat removal from the thermopile cold junctions to the cold heat exchanger is carried out due to thermal conductivity and is described by the equations [5]:

$$Q_1 = \frac{\lambda_T S_T}{l_T}(T_T - T_\Gamma), \tag{1}$$

$$Q_2 = \frac{\lambda_m S_m}{l_m}(T_X - T_m),, \tag{2}$$

where λ_T, λ_m is thermal conductivity of material of the hot and cold heat conductors; T_T, T_m are temperatures of the hot and cold heat conductors; T_Γ, T_X is temperature of the hot and cold side of thermopile, respectively.

Thermal power Q3 is removed from the cold heat conductor by free convection into the water contained in the cooling block (pot capacity):

$$Q_3 = \alpha(T_m - T_0)S_m\,, \tag{3}$$

where $\alpha(v)$ is the coefficient of convective heat transfer between the cold heat conductor and water in the cooling block; T_0 is the temperature of the liquid in the cooling block.

The electric power generated by the thermopile is proportional to Q_1 and the efficiency of the thermopile η:

$$P = P_{TEБ} = Q_1 \eta\,, \tag{4}$$

The main heat losses Q_4 occur on the thermopile through thermal insulation:

$$Q_4 = \frac{\lambda S_T}{L}(T_Б - T_0), \tag{5}$$

where λ is the thermal conductivity of the insulating material; S_T is the surface area of the hot heat conductor which is not occupied by the thermopile; L is the thickness of the insulating layer.

The heat balance equation for the selected model of the thermoelectric generator can be written as:

$$\begin{cases} Q_1 = P + Q_2 + Q_4, \\ Q_2 = Q_3 + Q_4 \end{cases} \tag{6}$$

The solution of the system of equations (6) makes it possible to determine the main energy and design parameters of the thermoelectric generator unit in particular and a complex unit with a portable heater in general.

Optimization of TEG design

Optimization of the generator unit was preceded by an experiment to determine the temperatures of the elements of the selected portable stove [6]. Fig. 2 presents the results of such measurements.

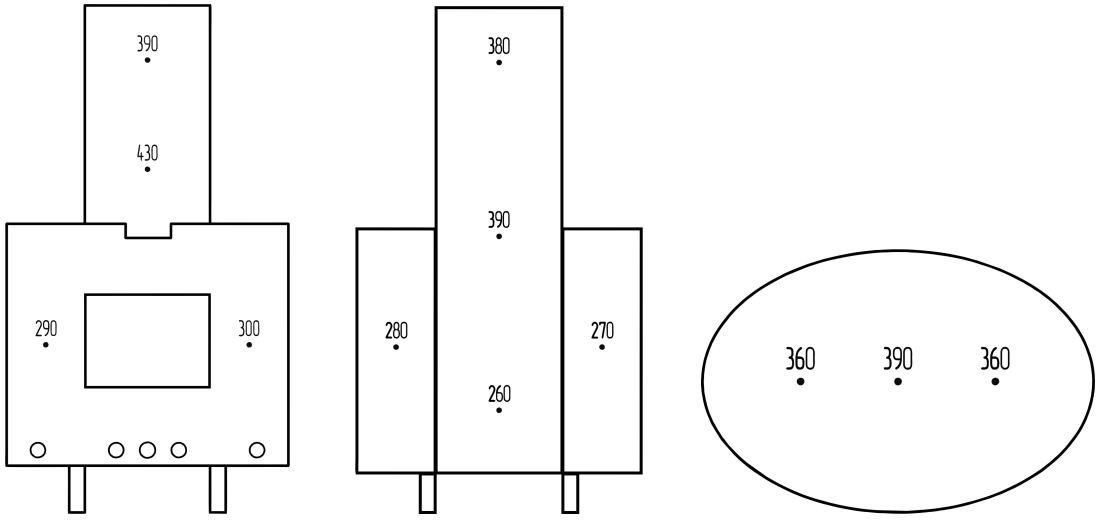

a) *b)* *c)*

Fig.2. Results of measuring the temperatures of the heater walls (°C)
a) – front view, b) – rear view, c) – top view.

Optimization computer calculations, which took into account the experimental temperature measurements, made it possible to determine the design parameters of the thermoelectric generator unit which was designed to be placed on the cooking surface of a portable stove.

From the computer analysis it followed that thermoelectric generator unit based on a military pot should contain two thermoelectric generator modules in its bottom facing the heat source. The

Altec-1061 module is installed as the optimal thermoelectric module for certain temperature and thermal conditions.

Calculation of energy characteristics of the TEG with a stove

The approximate calculated mass of firewood at one loading in the stove m = 60g = 0.06 кg. When burning one load of firewood, the released energy E is:

$$E = G \cdot m = 750 \text{ (kJ)} \tag{7}$$

where G=12.56 mJ/kg is calorific value of firewood.

Thermal power Q absorbed by thermoelectric modules:

$$\eta = \frac{P}{Q} \rightarrow Q = \frac{P}{\eta} = 110 \text{ (W)} \tag{8}$$

where P = 5 W is calculated electric power generated by modules, η = 0.045 is the efficiency of modules at the hot and cold side temperatures T_h = 300°C and T_c = 100°C, respectively.

Operating time t at one loading while minimizing heat losses:

$$Q = \frac{E}{t} \rightarrow t = \frac{E}{Q} = 2 \text{ (h)} \tag{9}$$

Thermal power $Q_н$ consumed to heat water in the generator pot:

$$Q_н = Q - P = 105 \text{ (W)} \tag{10}$$

Time t of heating water in the generator pot:

$$Q_н = \frac{c \cdot m \cdot (T_1 - T_0)}{t} \rightarrow t = \frac{c \cdot m \cdot (T_1 - T_0)}{Q_н} = 1 \text{ (h)} \tag{11}$$

where c=4.22 $kJ / kg \cdot K$ is heat capacity of water;

m=1l is the volume of water in the pot;

T_1=100 °C is the final water heating temperature;

T_2=20 °C is the initial temperature of water in the pot.

In the absence of heat loss, the operating time of the thermoelectric generator at one loading of fuel can be approximately 2 hours.

Calculation of energy characteristics of the TEG with a stove

The approximate calculated mass of firewood at one loading in the stove m = 60g = 0.06 кg. When burning one load of firewood, the released energy E is:

$$E = G \cdot m = 750 \text{ (kJ)} \tag{7}$$

where G=12.56 mJ / kg is calorific value of firewood.

Thermal power Q absorbed by thermoelectric modules:

$$\eta=\frac{P}{Q}\rightarrow Q=\frac{P}{\eta}=110\,(\mathrm{W}) \tag{8}$$

where $P = 5$ W is calculated electric power generated by modules, $\eta = 0.045$ is the efficiency of modules at the hot and cold side temperatures $T_h = 300°C$ and $T_c = 100°C$, respectively.

Operating time t at one loading while minimizing heat losses:

$$Q=\frac{E}{t}\rightarrow t=\frac{E}{Q}=2\,(\mathrm{h}) \tag{9}$$

Thermal power $Q_н$ consumed to heat water in the generator pot:

$$Q_н=Q-P=105\,(\mathrm{W}) \tag{10}$$

Time t of heating water in the generator pot:

$$Q_н=\frac{c\cdot m\cdot(T_1-T_0)}{t}\rightarrow t=\frac{c\cdot m\cdot(T_1-T_0)}{Q_н}=1\,(\mathrm{h}) \tag{11}$$

where c=4.22 $kJ/kg\cdot K$ is heat capacity of water;

m=1l is the volume of water in the pot;

T_1=100 °C is the final water heating temperature;

T_2=20 °C is the initial temperature of water in the pot.

In the absence of heat loss, the operating time of the thermoelectric generator at one loading of fuel can be approximately 2 hours.

Description of TEG design

The design of a thermoelectric unit for work with a portable stove is shown schematically in Fig. 3.

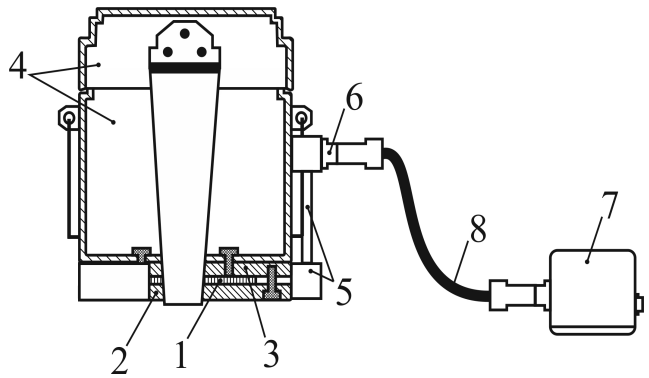

Fig.3. Schematic of thermoelectric generator unit.1 – thermopile; 2 – heat-conducting plate;3 – heat sink plate; 4 – army pot with a lid;5 – protective housing; 6 – electric output; 7 – electronic voltage stabilization unit; 8 – electric connecting cable.

To protect the electrical terminals of the thermopile from direct flame and external mechanical loads, the generator contains a protective housing **5**, which ends with an electrical output **6**. Using an electric cable **8,** the thermoelectric generator is connected to the electronic output voltage stabilization unit **7**. The appearance of the unit is shown in Fig. 4.

Fig. 4. Appearance of the thermoelectric unit

The Institute of Thermoelectricity of the National Academy of Sciences and the Ministry of Education and Science of Ukraine has developed, researched and standardized a thermoelectric unit for universal use with various heat sources and fuels. Table 1 shows the main parameters of the Altec - 8046 unit [7].

Table 1

Basic parameters of the Altec-8046 thermoelectric unit

1	Electric power, W	5
2	Electric voltage output, V	5.10
3	Pot volume, l	1.3
4	Overall dimensions, mm	170 × 170 × 100
5	Mass, kg	1

Methods of experimental research

The purpose of research conducted at the Institute of Thermoelectricity was to determine the energy characteristics of a thermoelectric army pot on a portable stove. The maximum electric power of the generator was measured in the range of water temperatures T_w = (20-100) °C every 10°C from the moment of ignition of the stove. The schematic of the experiment is shown in Fig. 5.

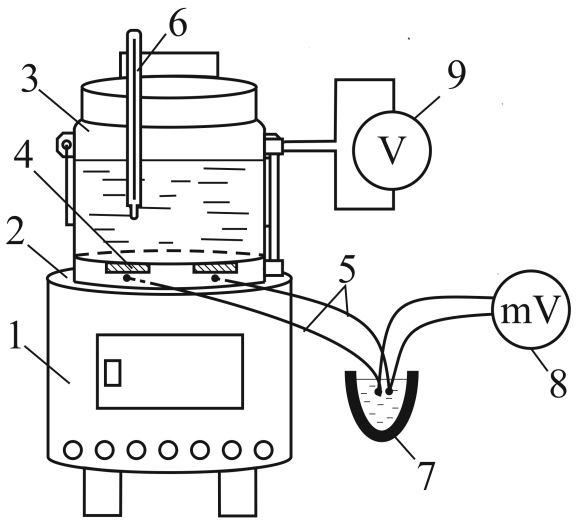

Fig.5 Schematic of the experiment to study the energy characteristics of thermoelectric army pot.
1 – tourist stove; 2 – cooking surface; 3 – thermoelectric generator;
4 – thermoelectric generator modules; 5 – thermocouples;
6 – thermometer; 7 – vessel with melting ice;8 – millivoltmeter; 9 – voltmeter.

When studying the energy characteristics of the generator, at all stages of the experiment, the fuel consumption was recorded to determine the obtained thermal power and the efficiency of thermoelectric conversion.

Research results

The time dependences of the energy characteristics of the Altec-8046 thermoelectric unit with a portable stove are presented in Fig. 6.

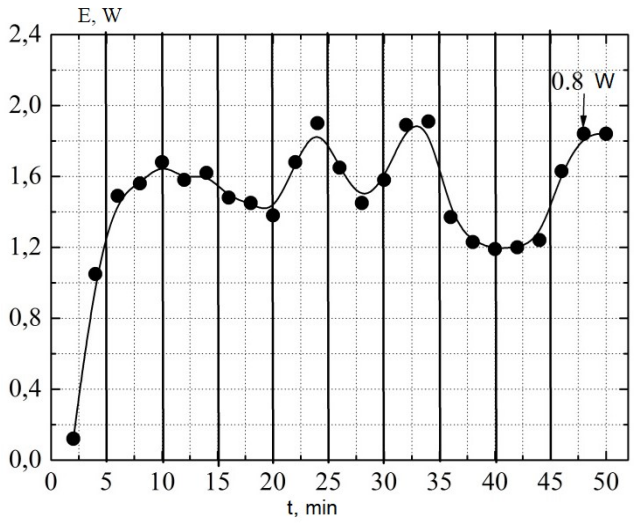

Fig. 6. Dependence of electromotive force E of thermoelectric modules on time
t. Vertical black lines indicate the moments of throwing fuel into the stove.

In these studies, firewood was used as fuel. Firewood consumption g = 840 g / hour. Thermal design power of the stove Q = 2.9 kW. For comparison, a study of a thermoelectric generator unit was carried out on an open flame from dry alcohol. Fig. 7 shows the obtained dependence of the electromotive force and the value of power on time.

The comparison of the obtained results showed the expediency of refining the portable stove, which would allow operation of the thermoelectric unit with an open flame. This design solution can improve the efficiency of TEG by a factor of ~ 1.6.

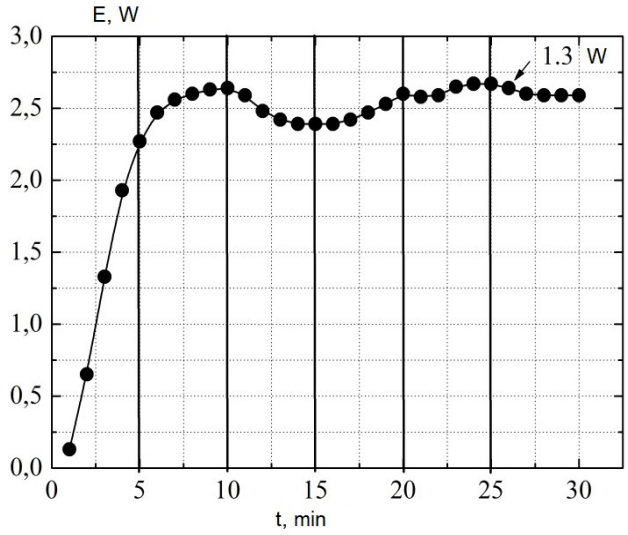

Fig. 7. Dependence of electromotive force on time in the variant of open flame

The consumption of dry alcohol g = 420 g / h. In this case, the thermal power of the stove was Q = 3.6 kW. The volume of water poured into the pot is 1 liter. The achieved efficiency values were about 1% for a TEG with a portable stove. The ratio of the output power to the weight of the device with a wood-fired stove is ~ 0.8, with an open flame - 1.3. These values are higher than those of the closest analogues.

Economic calculations of the cost of the developed device were carried out. Table 2 presents the cost of a single product of a thermoelectric generator with an army pot "Altec-8046" versus the batch size.

Table 2

The cost of thermoelectric generator versus the batch size

Batch size, pcs.	1	10	100	1000
Cost, $	190	178	163	150

Conclusions

1. A thermoelectric generator based on the Altec-8046 thermoelectric unit with a portable stove has been developed.
2. Studies carried out on various fuels have shown the possibility of using the developed device for power supply of modern means of communications and various gadgets.

3. The achieved values of the output electric power with respect to the weight of the device significantly outweigh the closest known analogues.
4. The expediency of constructive revision of the selected portable stove in terms of providing the possibility of using an open flame has been established.
5. The energy efficiency of a TEG with a portable stove after its improvement can increase by a factor of 1.6.
6. The economic calculations of the device have determined the average cost of the TEG as $170.

The authors express their sincere gratitude to the scientific supervisor, academician of the NAS of Ukraine LI Anatychuk, for the idea of work and valuable advice in its implementation.

References

1. https://turkul.net/nabor-biolite-basecamp.
2. https://www.treehugger.com/firebee-power-tower-turns.
3. Thermoelectric generator UA105730 U.
4. https://www.acsys.spb.ru/mini-generator-powerspot-mini-thermix/
5. Tourist heater UA 101649 U.
6. Anatychuk L.I. (1979). *Termoelementy i termoelektricheskiie ustroistva: Spravochnik [Thermoelements and thermoelectric devices: Handbook]*. Kyiv: Naukova dumka [in Russian].
7. Thermoelectric generator Altec-8046. *Operating instructions*.

Submitted 09.07.2020

Розвер Ю.Ю.[1], **Тінко Е.В.**[2]

[1]Інститут термоелектрики НАН і МОН України,
вул. Науки, 1, Чернівці, 58029, Україна;
e-mail: anatych@gmail.com;
[2]Чернівецький національний університет
ім. Юрія Федьковича, вул. Коцюбинського 2,
Чернівці, 58000, Україна

ТЕРМОЕЛЕКТРИЧНИЙ ГЕНЕРАТОР З ПОРТАТИВНОЮ ПІЧКОЮ

У роботі наводяться результати розробки та експериментального дослідження термоелектричного генератора, що складається з термоелектричного блоку на базі армійського казанка та портативної пічки широкого використання. Отримані результати підтверджують можливість використання термоелектричного генератора для живлення акумуляторів мобільних телефонів та різноманітних гаджетів. Досягнуті енергетичні параметри суттєво переважають найближчі існуючі аналоги. Встановлено доцільність конструктивного допрацювання вибраної портативної пічки в частині забезпечення

можливості використання відкритого полум'я .Економічні розрахунки пристрою визначили середню вартість ТЕГ на рівні 170 доларів США. Бібл. 7, рис. 7, табл. 2.
Ключові слова: *термоелектричний генератор, фізична модель, портативна пічка.*

Розвер Ю.Ю[1], Тинко Е.В.[2]

[1]Институт термоэлектричества НАН и МОН Украины,
ул. Науки, 1, Черновцы, 58029, Украина; e-mail: *anatych@gmail.com*
[2] Черновицкий Национальный университет им. Ю. Федьковича

ТЕРМОЭЛЕКТРИЧЕСКИЙ ГЕНЕРАТОР С ПОРТАТИВНОЙ ПЕЧЬЮ

В работе приводятся результаты разработки и экспериментального исследования термоэлектрического генератора, состоящего из термоэлектрического блока на базе армейского котелка и портативной печи широкого применения. Полученные результаты подтверждают возможность использования термоэлектрического генератора для питания аккумуляторов мобильных телефонов и различных гаджетов. Достигнутые энергетические параметры существенно превышают таковые, присущие ближайшим существующим аналогам. Установлена целесообразность конструктивной доработки выбранной портативной печи в части обеспечения возможности использования открытого пламени. Экономические расчеты устройства определили среднюю стоимость ТЭГ на уровне 170 долларов США. Библ. 7, рис. 7, табл. 2.
Ключевые слова: термоэлектрический генератор, физическая модель, портативная печь.

References

1. https://turkul.net/nabor-biolite-basecamp.
2. https://www.treehugger.com/firebee-power-tower-turns.
3. Thermoelectric generator UA105730 U.
4. https://www.acsys.spb.ru/mini-generator-powerspot-mini-thermix/
5. Tourist heater UA 101649 U.
6. Anatychuk L.I. (1979). *Termoelementy i termoelektricheskiie ustroistva: Spravochnik [Thermoelements and thermoelectric devices: Handbook]*. Kyiv: Naukova dumka [in Russian].
7. Thermoelectric generator Altec-8046. *Operating instructions*.

Submitted 09.07.2020

Dmytrychenko M.F., *Dr. of Technical Sciences*
Gutarevych Yu.F., *Dr. of Technical Sciences*
Trifonov D.M., *Cand. of Technical Sciences*
Syrota O.V., *Cand. of Technical Sciences*

National Transport University1,
M.Omelianovycha-Pavlenka Str., Kyiv, 01010, Ukraine,
e-mail: d.trifonov@ntu.edu.ua

THE USE OF THERMOELECTRIC ENERGY CONVERTERS TO REDUCE THE INFLUENCE OF NATURAL AND CLIMATIC FACTORS ON THE TECHNICAL READINESS OF A VEHICLE

The article discusses the problem associated with the operation of a vehicle at low ambient temperatures, substantiates the need for special measures to maintain the optimal thermal regime of the battery. The analysis of the factors influencing the start of a cold engine is carried out. The effect of low temperature of the storage battery on the energy performance of the electrical starting system is shown. Computational studies of the proposed system for compensating the heat losses of the storage battery during the maintenance of a vehicle at low temperatures by the method of thermostating with the use of thermoelectric energy converters are carried out. Bibl. 14, Fig. 4, Tabl. 3.
Key words: technical readiness, storage battery, thermoelectric generator, phase transition thermal accumulator, electric heating elements.

Introduction

The car has become an integral part of modern life. However, its use raises a number of problems primarily related to environmental pollution and low energy efficiency. Since the creation of the car, there has been a problem associated with ensuring a reliable and trouble-free start of the cold internal combustion engine (ICE) at low ambient temperatures. This problem is still relevant today.

The purpose of the work is to carry out computational studies of the system to ensure compensating the heat losses of the storage battery by the method of thermoelectric stabilization of its optimal temperature when a vehicle is kept out of the garage at low ambient temperatures.

Analysis of previous research

Review and analysis of literary sources related to the impact of natural and climatic factors on a vehicle during operation, primarily in urban conditions, characterized by long periods of inactivity, small movements, frequent and short stops and garage-free maintenance during the inter-shift period allows one to determine precisely the ambient air temperature as the main factor that affects the technical readiness of a vehicle.

Low temperatures complicate the start of a cold engine and lead to deterioration of its operating conditions, which generally reduces the technical readiness and use of the vehicle for its intended purpose.

The technical readiness of a vehicle at low ambient temperatures is mainly determined by the reliable start of a cold engine and the recovery time of its thermal regime. It is largely complicated as a result of a decrease in the discharge characteristics of storage battery in the mode of starting the engine due to an increase in the viscosity and resistance of the electrolyte, an increase in resistance to cranking of the engine crankshaft and deterioration of the conditions for the formation of the fuel-air mixture.

Mixing deteriorates due to a decrease in the intake temperature below the optimum, which leads to a deterioration in fuel evaporation and a decrease in the temperature of the working fluid at the end of the compression stroke. With a decrease in the ambient air temperature from 20 ° C to minus 30 ° C, the temperature at the end of the compression stroke decreases by 100 ... 210 ° C, while in diesel engines there is a delay in the autoignition of fuel two to three times in time, which leads to a deterioration of burning process. The viscosity of winter diesel fuel with a decrease in inlet air temperature from +20 ° C to minus 30 ° C increases 15 times. The viscosity of gasoline when the inlet temperature decreases from 0 ° C to minus 30 ° C is one and half times higher, and evaporation is 50 percent lower.

As the temperature decreases, the viscosity of the oil in the engine lubrication system increases. This leads to an increase in friction power losses in the conjugate parts of the cylinder-piston group and as a consequence to a decrease in the cranking speed of the engine crankshaft.

The reliability of starting the internal combustion engine at low ambient temperatures is largely determined by the performance of the battery. The battery performance is understood as the maximum possible number of crankshaft rotations with a duration of 15 seconds each [1].

The decrease in the temperature of the electrolyte is accompanied by an increase in its viscosity and internal resistance, which leads to a significant decrease in voltage at the terminals of the battery, which reduces the power developed by the starter in the cold engine start mode. With a decrease in the temperature of the electrolyte from + 30 ° C to minus 40 ° C, its resistivity increases 8 times [2]. According to the Research Institute of Starter Batteries, at a temperature of 0 ° C, the current efficiency of batteries is 90%, and at minus 40 ° C - 20%. At an electrolyte temperature below minus 20 ° C, an intensive deterioration in the efficiency of charging batteries from the on-board network was established. When charging the battery from a stationary device, the battery electrolyte is actively boiling at a constant density. Because the energy supplied is almost completely spent on water hydrolysis, batteries are practically inoperable at minus 30 ... 35 ° C [3].

A decrease in the battery capacity in the starting mode leads to a decrease in the starting crankshaft rotation speed, and a decrease in voltage leads to a decrease in the torque developed by the starter. Achieving the required starting speed of the crankshaft at low temperatures is difficult due to an increase in the cranking resistance torque of the engine crankshaft. In the process of starting the engine at low temperatures, the determining factor is the ratio of the moment of resistance of the engine crankshaft and the torque developed by the starter.

In this connection, the main concern of ensuring the operability of the battery and, as a consequence, of the technical readiness of a vehicle as a whole, should be the maintenance of the optimal temperature of the battery. The easiest way to solve this problem is to slow down the electrolyte cooling. For example, according to the Research Institute Avtoprilad uninsulated battery 6ST-132 is cooled from + 25 ° C to minus 30 ° C at a rate of 6.6 °C for one hour; and

insulated – 1.4 ° C for one hour.

In practice, there are many ways to ensure the technical readiness of a vehicle at low temperatures. However, most of them require the solution of complex design and technical problems and, under operating conditions, turn out to be ineffective or quite energy consuming. Therefore, the proposed work considers those that are based on the methods of storage battery thermal control through use of secondary energy resources of the internal combustion engine, which arise in large quantities during its operation.

Research results

With the rapid growth in the number of vehicles over the past decades, combined with the tightening of standards for fuel consumption and emissions of harmful substances, the utilization of thermal energy of exhaust gases as part of the secondary energy resources of a transport engine is becoming a promising direction for solving the above problem. This allows the implementation of energy-efficient technologies for road transport. Exhaust gases have a high thermal potential, take about 30% of the fuel energy into the environment, not only wasting primary energy resources, but also increasing the heat load on the environment.

Application of heat accumulators using phase transition heat-accumulating materials is an effective and promising way of storing heat energy on board a vehicle. This method makes it possible to provide a high density of accumulated energy with an isothermal nature of the accumulation process and makes it possible to store accumulated thermal energy on board a vehicle for quite a long time.

In this regard, it seems promising to develop systems that would have the ability to convert the thermal energy accumulated in phase transition heat accumulator into electrical energy. To solve this problem, according to the authors, thermoelectric energy converters can be effectively used [4]. The advantages of the latter are the absence of moving parts, silent operation, environmental friendliness, versatility in terms of methods of supply and removal of thermal energy, potentially high reliability [5, 6].

This article presents the results of computational studies of the thermoelectric system proposed in [7,8], which provides the optimal thermal regime of the starter battery at the end of the operation of the internal combustion engine during the maintenance of the vehicle at low ambient temperatures.

Thermoelectric generators (TEG), as autonomous direct current sources, received intensive development after semiconductor thermopiles were taken as the basis for their design. Over the past decades, there has been a constant improvement of semiconductor thermoelectric materials, which is aimed primarily at increasing their thermoelectric figure of merit in order to increase the electricity they produce and improve the efficiency [9].

Significant disadvantages of semiconductor TEGs are their fragility, high cost and complexity of the design of an automobile thermoelectric generator (ATEG) to ensure efficient operation, due to the need for an external source of cooling, which makes it possible to obtain the necessary (stable) temperature gradient and the presence of an electronic converter, which allows maintaining the necessary output voltage. The need for such a scheme is explained by the fact that the electromotive force generated by ATEG is not constant, since the temperature difference constantly changes its value in different operating modes of the transport ICE.

In the conditions of real operation of the vehicle, the ATEG, from the point of view of the efficiency and stability of its thermoelectric properties, must have the necessary mechanical strength and chemical resistance under the conditions of prolonged vibration and shock loads, with sharp drops in the temperature, pressure, and humidity.

Thus, it is fair to assume that in order to obtain electrical energy sufficient to power low-power devices under conditions of a small temperature gradient, metal conductors are more suitable for the manufacture of ATEG.

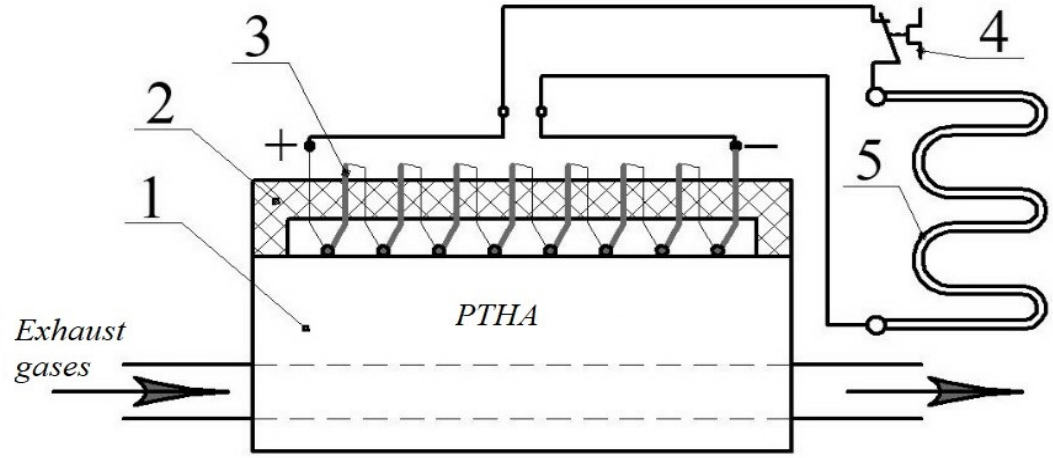

Fig. 1. Thermoelectric system for utilization of thermal energy of exhaust gases with phase transition heat accumulator:
1 – phase transition heat accumulator,
2 – layer of heat-resistant compound,
3 – thermoelectric generator,
4 – heat regulator, 5 – heating element.

Taking into account the above, the authors proposed a method for increasing the thermal readiness of a vehicle, in particular, the electrical starting system, under low temperatures. The implementation of this method and, as a consequence, the provision of the optimal thermal mode of the storage battery, is possible due to the use of a device for compensating heat losses of storage battery by thermostating with heating elements.

The heat capacity of the battery is quite high, so when you install it in a container with insulated walls (thermocase), the rate of drop of the electrolyte temperature will be quite low. Heating elements are added inside the thermocase. The built-in temperature regulator turns off heating on reaching + 25 ° C and turns it on again at + 15 ° C.

The operating principle of the proposed system is as follows (Fig. 2): after stopping the internal combustion engine the storage battery naturally cools down (section I), upon reaching the storage battery temperature 15 °C, electric heating elements are connected to ATEG to heat the storage battery to 25 °C (section II), following which the heating elements are turned off. After reducing the temperature of the storage battery to 15 °C (section III) – the process is repeated. Responsible for the switching of electrical circuits is the electronic control unit that receives information from the temperature sensor of the storage battery (the temperature sensor is installed on the negative terminal of the storage battery).

The proposed technical solution makes it possible to generate electrical energy without any additional energy transmitted to the system both the internal combustion engine is in operation and when the vehicle is kept in open areas under low temperatures. Based on the results of previous

experimental studies, the possibility of using metal TEGs for generating electrical energy for quite a long time after the end of the ICE operating cycle was confirmed [7].

Fig. 2. Operating principle of a device for compensating heat losses of storage battery

Computational studies

Calculation of the amount of energy required for thermal stabilization of the 6CT-44A battery of ZAZ Tavria class cars with a capacity of 44 A·h in the temperature range 15...25 °C.

The mass of the specified battery is 13.6 kg, of which the mass of the electrolyte is 3.6 kg. To simplify the calculation, we assume that another mass – 10.0 kg falls on lead (the mass of the body of the storage battery and separators is neglected). Some design parameters of the 6CT-44A battery are shown in Table 1 [10].

Table 1

Some design parameters of the 6CT-44A storage battery

Overall dimensions, mm			Mass, kg	
length	width	height	without electrolyte	with electrolyte
207	175	175	10	13,6

The amount of heat required to heat the battery (Q_b) is defined as the sum of the amount of heat for heating the lead (Q_{Pb}) and the amount of heat for heating the electrolyte (Q_{El}):

$$Q_{АБ} = Q_{Pb} + Q_{Ел} \quad (1)$$

The amount of heat is defined by the formula:

$$Q = m \cdot c_p \cdot \Delta t, \quad (2)$$

where m is mass of heated substance, kg;
c_p is specific heat, J/kg·K;
Δt is temperature difference, K.
The values of specific heats of storage battery components are given in Table 2.

Table 2

The values of specific heats of storage battery components

Storage battery components	c_p, J/(kg·K)
Water H_2O	4182
Sulphuric acid (100%) H_2SO_4	1380
Lead Pb	128

The heat capacity of electrolyte with a density of 1.28 g/cm^3 was determined using the data given in Table 3 [11].

Table 3

The amount of distilled water and acid, required to prepare 1 l of electrolyte with a density of 1.28 g/cm^3 (at 25 °C)

The required electrolyte density, g/cm^3	The amount of water, l	The amount of sulphuric acid with a density of 1.83 g/cm*	
		l	kg
1.28	0.781	0.285	0.523

Using the data in Table 1 and 3, we received the required amount of sulfuric acid with a density of 1.83 g / cm^3 - 1.88 kg; distilled water - 2.81 kg. Based on the obtained values and data of Table 2 we calculated the specific heat of the electrolyte with a density of 1.28 g/cm^3 - 1.15 kJ/(kg·K).

Based on the obtained values and formulae 1, 2, we calculated the amount of heat required to heat the 6ST-44A battery from 15 ° C to 25 ° C:

$$Q_b = 10 \cdot 10.0 \cdot 128 + 10 \cdot 3.6 \cdot 1150 \approx 54 \text{ (kJ)}$$

If the calculated thermal energy is converted into consumed electrical power, then we get about 15 W · h.

In practice, it is impossible to achieve the full use of storage battery active materials involved in current-forming process. Moreover, the electrolyte (height h_3), which is located in the mud space between prisms 5 and the electrolyte reserve (height h_2 in a battery with a sheet separator and height h_2+h_3 in a battery with an envelope separator), does not take part in current-generating process during electrical starting of the internal combustion engine. In this connection, the paper proposes to limit the heating area of storage battery (side and end surfaces with height h_1) by the height of the electrode to reduce the power of the electric heating element 7 (Fig. 3).

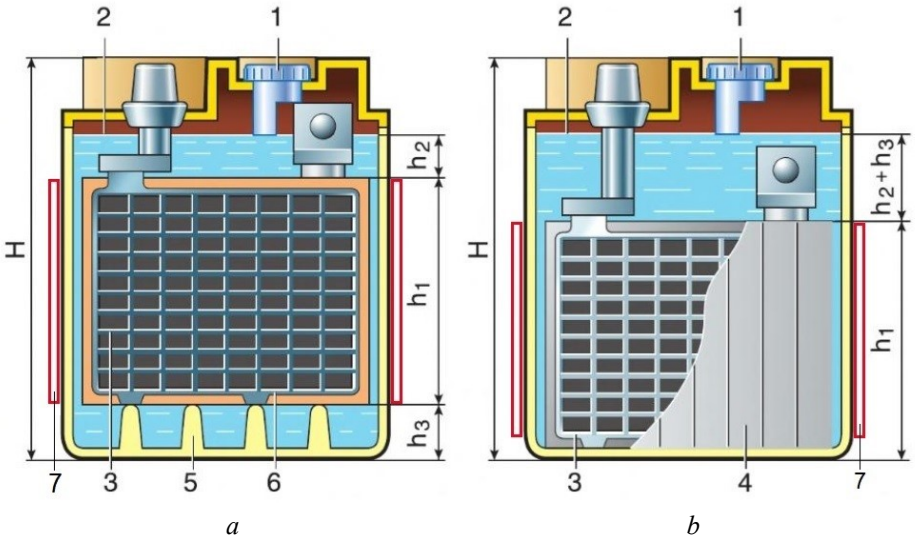

Fig. 3. Schematic of storage battery: [12]
a – conventional battery; b – battery with unattended envelope separators;
1 - plug; 2 – electrolyte level in a battery; 3 - electrode; 4 – envelope separator;
5 – mud space prisms; 6 – card separator;7 – electric heating element;
H – battery height; h_1 – electrode height; h_2 – electrolyte reserve in a battery with a sheet separator; h_3 – height of prisms; $h_2 + h_3$ – electrolyte reserve in a battery with an envelope separator

Therefore, the value of the required electric power of the electric heating element can be much lower than the calculated and with regard to the volume of electrolyte that does not participate in the current-generating process it can be reduced by 40… 60%, which will make up to 9 W · h.

Calculation of thermoelectric generator.

Based on the analysis of possible electric heating materials for heating storage battery, the use of carbon fiber material as an external electric heater of storage battery is proposed (Fig. 4).

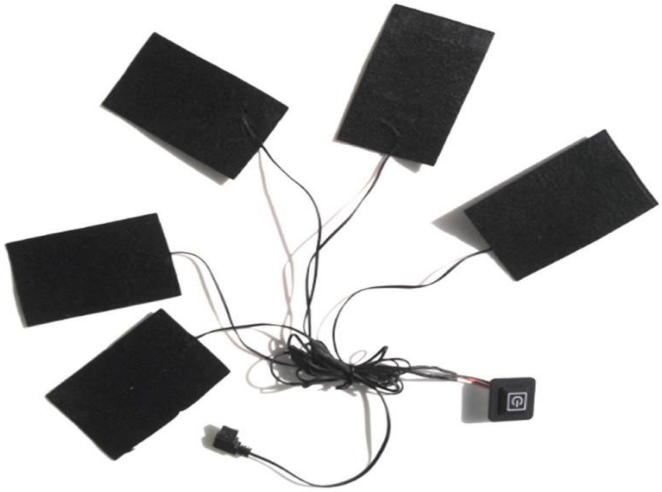

Fig. 4. Electric heating elements based on carbon fiber materials

The use of carbon fiber materials as heating elements helps provide:
• larger area with a uniform temperature distribution on the surface;
• high heat transfer rates;
• reliable operation for a long time;
• low cost of electricity consumption compared to counterparts about 30%;
• heating in 3s after power supply and the same fast cooling.
The technical characteristics of the proposed heating element are as follows:
• thickness: about 0.3 mm
• substrate size: about 110 * 70 mm
• heating temperature: 50…55 ℃
• voltage: 3.7 ... 5.0 V
• current: 1.85 ± 0.05 A
• power output: 8.5 ± 0.2 W
• resistance: 3 Ohm

Based on the technical characteristics of the heating element, we calculated a thermoelectric generator based on chromel-copel (L) thermocouples to power an external electric heater of 6CT-44A storage battery. As a heat source, a phase transition thermal accumulator was used, assuming its average temperature in the zone of contact with TEG (t_h) = 78.5 °C, the temperature of the cold junction (t_c) = 0 °C. The calculations used the method proposed in [13].

The purpose of the calculation is to determine the required number of series-connected *L* type thermocouples to ensure the operation of the external electric heater of storage battery.

The required number K of thermocouples in TEG, each of which having internal resistance *r* and thermoEMF e_t, was calculated by the formula (3):

$$K = \frac{U}{e_t - Ir} \tag{3}$$

where U is voltage on the load, V;
e_t is thermoEMF developed by thermocouple, V;
I is current flowing in the thermocouple circuit, A
r is internal resistance of thermocouple, Ohm.

Current flowing in the thermocouple circuit was calculated by the formula (4):

$$I = \frac{e_t}{r + R} \tag{4}$$

where R is load resistance, Ohm.

The internal resistance of thermocouple was calculated by the formula (5):

$$r = \frac{\rho_1 l}{s_1} + \frac{\rho_2 l}{s_2} \tag{5}$$

where ρ_1, ρ_2 are the resistivities of materials of which thermocouples are made, Ohm·mm^2/m;
l is the length of thermocouple conductor (assumed to be equal for both conductors), m;
s_1, s_2 are cross-sectional areas of thermocouple conductors, mm^2.

According to [14], the thermoEMF developed by thermocouple of L type is on the average 4.1 mV. According to [14], the resistivity of chromel metal alloy was assumed to be 0.038 Ohm•mm^2/m and the resistivity of copel alloy – 0.027 Ohm•mm^2/m, with the wire diameter 0.7 mm and the length of both thermocouple conductors assumed to be 0.02 m.

Based on the results of calculating the cross-sectional area of the thermocouple conductors, we obtained 0.38 mm^2.

According to formula (5), the resistance of thermocouple was determined as r = 0.0034 Ohm. Formula (4) was used to calculate current flowing in thermocouple circuit, I = 0.0014 A, formula (3) – to determine the required number of thermocouples in TEG, K ≈ 1200 pcs.

Conclusions

1. Based on the results of the studies, a system was proposed for compensating the heat losses of the battery during the maintenance of the vehicle at low temperatures by the thermostating method using thermoelectric energy converters.
2. The proposed technical solution makes it possible to generate electrical energy, both when the internal combustion engine is operating and when the vehicle is kept in open areas at low temperatures, using a phase transition heat accumulator as a heat exchanger, which accumulates the thermal energy of exhaust gases.
3. To power the external electric heater of a car battery, it is proposed to use a thermoelectric generator on chromel-copel (L) thermocouples.
4. According to the calculation results, to ensure thermoelectric stabilization of the optimal temperature of the 6ST-44A automobile battery, the required number of series-connected L type thermocouples was determined, to ensure the operation of an external electric heater with a total power of up to 9 W - about 1200 pieces.

References

1. Krokhta G.M., Usatykh N.A., Guskov Yu.A., Voronin D.M. (2016). Osobennosti raboty starternykh akkumuliatornykh batarei pri samoprogreve dvigatelia v zimnii period [Operating peculiarities of starter storage batteries during self-heating of the engine in winter]. *Dostizheniia nauki i tekhniki APK – Achievements of Science and Technology of Agro-Industrial Complex,* 30 (12), 94-97 [in Russian].
2. Timinskii V.I. (1985). *Spravochnik po elektrooborudovaniiu avtomobilei, traktorov, kombainov*

[Handbook of the electrical equipment of cars, tractors, combines]. Minsk: Uradzhai [in Russian].

3. Pankratov N.I. (1985). Ekspluatatsiia akkumuliatornykh batarei pri nizkikh temperaturakh [Operation of storage batteries at low temperatures]. *Avtomobilnyi Transport*, 2, 16–19 [in Russian].
4. Kajikawa T., Funahashi R. (2016). Recent activity on thermoelectric power generation technology in Japan. *J. Thermoelectricity*, 1, 5-15.
5. Anatychuk L.I., Prybyla A.V. (2016). Comparative analysis of thermoelectric and compression heat pumps for individual air-conditioners. *J.Thermoelectricity*, 2, 31-39.
6. Anatychuk L.I., Lysko V.V. (2019). On the possibility of using thermoelectric generators for high-power transport starting pre-heaters. *J.Thermoelectricity*, 3, 80-92.
7. Dmytrychenko M.F., Gutarevych Y.F., Trifonov D.M., Syrota O.V., Shuba E.V. (2018). On the prospects of using thermoelectric generators with the cold start system of an internal combustion engine with a thermal battery. *J.Thermoelectricity*, 4, 49-54.
8. *Patent of Ukraine №136638* (2019). Dmytrychenko M.F., Gutarevych Yu.F., Trifonov D.M., Syrota O.V., Shuba S.V. Thermoelectric system of thermal energy utilization with thermal accumulator of phase transition [in Ukrainian].
9. Zu-Guo Shen, Lin-Li Tian, Xun Liu. (2019). Automotive exhaust thermoelectric generators: Current status, challenges and future prospects. *Energy Conversion and Management*, 195, 1138-1173.
10. Bykov K.P., Shlenchik T.A. (2006). *Avtomobili "Tavria", "Slavuta" ZAZ-1102, ZAZ-1103, ZAZ-1105 i ikh modifikatsii. Ustroistvo, ekspluatatsiia, remont, posobiie po remontu. [Automobiles "Tavriia", "Slavuta" ZAZ-1102, ZAZ 1103, ZAZ 11-05 and their modifications. Design, operation, repair, repair manual]*. T.A.Shlenchik (Ed.). Chernigiv: PKF "Ranok" [in Russian].
11. Kashtanov V.P., Titov V.V., Uskov A.F. (1983). *Svintsovyie starternyie akkumuliatornyie batarei. Rukovodstvo [Lead starter batteries. Manual]*. Moscow [in Russian].
12. Kurzukov N.I., Yagniatinskii V.M. (2008). *Akkumuliatornyie batarei. Kratkii spravochnik. [Storage batteries. Quick reference book]*. Moscow: LLC "Book publishing house "Za rulem" [in Russian].
13. Bernshtein A.S. (1956). *Termoelektricheskiie generatory. Massovaia radio biblioteka. Vypusk 252 [Thermoelectric generators. Mass radio library. Issue 252]*. Moscow; Leningrad; Gosenergoizdat [in Russian].
14. *State Standards Committee of the USSR*. Wire made of chromel, alumel, kopel and constantan alloys for thermoelectrodes of thermoelectric converters. Technical Specifications. GOST 1790-77.

Submitted 20.07.2020

Дмитриченко М.Ф. *доктор техн. наук*
Гутаревич Ю.Ф. *доктор техн. наук*
Тріфонов Д.М. *канд. техн. наук*
Сирота О.В. *канд. техн. наук*

Національний транспортний університет
вул. М. Омеляновича-Павленка, 1, м. Київ,
01010, Україна, *e-mail: d.trifonov@ntu.edu.ua*

ЗАСТОСУВАННЯ ТЕРМОЕЛЕКТРИЧНИХ ПЕРЕТВОРЮВАЧІВ ЕНЕРГІЇ ДЛЯ ЗМЕНШЕННЯ ВПЛИВУ ПРИРОДНО-КЛІМАТИЧНИХ ФАКТОРІВ НА ТЕХНІЧНУ ГОТОВНІСТЬ ТРАНСПОРТНОГО ЗАСОБУ

У статті розглядається проблема, пов'язана з експлуатацією транспортного засобу в умовах низьких температур оточуючого повітря, обґрунтовується необхідність прийняття спеціальних заходів для підтримки оптимального теплового режиму акумуляторної батареї. Проведено аналіз факторів, що впливають на пуск холодного двигуна. Показано вплив низької температури акумуляторної батареї на енергетичні показники електростартерної системи пуску. Проведені розрахункові дослідження запропонованої системи для компенсації теплових втрат акумуляторної батареї під час утримання транспортного засобу в умовах низьких температур методом термостатування з застосуванням термоелектричних перетворювачів енергії. Бібл.14, рис.4, табл. 3.

Ключові слова: технічна готовність, акумуляторна батарея, термоелектричний генератор, тепловий акумулятор фазового переходу, електронагрівальні елементи.

Дмитриченко М.Ф., *доктор техн. наук*
Гутаревич Ю.Ф., *доктор техн. наук*
Трифонов Д.Н., *канд. техн. наук*
Сирота А.В., *канд. техн. наук*

Национальный транспортный университет
ул. М. Емельяновича-Павленко, 1, г. Киев, 01010, Украина,
e-mail: d.trifonov@ntu.edu.ua

ПРИМЕНЕНИЕ ТЕРМОЭЛЕКТРИЧЕСКОГО ПРЕОБРАЗОВАТЕЛЯ ЭНЕРГИИ ДЛЯ УМЕНЬШЕНИЯ ВЛИЯНИЯ ПРИРОДНО-КЛИМАТИЧЕСКИХ ФАКТОРОВ НА ТЕХНИЧЕСКУЮ ГОТОВНОСТЬ ТРАНСПОРТНОГО СРЕДСТВА

В статье рассматривается проблема, связанная с эксплуатацией транспортного средства в условиях низких температур окружающего воздуха, обосновывается необходимость принятия специальных мер для поддержания оптимального теплового режима аккумуляторной батареи. Проведен анализ факторов, влияющих на пуск холодного двигателя. Показано влияние низкой температуры аккумуляторной батареи на энергетические показатели электростартерной системы пуска. Проведены расчетные исследования предложенной системы для компенсации тепловых потерь аккумуляторной батареи во время содержания транспортного средства в условиях низких температур методом термостатирования с применением термоэлектрических преобразователей энергии. Библ.14, рис.4, табл. 3.

Ключевые слова: техническая готовность, аккумуляторная батарея, термоэлектрический генератор, тепловой аккумулятор фазового перехода, электронагревательные элементы.

References

1. Krokhta G.M., Usatykh N.A., Guskov Yu.A., Voronin D.M. (2016). Osobennosti raboty starternykh akkumuliatornykh batarei pri samoprogreve dvigatelia v zimnii period [Operating peculiarities of starter storage batteries during self-heating of the engine in winter]. *Dostizheniia nauki i tekhniki APK – Achievements of Science and Technology of Agro-Industrial Complex,* 30 (12), 94-97 [in Russian].
2. Timinskii V.I. (1985). *Spravochnik po elektrooborudovaniiu avtomobilei, traktorov, kombainov [Handbook of the electrical equipment of cars, tractors, combines].* Minsk: Uradzhai [in Russian].
3. Pankratov N.I. (1985). Ekspluatatsiia akkumuliatornykh batarei pri nizkikh temperaturakh [Operation of storage batteries at low temperatures]. *Avtomobilnyi Transport*, 2, 16–19 [in Russian].
4. Kajikawa T., Funahashi R. (2016). Recent activity on thermoelectric power generation technology in Japan. *J. Thermoelectricity*, 1, 5-15.
5. Anatychuk L.I., Prybyla A.V. (2016). Comparative analysis of thermoelectric and compression heat pumps for individual air-conditioners. *J.Thermoelectricity*, 2, 31-39.
6. Anatychuk L.I., Lysko V.V. (2019). On the possibility of using thermoelectric generators for high-power transport starting pre-heaters. *J.Thermoelectricity*, 3, 80-92.
7. Dmytrychenko M.F., Gutarevych Y.F., Trifonov D.M., Syrota O.V., Shuba E.V. (2018). On the prospects of using thermoelectric generators with the cold start system of an internal combustion engine with a thermal battery. *J.Thermoelectricity*, 4, 49-54.
8. *Patent of Ukraine №136638* (2019). Dmytrychenko M.F., Gutarevych Yu.F., Trifonov D.M., Syrota O.V., Shuba S.V. Thermoelectric system of thermal energy utilization with thermal accumulator of phase transition [in Ukrainian].
9. Zu-Guo Shen, Lin-Li Tian, Xun Liu. (2019). Automotive exhaust thermoelectric generators: Current status, challenges and future prospects. *Energy Conversion and Management*, 195, 1138-1173.

10. Bykov K.P., Shlenchik T.A. (2006). *Avtomobili "Tavria", "Slavuta" ZAZ-1102, ZAZ-1103, ZAZ-1105 i ikh modifikatsii. Ustroistvo, ekspluatatsiia, remont, posobiie po remontu. [Automobiles "Tavriia", "Slavuta" ZAZ-1102, ZAZ 1103, ZAZ 11-05 and their modifications. Design, operation, repair, repair manual]*. T.A.Shlenchik (Ed.). Chernigiv: PKF "Ranok" [in Russian].
11. Kashtanov V.P., Titov V.V., Uskov A.F. (1983). *Svintsovyie starternyie akkumuliatornyie batarei. Rukovodstvo [Lead starter batteries. Manual]*. Moscow [in Russian].
12. Kurzukov N.I., Yagniatinskii V.M. (2008). *Akkumuliatornyie batarei. Kratkii spravochnik. [Storage batteries. Quick reference book]*. Moscow: LLC "Book publishing house "Za rulem" [in Russian].
13. Bernshtein A.S. (1956). *Termoelektricheskiie generatory. Massovaia radio biblioteka. Vypusk 252 [Thermoelectric generators. Mass radio library. Issue 252]*. Moscow; Leningrad; Gosenergoizdat [in Russian].
14. *State Standards Committee of the USSR*. Wire made of chromel, alumel, kopel and constantan alloys for thermoelectrodes of thermoelectric converters. Technical Specifications. GOST 1790-77.

Submitted 20.07.2020

Анатичук Л.І.

L.I. Anatychuk *acad. National Academy of Sciences of Ukraine*[1,2]
R.V. Kuz *cand. phys. - math. Sciences*[1,2]

Кузь Р.В.

[1]Institute of Thermoelectricity of the NAS
and MES of Ukraine,
1, Nauky str., Chernivtsi, 58029, Ukraine;
[2]Yu.Fedkovych Chernivtsi National University,
2, Kotsiubynskyi str., Chernivtsi, 58000, Ukraine
e-mail: anatych@gmail.com

EFFECTIVENESS OF THERMOELECTRIC RECUPERATORS FOR RATIONAL TEMPERATURES OF HEAT SOURCES

The paper presents the results of analysis of thermoelectric recuperators of waste heat for the temperature range 100 -300^{O}C of the heat carrier. Based on computer model, optimization of sectional recuperators is carried out, the efficiency of each section and recuperator as a whole is calculated. The specific cost and payback time of sectional generators is calculated. Conclusions are made on the economic feasibility of using such recuperators. Bibl. 130, Fig. 9, Tabl. 1.
Key words: thermoelectric recuperator, waste heat, efficiency, power, specific cost.

Introduction

General characterization of the problem. Most types of equipment for technological processes in industry, heat engines (turbines, internal combustion engines, etc.) generate a large amount of waste heat during their operation. In so doing, more than half of this heat is not only not used in any way, but also leads to negative consequences for the environment – to its thermal pollution [1 – 4]. In this case, the majority of thermal waste (nearly 90 %) has temperature up to 300 °C (Fig. 1). This determines the relevance of creation of waste heat recuperators for this temperature level.

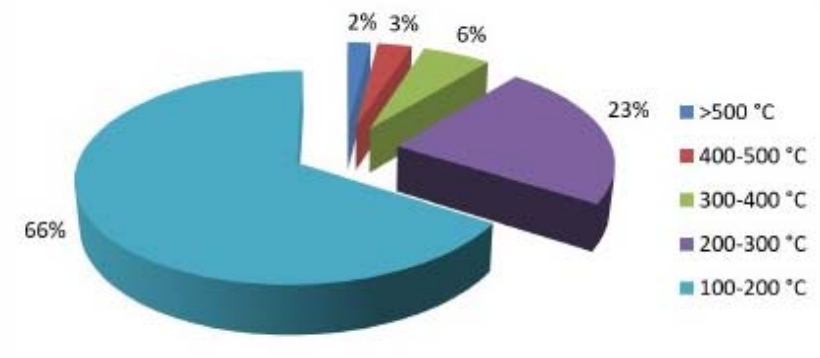

Fig. 1. Distribution of thermal waste sources by temperature range [6].

The most popular ways of thermal into electrical energy conversion are mechanical. Their characteristics are shown in the table. As is seen from the table, mechanical methods are efficient at

high temperatures. At low temperatures (up to 300°C) they considerably lose their effectiveness or do not work altogether. Another disadvantage is the need to use bulky equipment (boilers, evaporators, turbines). Under such circumstances, direct thermal into electrical energy conversion by means of thermoelectricity can become a competitive mechanical method.

Table.

Mechanical methods of waste heat conversion into electrical energy [7- 11]

№	Method	Efficiency	Operating temperatures	Electrical energy cost	Service life
1.	Rankine cycle	20-30 %	> 350 °C	0.8 – 1.8 $ / Wт	15 - 20 years
2.	Kalina cycle	~ 15 %	100 – 540 °C	1.2 – 1.8 $/Wт	20 - 30 years
3.	Organic Rankine cycle	~ 8-15 %	100 – 590 °C	1.4 – 2.2 $/W	20 - 30 years

Therefore, *the purpose of the work* is to establish general features that thermoelectric recuperators must meet, which will ensure their rational use.

Unlike thermoelectric generators which use costly heat sources and for which the main criterion of effectiveness is their efficiency, thermoelectric recuperators use waste heat. Therefore, to determine their effectiveness, it is necessary to apply other approaches, namely to establish their specific cost and payback time [129].

Known thermoelectric recuperators of waste heat

Based on the analysis of literature data, it is possible to identify the most common areas of using thermoelectric heat recuperators, namely industrial plants, internal combustion engines, thermal power plants, boilers, gas turbines, and domestic heat. Waste heat recuperators [43-51] from such energy-intensive industrial facilities as steel plants [26, 36-41, 54, 55], cement kilns [27-35, 38-40, 52, 54], glass furnaces [38-40, 52], furnaces for annealing lime [38, 39, 52], furnaces for the production of ethylene [38, 39], garbage recycling plants [104, 105], furnaces for smelting aluminum and other metals [38, 39, 52] are under active investigation.

Thus, the scientists of KELK Ltd. and JFE Steel Corporation (Japan) [36, 37] jointly developed and tested a thermoelectric recuperator using waste heat from a steel furnace. Its power is about 9 kW with the efficiency of 8%.

A thermoelectric recuperator using waste heat from a cement kiln was installed at the Awazu plant of Komatsu (Japan). The power of such a recuperator is about 10 kW. The waste heat recuperator from cement kilns [35] was also developed by scientists from Industrial Technology

Research Institute (Taiwan) and Institute of Thermoelectricity (Ukraine). The feature of this generator is its placement at some distance from the cement kiln which rotates, while it does not affect the technological processes inside the kiln. The project for waste heat recovery from garbage recycling plants using thermoelectricity was implemented jointly by Fujitaka (Japan) and Institute of Thermoelectricity (Ukraine) [104, 105].

A large number of publications are devoted to heat recovery from internal combustion engines of cars [28, 29, 52, 56 - 103] and motorcycles [28, 29]. However, it should be noted that the use of thermoelectric recuperators in cars has a number of disadvantages [60, 70, 71]. The real power gain is not significant enough. This leads to a search for more efficient applications of thermoelectricity. First of all, it looks promising to recover heat from diesel engines of large ships (in addition to high power, their advantage is the ability to remove heat from the thermoelectric converter to the surrounding water), as well as large trucks and special equipment [75, 80, 82, 93, 97]. There are also interesting works devoted to the use of thermoelectric recuperators in hybrid vehicles [71], where the energy generated during the operation of an internal combustion engine is used to recharge the batteries of the vehicle.

Ref.[106] presents the results of studies on a thermoelectric heat recuperator, which uses waste heat energy from power plants of Tokyo Electric Power. By joint efforts of the Komatsu Research Center and KELK [107], such a thermoelectric recuperator was created and its experimental studies were carried out.

In [38, 39], studies of a thermoelectric recuperator, which uses waste heat from industrial boilers, are presented. The efficiency of such a converter reaches 2%.

The Brno University of Technology (Czech Republic) has developed a thermoelectric recuperator for recovery of waste heat from a boiler, which uses biomass as a fuel [108].

The topic of heat recovery from gas turbines is discussed in [23, 110]. The exhaust gases from the turbine of pumping stations on gas mains were used as a source of thermal energy.

Refs. [111-115] present the results of development of a thermoelectric recuperator of heat from the combustion of biomass in a household kitchen stove. The temperature difference on thermoelectric modules is created on the one hand by flame, and on the other – by water tank.

One of the applications of thermoelectricity for waste heat recovery is a recuperator that uses waste heat from the biomass drying process [116]. The power generated by it is used to power the fans that circulate hot air in such a system.

Toshiba has developed a thermoelectric recuperator for an electric transformer [111].

Miniature thermoelectric recuperators used to power low-power equipment and sensors on board the aircraft are considered in [117-122]. Such devices are mounted under the wing of the aircraft and use the hot heat of the turbine.

It should be noted that heat recovery from stationary industrial plants (especially at temperatures below 600 K) is of great interest for thermoelectricity, since it allows one to fully realize its advantages. Estimates show that in the United States alone, about 3.300 TJ of energy are released annually from thousands of industrial processes [38, 53], some of which can be returned to active balance by direct thermoelectric energy conversion. Moreover, thermoelectric recuperators can be used not only to increase the overall efficiency of energy conversion, but also to provide backup power to the most critical units of industrial installations, which can significantly increase their reliability [23-25].

Determination of general properties of thermoelectric recuperators

Physical model of a thermoelectric sectional heat recuperator is shown in Fig.2.

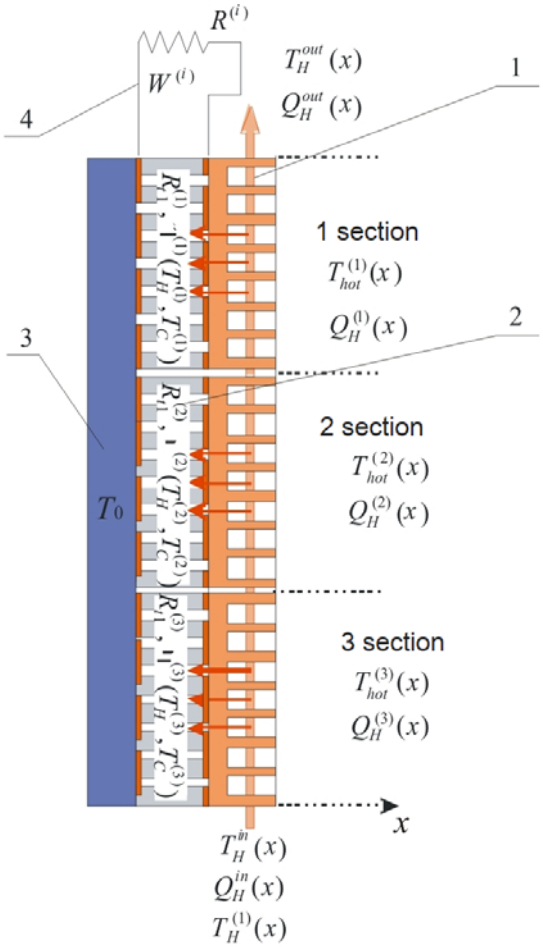

Fig. 2. Physical model of thermoelectric sectional heat recuperator:
1 – hot heat exchanger; 2 – thermopiles
3 – cold heat exchanger 4 – matched electrical load of the section.

Each section of the recuperator consists of hot heat exchanger (1), thermopile (2) with thermal resistance $R_{t2}^{(i)}$ and efficiency $\eta(T_H, T_0)$; cold heat exchanger (3) with temperature T_0. Thermopiles of each recuperator section are loaded on matched electrical load $R^{(i)}$ (4). Hot gas input flow has temperature T_H^{in} and thermal power Q_H^{in}. Hot gas gives part of heat $Q_H^{(i)}(x)$ at temperature $T_{hot}^{(i)}(x)$ to the hot heat exchanger. At the recuperator outlet the gas flow has temperature T_H^{out} and thermal power Q_H^{out}. From the hot heat exchanger heat is passed to the thermopile, heating its hot side to temperature $T_H^{(i)}(x)$. To calculate maximum possible recuperator power, we will ignore thermal losses. For the optimization of TEG it is necessary to find the distribution of temperatures and heat flows in thermopiles of each section. Such a calculation for this model was made through use of numerical computer methods.

To calculate the electrical power of TEG, we use the equation of energy balance in the form

$$W = \sum_{i=1}^{N}\left[\int\left(Q_H^{(i)}(x) - Q_C^{(i)}(x)\right)dx\right]. \qquad (1)$$

The necessary temperatures and heat flows are found from thermal conductivity equation

$$-\nabla\left(\kappa_{TE}(T)\nabla T\right) = Q_J, \qquad (2)$$

where κ_{TE} is effective thermal conductivity of thermopile, Q_J is the Joule heat which is released in the bulk of the thermopile.

The boundary conditions for (2) will be given by

$$Q_H^{in(1)} = Q_H^{in},\ Q_H^{in(i+1)} = Q_H^{out(i)},\ Q_H^{out(N)} = Q_H^{out}\ , \tag{3}$$

$$Q_H^{(i)}(x) = \left(T_H^{(i)}(x) - T^{(i)}(x)\right) / R_t^{(i)}\ , \tag{4}$$

$$Q_C^{(i)}(x) = \left(T_0\ (x) - T^{(i)}(x)\right) / R_{t2}^{(i)}\ , \tag{5}$$

The set of relations (1) - (5) makes it possible to determine the distribution of temperatures and heat flows in each of the sections

To restrict the hot temperature of the module, the thermal resistance between the hot heat exchanger and the thermoelectric module is determined from equation (4).

The power of each section and total efficiency of TEG can be found from equations

$$W^{(i)} = \int Q_H^{(i)}(x)\eta(T_H^{(i)}(x), T_0)dx\ , \tag{6}$$

$$\eta_{TEG} = \frac{1}{Q_H^{in}}\sum_{i=1}^{N} W^{(i)}\ . \tag{7}$$

The system of equations (1) - (5) was solved by numerical methods on a two-dimensional mesh of finite elements.

To calculate the efficiency of the thermoelectric recuperator, thermoelectric materials based on Bi-Te were selected which are one of the best in terms of quality in the considered temperature range [127].

At the first stage, the optimization of the hot temperatures of the recuperator sections was carried out (Fig. 3). Fig. 4 shows the relative number of thermoelectric modules of the same type in a section to achieve optimal temperature distribution.

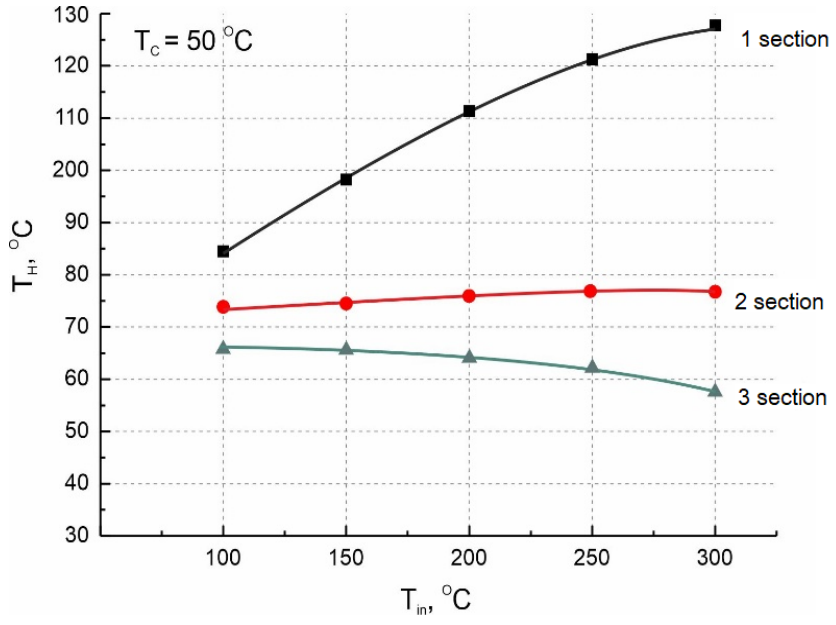

Fig. 3. Dependence of the optimal hot temperature of the sections on the temperature of heat carrier.

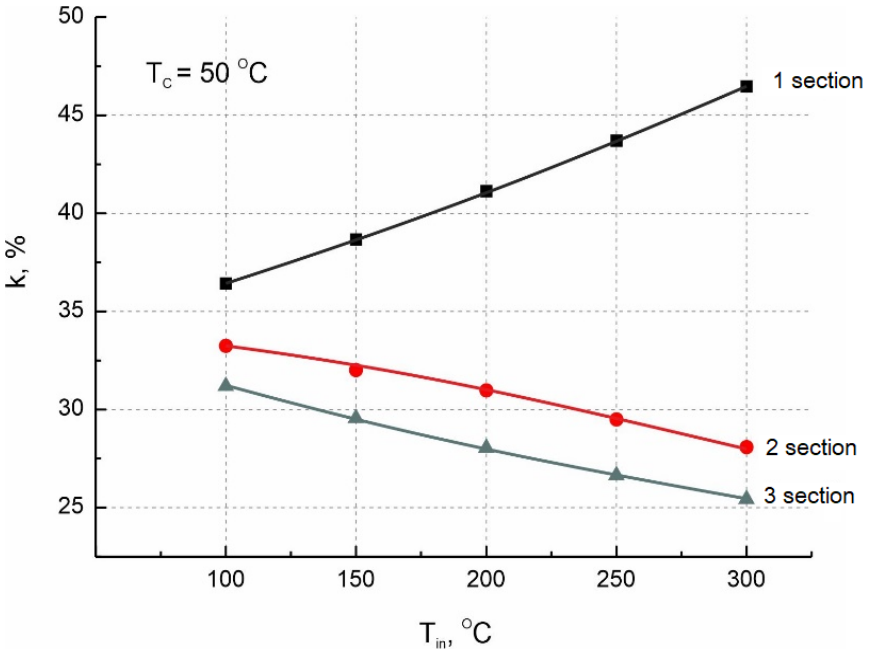

Fig. 4. Relative number of thermoelectric modules in a section to achieve optimal temperature distribution.

The next step is to determine the dependence of the efficiency of thermoelectric modules (Fig. 5) and the recuperator as a whole (Fig. 6) on the temperatures of the input heat carrier.

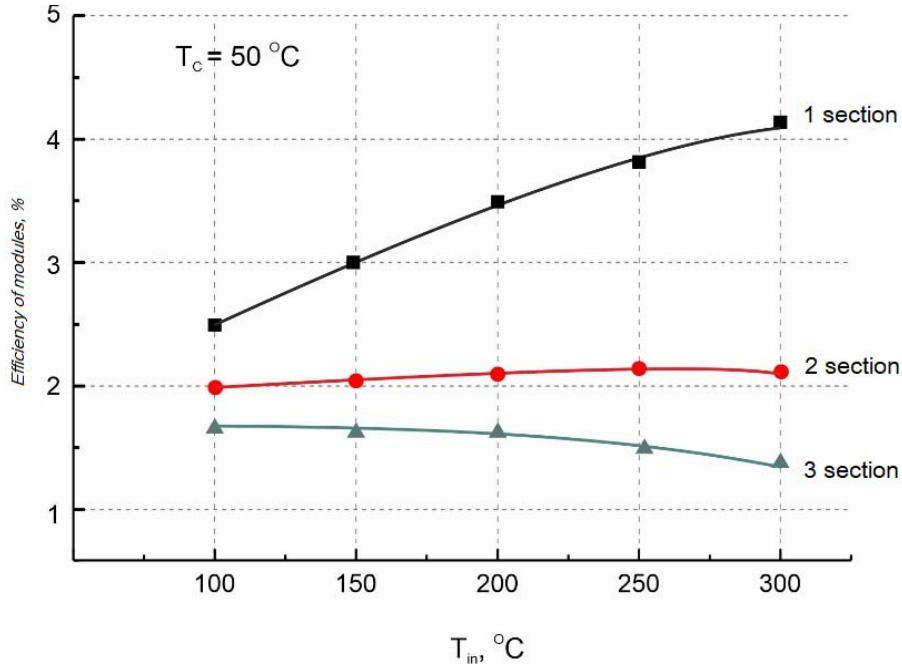

Fig. 5. Dependence of the efficiency of modules of sections on the temperature of inlet heat carrier.

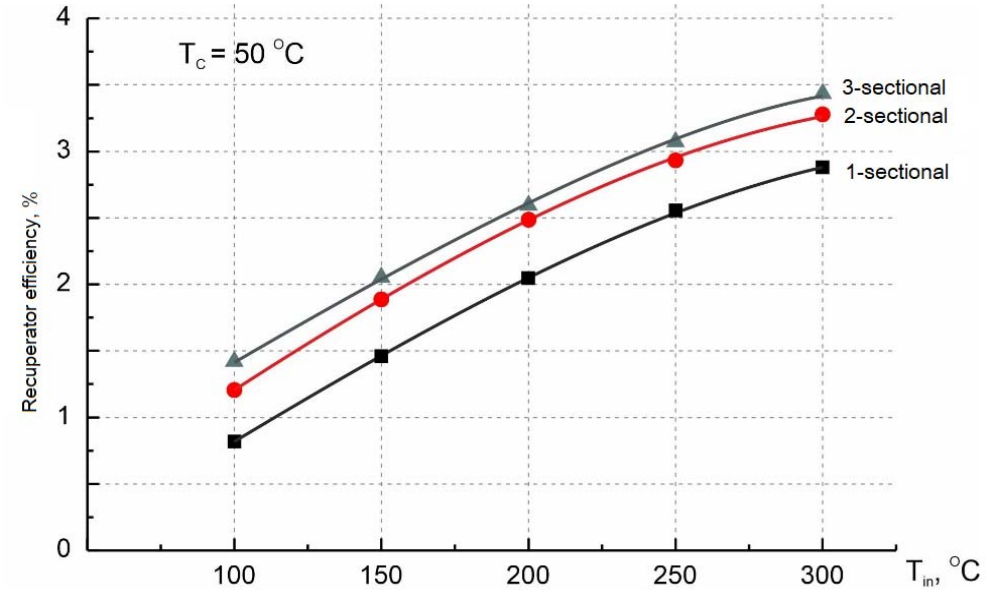

Fig. 6. Dependence of recuperator efficiency on the temperature of inlet heat carrier.

As is evident from Fig. 6, the use of the second section of the thermoelectric heat recuperator leads to an increase in efficiency by ~18%, and the third – only by 3%.

The percentage contribution of each section of thermoelectric heat recuperator to its total power is shown in Fig. 8. As can be seen from the figure, the percentage contribution of the first section of recuperator to total power is 85 – 90%, the second – 8 – 12%, the third – about 2%.

To assess the economic feasibility of using a thermoelectric recuperator, its specific cost was calculated (Fig. 8), based on the results obtained in [128]. As can be seen from the figure, the use of the third section in the considered temperature range is not economically feasible. The use of the second section is also questionable.

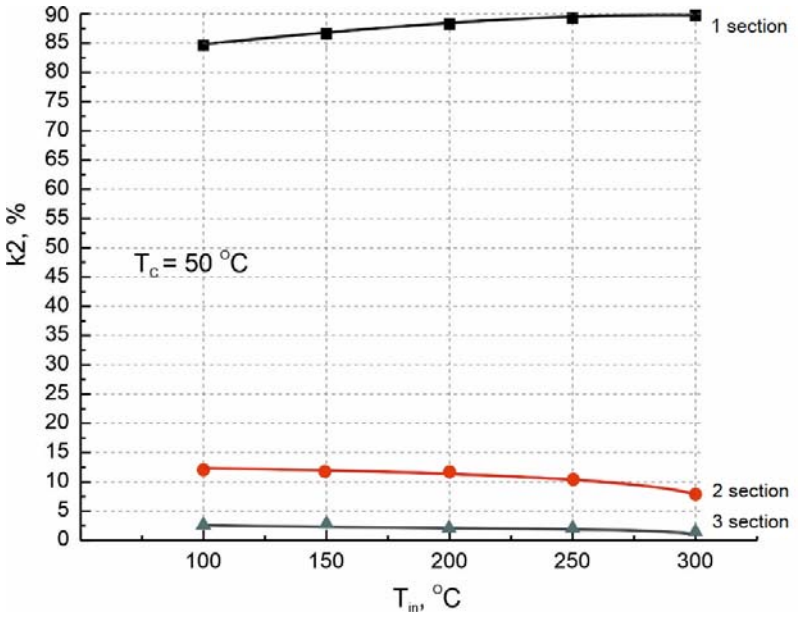

Fig. 7. Contribution of each section to total power of recuperator.

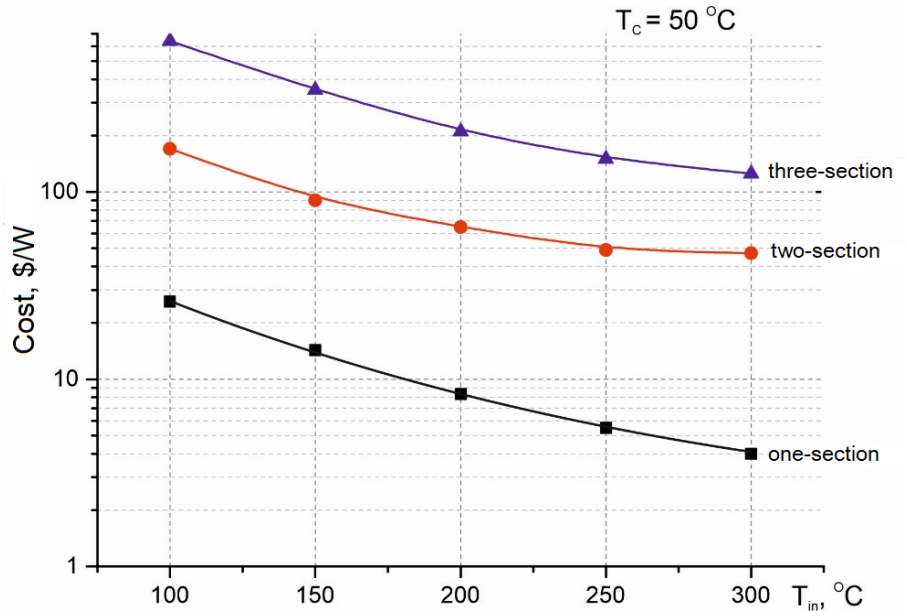

Fig. 8. Specific cost of sectional recuperators.

For a better understanding of the economic efficiency of thermoelectric recuperators, we will calculate their payback time, based on a comparison of the cost of their electrical energy with the cost of industrial electrical energy. Fig. 9 shows the results of such calculations. For example, a comparison was made with the average cost of electricity in Ukraine 0.12 $ / (kWh) (according to the data of the company Ukrenergo [130]).

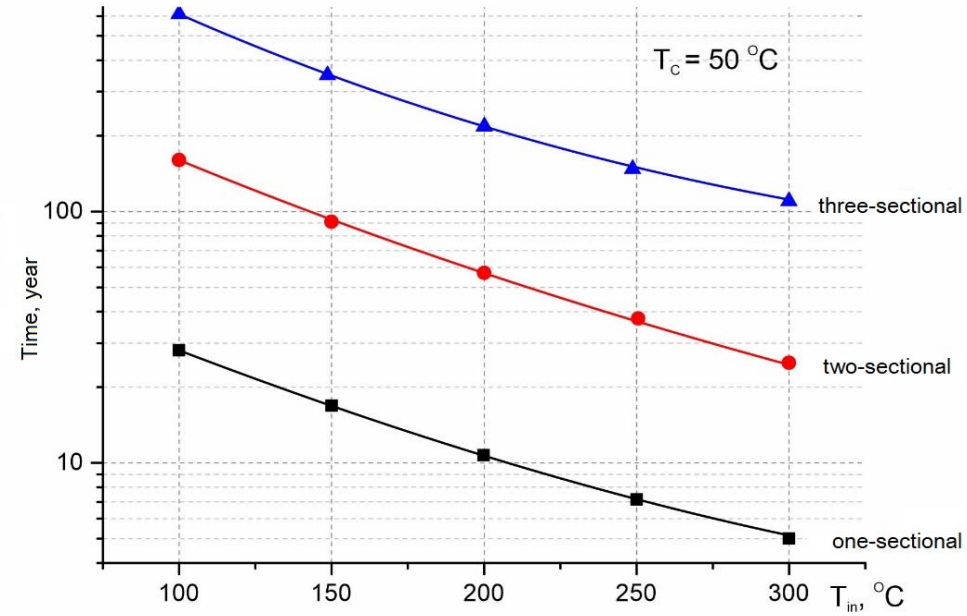

Fig. 9. Payback time of sectional recuperators.

From the analysis of Fig. 9 it becomes clear that for the specified temperature range (100 - 300 ° C) it is economically feasible to use only one section. A small gain in power when using other sections does not cover material costs.

Conclusions

1. The dependences of the optimal temperatures of the recuperator sections on the inlet gas temperature in the range from 100 to 600 ° C are established. For the first section from 37 to 47 ^{O}C, the second - from 33 to 27 ^{O}C, the third - from 32 to 25 ^{O}C.
2. The number of thermoelectric converters in each section is determined to achieve the optimal temperature distribution in the sections. For low inlet gas temperatures the number of thermocouples in the sections is approximately the same. With a rise in temperature, the share of thermocouples in the first section increases.
3. The specific cost of a thermoelectric recuperator and its payback time are calculated. It is shown that the cost of each subsequent section is approximately an order of magnitude greater than the cost of the previous one. Therefore, for the range of hot temperatures of the heat carrier 100-300^{O}C it is economically feasible to use only one section.

References

1. Rowe, M.D., Gao Min, Williams, S.G.K., Aoune A., Matsuura K., Kuznetsov V.L., Li Wen Fu. (1997). Thermoelectric recovery of waste heat-case studies. *Energy Conversion Engineering Conference* (1997, vol.2, 1075 – 1079).
2. Basic research needs for solar energy utilization. Report of the Basic Energy Sciences Workshop on Solar Energy Utilization. USA: DOE, April 18−21, 2005.
3. European Commission. Energy. Energy 2020: *Roadmap* 2050. – http://ec.europa.eu/energy/energy2020/roadmap/index_en.htm.
4. Paniakin V. (2010). Kogeneratsiia: Kak eto rabotaiet [Cogeneration: How it works]. *Seti i biznes – Networks and Business*, 4 [in Russian].
5. Waste heat recovery:technology and opportunities in U.S. industry. *Report of BCS, Incorporated*, USA. – 2008.
6. Cynthia Haddad, et al. (2014). Some efficient solutions to recover low and medium waste heat: competitiveness of the thermoacoustic technology. *Energy Procedia*, 50, 1056 – 1069.
7. Thekdi, Arvind C. (2007). Waste heat to power economic tradeoffs and considerations. *Proc. of the 3rd Annual Waste Heat to Power Workshop* (USA, 2007).
8. Paul Cunningham P.E. (2002). Waste heat/cogen opportunities in the cement industry. *Cogeneration and Competitive Power Journal*, 17 (3), 31-51.
9. Quoilinetal S. (2013). Techno-economic survey of organic Rankine cycle (ORC) systems. *Renewable and Sustainable Energy Reviews*, 22, 68–186.
10. Zhang C., et al. (2017). Implementation of industrial waste heat to power in Southeast Asia: an outlook from the perspective of market potentials, opportunities and success catalysts. *Energy Policy*, 106, 525–535.
11. Milewskia Jarosław, Krasuckib Janusz (2017). Comparison of ORC and Kalina cycles for waste heat recovery in the steel industry. *Journal of Power Technologies*, 97 (4), 302–307.
12. Anatychuk L.I. (1979). *Termoelementy i termoelektricheskiie ustroistva: Spravochnik [Thermoelements and thermoelectric devices: Reference book]*. Kyiv: Naukova dumka [in Russian].
13. Bernshteyn A.S. (1956). Termoelektricheskiie generatory [Thermoelectric generators]. Moscow: Gosenergoizdat [in Russian].
14. Anatychuk L.I. (2001). Rational areas of research and applications of thermoelectricity.

J.Thermoelectricity, 1, 3 – 14.

15. Anatychuk L.I. (2007). Current state and some prospects of thermoelectricity. *J.Thermoelectricity*, 2, 7 – 20.
16. Freik D.M., Nykyrui L.I., Krynytskyi O.S. (2012). Dosiahnennia i problemy termoelektryky [Achievements and problems of thermoelectricity]. *Fizyka i khimiia tverdoho tila - Physics and Chemistry of Solid State*, 13(2), 297-318 [in Ukrainian].
17. Y. Chen, et al. (2006). A comparative study of the carbon dioxide transcritical power cycle compared with an organic Rankine cycle with R123 as working fluid in waste heat recovery. *Applied Thermal Engineering*. 26, 2142–2147.
18. Zhang X., Wu L., Wang X., Ju G. (2016). Comparative study of waste heat steam SRC, ORC and S-ORC power generation systems in medium-low temperature. *Applied Thermal Engineering*. doi: http://dx.doi.org/10.1016/j.applthermaleng.2016.06.108
19. Kishore R.A., Priya S. (2018). A review on low-grade thermal energy harvesting: materials, methods and devices. *Materials*, 11 (8), 1433. doi:10.3390/ma11081433.
20. Aladayleh Wail, Alahmer Ali. (2015). Recovery of exhaust waste heat for ICE using the beta type Stirling engine. *Journal of Energy*. Article ID 495418, https://doi.org/10.1155/2015/495418.
21. Takahashi Y., Yamamoto K., Nishikawa M. (2006). Fundamental performance of triple magnetic circuit type cylindrical thermomagnetic engine. *Electrical Engineering in Japan*, 154 (4).
22. Huffman F.N., Sommer A.H., Balestra C.L., Briere D.P., Oettinger P.E. (1976). High efficiency thermionic converter studies. *NASA Technical Report. – NASA-CR-135125*.
23. Anatychuk L.I., Prybyla A.V. (2012). Thermoelectric heat recuperator for gas turbines. *XIII Interstate Workshop "Thermoelectrics and their applications"* (Russia, Saint-Petersburg, November 13-14, 2012).
24. Malygin N.D., Stoianov V.U. (2004). Primeneniie termoelektricheskogo generatora v istochnike bespereboinogo pitaniia povyshennoi nadezhnosti dlia osobo vazhnykh potrebitelei [The use of thermoelectric generator in high reliability uninterupted supply for critical consumers]. *Stroitelstvo i tekhnogennaia bezopasnost'*, 9, 153 – 156 [in Russian].
25. Shostakovskiy P. (2013). Alternativnyie istochniki elektricheskoi energii promyshlennogo primeneniia na osnove termoelektricheskikh generatorov [Alternative sources of electric energy for industrial use based on thermoelectric generators]. *Control Engineering Russia*, 3 (45), 52 – 56 [in Russian].
26. Anatychuk L.I., Hwang J.D., Chu H.S., Hsieh H.L. (2011). The design and application of thermoelectric generators on the waste heat recovery of heating furnace in steel industry. *XIV International Forum on Thermoelectricity (May 17-20, 2011, Russian Federation, Moscow).*
27. Kaibe H., Kaijihara T., Fujimoto S., Makino K., Hachiuma H. (2011) Recovery of plant waste heat by a thermoelectric generating system [S. Sano] *KOMATSU technical report*, 57(164), 26 – 30.
28. Kajikawa T. (2010). Thermoelectric application for power generation in Japan. *Advances in Science and Technology*, 74, 83-92.
29. Kajikawa T. (2011). Advances In thermoelectric power generation technology in Japan. *J. of Thermoelectricity*, 3 (5 – 19).
30. Kaibe H., Fujimoto S., Mizukami H., Morimoto S. (2010). Field test of thermoelectric generating system at Komatsu Plant. *Proceedings of Automotive 2010, Berlin (2010.12).*
31. Kaibe H., Fujimoto S., Kajihara T., Makino K., Hachiuma H. (2011). Thermoelectric generating system attached to a carburizing furnace at Komatsu Ltd., Awazu Plant. *Proc of 9th European Conference on Thermoelectrics (Thessaloniki, Greece, September 2011, 201E_10_O.)*

32. Kaibe H., Makino K., Kajihara K., Fujimoto S. and Hachiuma H. (2012). Thermoelectric generating system attached to a carburizing furnace at Komatsu Ltd., Awazu Plant. *AIP Conf. Proc. 1449, 524*; http://dx.doi.org.sci-hub.org/10.1063/1.4731609.
33. Kaibe H., Makino K., Kajihara K., Lee Y.-H. and Hachiuma H. *Study of thermoelectric generation unit for radiant waste heat.*
34. Kaibe H., Kajihara T., Nagano K., Makino K., Hachiuma H., Natsuume D. (2014). Power delivery from an actual thermoelectric generation system. *Journal of Electronic Materials*.
35. Anatychuk L.I., Hwang Jenn-Dong, Lysko V.V., Prybyla A.V. (2013). Thermoelectric heat recuperators for cement kilns. *J.Thermoelectricity*, 5, 39-45.
36. Kuroki T., Kabeya K., Makino K., Kajihara T., Kaibe H., Hachiuma H., Matsuno H. (2014). Thermoelectric generation using heat in steal works. *Journal of Electronic Materials.*
37. Amaldi A., Tang F. (2014). *Proceedings of the 11th European conference on thermoelectrics : ECT 2013. Chapter 17. Waste heat recovery in steelworks using a thermoelectric generator.* Springer, 143-149.
38. Hendricks T. and Choate W.T. (2006). *Engineering Scoping Study of Thermoelectric Generator Systems for Industrial Waste Heat recovery* (Washington, D.C.: Industrial Technologies Program, U.S. Department of Energy, 2006), 1–76.
39. Waste heat recovery: Technology and opportunities in U.S. industry.– *U.S. department of energy: Industrial technologies program*, 2008, 112.
40. Waste heat to power systems.– Combined heat and power partnership. *U.S. environmental protection agency*, 2012, 9.
41. Villar A., Arribas J. (2012). Waste-to-energy thechnologies in continuous process industries. *Clean Techn Environ Policy*, 14, 29-39.
42. Joshi J., Patel N. (2012). Thermoelectric system to generate electricity from waste heat of the flue gases. *Advances in Applied Science Research*, 3(2), 1077-1084.
43. Amaldi A., Tang F. (2014). *Proceedings of the 11th European conference on thermoelectrics : ECT 2013. Chapter 26. Modeling and design of tubular thermoelectric generator used for waste heat recovery.* Springer.
44. Zhang Y., D'Angelo J., Wang X.,Yang J. (2012) Multi-physics modeling of thermoelectric generators for waste heat recovery applications. *(DEER Conference, Michigan).*
45. Faraji A., Singh R., Mochizuki M., Akbarzadeh A. (2013). Design and numerical simulation of a symbiotic thermoelectric generation system fed by a low-grade heat sorce. *Journal of Electronic Materials*.
46. Brazdil M., Pospisil J. (2012). A way tox use waste heat to generate thermoelectric power. *Acta Polytechnica*, 52(4), 21-25.
47. Qiu K., Hayden A. (2009). A natural-gas-fired thermoelectric power generation system. *Journal of Electronic Materials*, 38(7).
48. Ono K., Suzuki R. (1998). Thermoelectric power generation: Converting low-grade heat into electricity. *JOM*, 49-51.
49. Sasaki K., Horikawa D., Goto K. (2014). Consideration of thermoelectric power generation by using hot spring thermal energy or industrial waste heat. *Journal of Electronic Materials*.
50. Miller E., Hendricks T., Peterson R. (2009). Modeling energy recovery using thermoelectric conversion with an organic Rankine bottomig cycle. *Journal of Electronic Materials*, 38(7).
51. Miller E. (2010). Integrated dual cycle energy recovery using thermoelectric conversion with an organic Rankine bottomig cycle. *An abstract of the thesis for the degree of Master of Science in*

mechanical engineering.
52. Fleurial J.-P., Gogna P., Li, B.C-Y., Firdosy S., Chen B.J., Huang C.-K., Ravi V., Caillat T., Star K.(2009). Waste heat recovery opportunities for thermoelectric generator. *Thermoelectric Applications Workshop.*
53. Energy Use, Loss and Oppor tunity Analysis: U. S. Manufacturing and Mining, December 2004, Energetics, Inc., E3M, Incorporated, page 10.
54. Hachiuma H. (2013). Thermoelectric energy harvesting for industrial waste heat recovery. *Energy Harvesting and Storage USA*.
55. Anatychuk L.I., Jenn-Dong Hwang, Prybyla A.V. (2010). Thermoelectric generator for conversion of heat from gas rolling furnaces. *29-th International Conference on Thermoelectrics* (China, Shanghai).
56. Saqr K.M., Mansour M.K., Musa M.N. (2008). Thermal design of automobile exhaust based thermoelectric generators: objectives and challenges. *J.Thermoelectricity*, 1, 64 – 73.
57. Anatychuk L.I., Kuz R.V. (2014). Effect of air cooling on the efficiency of sectional thermoelectric generator in a car with a diesel engine. *J.Thermoelectricity*, 4, 84 – 91.
58. Anatychuk L.I., Kuz R.V. (2014). Effect of air cooling on the efficiency of thermoelectric generator in a diesel-engined car. *J.Thermoelectricity*, 2, 61 – 69.
59. Anatychuk L.I., Kuz R.V. (2014). Effect of air cooling on the efficiency of a thermoelectric generator in a car with a petrol engine. *J. Thermoelectricity*, 3, 84 – 87.
60. Korzhuev M.A., Svechnikova T.E. (2013). Thermodynamic restrictions for the net power of automotive thermoelectric generators and prospects of their use in transport. *J.Thermoelectricity*, 3, 58 – 73.
61. Saqr K.M., Mansour M.K., and Musa M.N. (2008). Thermal design of automobile exhaust-based thermoelectric generators: objectivities and challenges. *International J. Automotive Technology*, 9(2), 155-160.
62. Rowe D.M., Smith J., Thomas G. and Min G. (2011). Weight penalty incurred in thermoelectric recovery of automobile exhaust heat. *J. Electronic Materials*, 40 (5), 784-788.
63. Lieb J., Neugebauer S., Eger A., Linde M., Masar B., Stűtz W. (2009). The thermoelectric generator from BMW is making use of waste heat. *MTZ*, 70 (4), 4-11.
64. Eger A., Linde M. (2011). The BMW Group. Roadmap for the application of thermoelectric generators (San Diego, 2011), 23 p.
65. Espinosa N., Lazard M., Aixala L., and Scherrer H. (2010). Modeling thermoelectric generator applied to diesel automotive heat recovery. *JEMS* 39 (9), 1446-1455.
66. Anatychuk L.I., Luste O.J., and Kuz R.V. (2011). Theoretical and experimental study of thermoelectric generators for vehicles. *JEMS* 40(5), 1326-1331.
67. Anatychuk L.I., Luste O.J., and Kuz R.V. (2011). Theoretical and experimental study of thermoelectric generators for vehicles. *JEMS* 40 (5), 1326-1331.
68. Fairbanks W. (2011). Development of automotive thermoelectric generators and air conditioner / heaters. Proceedings of XIV International Forum on Thermoelectricity (Moscow 17-20.05.2011), [On line:http://forum.inst.cv.ua/].
69. Anatychuk L.I., Kuz R.V., Rozver Yu.Yu. (2012). Thermoelectric generator for petrol engine. *J.Thermoelectricity*, 2, 81 – 94.
70. Fainzilber E.M., Drabkin L.M. (1966). Ispolzovaniie tepla otrabotavshikh gazov dvigatelei v termoelektricheskom generatore dlia pitaniia elementov elektrooborudovaniia avtomobilei [Use of heat from exhaust gases of engines in a thermo-electric generator for powering elements of electrical equipment of cars]. *Avtomobilnaya promyshlennost*, 7, 9 – 10 [in Russian].

71. Korzhuev M.A., Granatkina Yu.V. (2012). Some bottlenecks of automobile thermoelectric generators and search for new materials to eliminate them. *J.Thermoelectricity*, 1, 81 – 94.
72. Korzhuev M.A. (2011). On the conflict of internal combustion engines and thermoelectric generators in the recovery of heat losses in cars. *Letters to JTP*, 37(4), 8 – 15.
73. Anatychuk L.I., Kuz R.V., Rozver Yu.Yu. (2011). Efficiency of thermoelectric recuperators of the exhaust gas heat of internal combustion engines. *J.Thermoelectricity*, 4, 80-85.
74. Anatychuk L.I., Rozver Yu.Yu., Misawa K., and Suzuki N. (1997). Thermal generators for waste heat utilization. *Proc. of 16th International Conference on Thermoelectrics* (Dresden, 1997), p. 586 – 587.
75. Zhang X., Chau K.T., and Chan C.C. (2008). Overview of thermoelectric generation for hybrid vehicles. *J. Asian Electric Vehicles,* 6 (2), 1119 – 1124.
76. Elsner N., Bass J., Ghamaty S., Krommenhoek D., Kushch A., and Snowden D. (2005). Diesel truck thermoelectric generator. Advanced combustion engine technologies. *FY 2005 Progress Report*, p. 301 – 305.
77. Yang Jihui, Seker F., Venkatasubramanian R., Nolas G.S., Uher C., and Wang H. (2006). Developing thermoelectric technology for automotive waste heat recovery. Advanced combustion engine technologies. *FY 2006 Progress Report*, p. 227 – 231.
78. Ikoma K., Munekiyo M., Furuya K., Kobayashi M., Izumi T., and Shinohara K. (1998). Thermoelectric module and generator for gasoline engine vehicles. *Proc. ICT'98. XVII International Conference on Thermoelectrics* (Nagoya, Japan, 1998), p. 464 – 467.
79. Takanose E., Tamakoshi H. (1993). The development of thermoelectric generator for passenger car. *Proc.12th International Conference on Thermoelectrics* (Yokohama, Japan, 1993), p. 467 – 470.
80. Stabler F. (2002). Automotive application of hight efficiency thermoelectrics. DARPA/ONR Program rewiew and DOE hight efficiency thermoelectric workshop. (San Diego (CA), March 24-27).
81. Bass J. et al. (1992). Thermoelectric generator development for heavy-duty truck applications. *Proceedings of Annual Automotive Technology Development Contractors Coordination Meeting* (Dearborn (USA). – P. 743-748.
82. Bass J. et al. (1995). Performance 1 kW thermoelectric generator for diesel engines. *Proc. AIP Conference*, P. 295-298.
83. Thacher E. F., Helenbrook B. T., Karri M. A. and Richter C. J. (2007). Testing an automobile thermoelectric exhaust based thermoelectric generator in a light truck. Proceedings of the I MECH E Part D. *Journal of Automobile Engineering*, 221(1), 95-107(13).
84. Kushch A., Karri M. A., Helenbrook B. T. and Richter C. J. (2004). The effects of an exhaust thermoelectric generator of a GM Sierra pickup truck. *Proceedings of Diesel Engine Emission Reduction (DEER) Conference* (Coronado, California, USA).
85. Jadhao J., Thombare D. (2013). Rewiew on exhaust gas heat recovery for I.C. engine. *International Journal of Engineering and Innovate Technology*, 2(12), 93-100.
86. Baker C., Vuppuluri P., Shi L., Hall M. (2012). Model of heat exchangers for waste heat recovery from diesel engine exhaust for thermoelectric power generation. *Journal of Electronic Materials*, 41(6).
87. Kim S., Won B., Rhi S., Kim S.H., Yoo J. (2011). Thermoelectric power generation system for future hybrid vehicles using hot exhaust gas. *Journal of Electronic Materials*, 40(5).
88. Su C., Ye B., Guo X., Hui P. (2012). Acoustic optimization of automotive exhaust heat

thermoelectric generator. *Journal of Electronic Materials*, 41(6).

89. Deng Y., Zhang Y., Su C. (2014). Modular analysis of automotive exhaust thermoelectric power generation system. *Journal of Electronic Materials*.
90. Quan R., Tang X., Quan S., Huang L. (2013). A novel optimization method for the electric topology of thermoelectric modules used in an automobile exhaust thermoelectric generator. *Journal of Electronic Materials*, 42(7).
91. Fleurial G.-P. (2009). Thermoelectric power generation materials: technology and application opportunities. *JOM*, 61(4), 79-85.
92. Kumar C., Sonthalia A., Goel R. (2011). Experimental study on waste heat recovery from an IC Engine using thermoelectric technology. *Thermal Science*, 15(4), 1011-1022.
93. Vázquez, J., et al., State of the art of thermoelectric generators based on heat recovered from the exhaust gases of automobiles. *Proceedings of 7th European Workshop on Thermoelectrics*, Paper 17 (Pamplona, Spain, 2002).
94. Wojciechowski K.T., Zybala R., Leszczynski J., Nieroda P., Schmidt M., Merkisz J., Lijewski P., Fuc P. (2012). Analysis of possibilities of waste heat recovery in off-road vehicles. *AIP Conf. Proc*., 1449, 501 – 504.
95. Wojciechowski K. T., Zybala R., Tomankiewicz J., Fuc P., Lijewski P., Wojciechowski J., Merkisz J. (2012). Influence of back pressure on net efficiency of TEG generator mounted in the exhaust system of a diesel engine, published in book: *Thermoelectrics Goes Automotive II.* Daniel Jänsch (Ed.). Expert Verlag.
96. Baskar P., Seralathan S., Dipin D., Thangavel S. (2014). Experimental analysis of thermoelectric waste heat recovery system retrofitted to two stroke petrol engine. *International Journal of Advanced Mechanical Engineering,* 4(1), 9-14.
97. LaGrandeur J., Crane D., Hung S. (2006). Hight-efficiency thermoelectric waste energy recovery system for passenger vehicle application. *Advanced Combustion Engine Technologies*. *FY 2006 Progress Report,* p. 232 – 236.
98. Willigan R., Hautman D., Krommenhoek D., Martin P. (2006). Cost-effective fabrication routes for the production of quantun well structures and recovery of waste heat from heavy duty trucks. Advanced Combustion Engine Technologies. *FY 2006 Progress Report*.
99. Nelson C. (2006). Exhaust energy recovery. Advanced Combustion Engine Technologies. *FY 2006 Progress Report*, p. 247 – 250.
100. Schock H., Case E., Downey A. (2006)ю Thermoelectric conversion of waste heat to electricity in an IC engine powered vehicle. Advanced Combustion Engine Technologies. *FY 2006 Progress Report*, p. 242 – 246.
101. Shu G., Zhao J., Tian H., Liang X., Wei H. (2012). Parametric and exergetic analysis of waste heat recovery system based on thermoelectric generator and organic rankine cycle utilizing R123. *Energy*, 45, 806-816.
102. J. Merkisz, P. Fuc, P. Lijewski, A. Ziolkowski, K. Wojciechowski (2014). The analysis of exhaust gas thermal energy recovery through a TEG generator in city traffic conditions reproduced on a dynamic engine test bed. *Journal of Electronic Materials*.
103. Nadaf S.L., Gangavat P.B. (2014). A review on waste heat recovery and utilization from diesel engines. *International Journal of Engineering and Innovate Technology*, 5(4), 31-39.
104. Noor A., Puteh R., Rajoo S. (2014). Waste heat recovery technologies in turbocharged automotive engine – A Review. Journal of Modern Science and Technology, 2(1), 108-119.
105. Anatychuk. L.I., Rozver. Yu.Yu., Misawa. K., Suzuki. N. (1997). Thermal generators for waste heat utilization. *Report on ICT'97*.

106. Anatychuk L.I., Razinkov V.V., Rozver Yu. Yu., Mikhailovsky V.Ya.(1997). Thermoelectric generator modules and blocks. *Report on ICT'97*.
107. Uemura K. (2002). History of thermoelectricity development in Japan. *J. of Thermoelectricity*, 3, 7 – 16.
108. Ohba R. and Nakamura S. (1986). Wind tunnel experiment of gas diffusion in thermally stratified flow. *Proc. 3rd Int. Workshop on Wind & Water Tunnel Modelling Atmospheric Flow & Dispersion* (Lausanne, YMG-1, 1986).
109. Brazdil M., Pospil J. (2013). Thermoelectric power generation utilizing the waste heat from a biomass boiler. *Journal of Electronic Materials*, 42(7).
110. *Characterization of the U.S. Industrial/Commercial boiler population.* Oak Ridge National Laboratory, May 2005. Prepared by Energy and Enviromental Analysis, Inc.
111. Anatychuk L.I., Morozov V.I., Mitin V.P., Prybyla A.V. (2012). Thermoelectric recupirator for gas turbines. *31-th International and 10-th European Conference on Thermoelectrics* (Aalborg, Denmark).
112. Date As., Date Ab., Dixon C., Akbarzadeh A. (2014). Progress of thermoelectric power generation systems: Prospect for small to medium scale power generation. *Renewable and Sustainable Energy Reviews*, 33, 371-381.
113. Champier D, Bedecarrats JP, Rivaletto M, Strub F. (2010). Thermoelectric power generation from biomass cook stoves. *Energy*, 35(2), 935–42.
114. Nuwayhid R.Y., Rowe D.M., Min G. (2003). Low cost stove-top thermoelectric generator for regions with unreliable electricity supply. *Renew Energy*, 28 (2), 205–22.
115. Nuwayhid RY, Shihadeh A, Ghaddar N. (2005). Development and testing of a domestic woodstove thermoelectric generator with natural convection cooling. *Energy Convers Manag*, 46(9–10), 1631–43.
116. Lertsatitthanakorn C. (2007). Electrical performance analysis and economic evaluation of combined biomass cook stove thermoelectric (BITE) generator. *Bioresour Technol*, 98(8), 1670–4.
117. Maneewan S., Chindaruksa S. (2009). Thermoelectric power generation using waste heat from a biomass drying. *Journal of Electronic Materials*, 38, 7.
118. Elefsiniotis A., Becker Th., Schmid U. (2013). Thermoelectric energy harvesting using phase change materials in high temperature enviroments in aircraft. *Journal of Electronic Materials*, 43 (6).
119. Elefsiniotis A., Kiziroglou M., Wright S., Becker Th., Yeatman E., Schmid U. (2013). Performance evaluation of a thermoelectric energy harvesting device using various change materials. *Journal of Physics: Conference Series*, 476.
120. Elefsiniotis A., Kokorakis N., Becker Th., Schmid U. (2014). A novel high-temperature aircraft-specific energy harvester using PCMs and state of the art TEGs. *12-th European Conference on Thermoelectrics*.
121. Samson D, Kluge M., Fuss T., Becker Th., Schmid U. (2012). Flight test results of a thermoelectric energy harvester for aircraft. *Journal of Electronic Materials*, 41 (6).
122. Elefsiniotis A., Weiss M., Becker Th., Schmid U. (2013). Efficient power management for energy-autonomous wireless sensor nodes for aeronautical application. *Journal of Electronic Materials*, 42 (7).
123. Samson D, Kluge M., Otterpohl T., Becker Th., Schmid U. (2010). Aircraft-specific thermoelectric generator module. *Journal of Electronic Materials*, 39(9).

124. Shan Yeung (2010). Thermoelectricity: Experiments, Application and Modelling.– *An abstract of the Thesis for the Degree of Master of Science in materials engineering and nanotechnology.*
125. http://kryothermtec.com/ru/thermoelectric-generator-b25-12.html
126. Shostakovskii P. (2010). Termoelektricheskiie istochniki alternativnogo pitaniia [Thermoelectric sources of alternative power supply]. *Novyie Tekhnologii – Novel Technologies*, 12, 131-138-(2010) [in Russian].
127. Hendricks T., Yee Shannon, Leblanc S. (2016). Cost scaling of a real-world exhaust waste heat recovery thermoelectric generator: a deeper dive. *Journal of Electronic Materials*, 45(3).
128. Anatychuk L.I., Kuz R.V. (2011). Materials for vehicular thermoelectric generators. Proc. of ICT'2011 (Michigan, USA).
129. Anatychuk L.I., Kuz R.V., Hwang J.D. (2012). The energy and economic parameters of Bi-Te based thermoelectric generator modules for waste heat recovery. *J. of Thermoelectricity*, 4, 73 - 79.
130. Anatychuk L.I., Kuz R.V., Prybyla A.V. (2014). Efficiency improvement of sectional thermoelectric heat recuperators. *J.Thermoelectricity*, 6, 77-88.
131. https://ua.energy

Submitted 17.07.2020

Анатичук Л.І., *акад. НАН України*[1,2]
Кузь Р.В., *канд. фіз.-мат. наук*[1,2]

[1]Інститут термоелектрики НАН і МОН України,
вул. Науки, 1, Чернівці, 58029, Україна;
e-mail: anatych@gmail.com;
[2]Чернівецький національний університет
ім. Юрія Федьковича, вул. Коцюбинського 2,
Чернівці, 58000, Україна

ЕФЕКТИВНІСТЬ ТЕРМОЕЛЕКТРИЧНИХ РЕКУПЕРАТОРІВ ДЛЯ РАЦІОНАЛЬНИХ ТЕМПЕРАТУР ДЖЕРЕЛ ТЕПЛА

У роботі наводяться результати аналізу термоелектричних рекуператорів теплових відходів для діапазону температур теплоносія 100 -300°С. На основі комп'ютерної моделі проведено оптимізацію секційних рекуператорів, розраховано ККД кожної секції та рекуператора в цілому. Розраховано питому вартість та час окупності секційних генераторів. Зроблено висновки про економічну доцільність використання таких рекуператорів. Бібл. 130, рис. 9, табл. 1.

Ключові слова: термоелектричний рекуператор, відпрацьоване тепло, ККД, потужність, питома вартість.

Анатычук Л.И., *акад. НАН Украины*[1,2]

Кузь Р.В., *канд. физ.-мат. наук*[1,2]

[1]Институт термоэлектричества НАН и МОН Украины,
ул. Науки, 1, Черновцы, 58029, Украина, *e–mail: anatych@gmail.com;*
[2]Черновицкий национальный университет
им. Юрия Федьковича, ул. Коцюбинского, 2,
Черновцы, 58012, Украина

ЭФФЕКТИВНОСТЬ ТЕРМОЭЛЕКТРИЧЕСКИХ РЕКУПЕРАТОРОВ ДЛЯ РАЦИОНАЛЬНЫХ ТЕМПЕРАТУР ИСТОЧНИКОВ ТЕПЛА

В работе приводятся результаты анализа термоэлектрических рекуператоров тепловых отходов для диапазона температур теплоносителя 100 -300^{0}C. На основе компьютерной модели проведена оптимизация секционных рекуператоров, рассчитан КПД каждой секции и рекуператора в целом. Рассчитаны удельная стоимость и время окупаемости секционных генераторов. Сделаны выводы об экономической целесообразности использования таких рекуператоров. Библ. 130, рис. 9, табл. 1.

Ключевые слова: термоэлектрический рекуператор, отработанное тепло, КПД, мощность, удельная стоимость.

References

1. Rowe, M.D., Gao Min, Williams, S.G.K., Aoune A., Matsuura K., Kuznetsov V.L., Li Wen Fu. (1997). Thermoelectric recovery of waste heat-case studies. *Energy Conversion Engineering Conference* (1997, vol.2, 1075 – 1079).
2. Basic research needs for solar energy utilization. Report of the Basic Energy Sciences Workshop on Solar Energy Utilization. USA: DOE, April 18−21, 2005.
3. European Commission. Energy. Energy 2020: *Roadmap* 2050. – http://ec.europa.eu/energy/energy2020/roadmap/index_en.htm.
4. Paniakin V. (2010). Kogeneratsiia: Kak eto rabotaiet [Cogeneration: How it works]. *Seti i biznes – Networks and Business*, 4 [in Russian].
5. Waste heat recovery:technology and opportunities in U.S. industry. *Report of BCS, Incorporated*, USA. – 2008.
6. Cynthia Haddad, et al. (2014). Some efficient solutions to recover low and medium waste heat: competitiveness of the thermoacoustic technology. *Energy Procedia*, 50, 1056 – 1069.
7. Thekdi, Arvind C. (2007). Waste heat to power economic tradeoffs and considerations. *Proc. of the 3rd Annual Waste Heat to Power Workshop* (USA, 2007).
8. Paul Cunningham P.E. (2002). Waste heat/cogen opportunities in the cement industry. *Cogeneration and Competitive Power Journal*, 17 (3), 31-51.
9. Quoilinetal S. (2013). Techno-economic survey of organic Rankine cycle (ORC) systems. *Renewable and Sustainable Energy Reviews*, 22, 68–186.
10. Zhang C., et al. (2017). Implementation of industrial waste heat to power in Southeast Asia: an outlook from the perspective of market potentials, opportunities and success catalysts. *Energy Policy*, 106, 525–535.

11. Milewskia Jarosław, Krasuckib Janusz (2017). Comparison of ORC and Kalina cycles for waste heat recovery in the steel industry. *Journal of Power Technologies*, 97 (4), 302–307.
12. Anatychuk L.I. (1979). *Termoelementy i termoelektricheskiie ustroistva: Spravochnik [Thermoelements and thermoelectric devices: Reference book]*. Kyiv: Naukova dumka [in Russian].
13. Bernshteyn A.S. (1956). Termoelektricheskiie generatory [Thermoelectric generators]. Moscow: Gosenergoizdat [in Russian].
14. Anatychuk L.I. (2001). Rational areas of research and applications of thermoelectricity. *J.Thermoelectricity*, 1, 3 – 14.
15. Anatychuk L.I. (2007). Current state and some prospects of thermoelectricity. *J.Thermoelectricity*, 2, 7 – 20.
16. Freik D.M., Nykyrui L.I., Krynytskyi O.S. (2012). Dosiahnennia i problemy termoelektryky [Achievements and problems of thermoelectricity]. *Fizyka i khimiia tverdoho tila - Physics and Chemistry of Solid State*, 13(2), 297-318 [in Ukrainian].
17. Y. Chen, et al. (2006). A comparative study of the carbon dioxide transcritical power cycle compared with an organic Rankine cycle with R123 as working fluid in waste heat recovery. *Applied Thermal Engineering*. 26, 2142–2147.
18. Zhang X., Wu L., Wang X., Ju G. (2016). Comparative study of waste heat steam SRC, ORC and S-ORC power generation systems in medium-low temperature. *Applied Thermal Engineering*. doi: http://dx.doi.org/10.1016/j.applthermaleng.2016.06.108
19. Kishore R.A., Priya S. (2018). A review on low-grade thermal energy harvesting: materials, methods and devices. *Materials*, 11 (8), 1433. doi:10.3390/ma11081433.
20. Aladayleh Wail, Alahmer Ali. (2015). Recovery of exhaust waste heat for ICE using the beta type Stirling engine. *Journal of Energy*. Article ID 495418, https://doi.org/10.1155/2015/495418.
21. Takahashi Y., Yamamoto K., Nishikawa M. (2006). Fundamental performance of triple magnetic circuit type cylindrical thermomagnetic engine. *Electrical Engineering in Japan*, 154 (4).
22. Huffman F.N., Sommer A.H., Balestra C.L., Briere D.P., Oettinger P.E. (1976). High efficiency thermionic converter studies. *NASA Technical Report. – NASA-CR-135125*.
23. Anatychuk L.I., Prybyla A.V. (2012). Thermoelectric heat recuperator for gas turbines. *XIII Interstate Workshop "Thermoelectrics and their applications"* (Russia, Saint-Petersburg, November 13-14, 2012).
24. Malygin N.D., Stoianov V.U. (2004). Primeneniie termoelektricheskogo generatora v istochnike bespereboinogo pitaniia povyshennoi nadezhnosti dlia osobo vazhnykh potrebitelei [The use of thermoelectric generator in high reliability uninterupted supply for critical consumers]. *Stroitelstvo i tekhnogennaia bezopasnost'*, 9, 153 – 156 [in Russian].
25. Shostakovskiy P. (2013). Alternativnyie istochniki elektricheskoi energii promyshlennogo primeneniia na osnove termoelektricheskikh generatorov [Alternative sources of electric energy for industrial use based on thermoelectric generators]. *Control Engineering Russia*, 3 (45), 52 – 56 [in Russian].
26. Anatychuk L.I., Hwang J.D., Chu H.S., Hsieh H.L. (2011). The design and application of thermoelectric generators on the waste heat recovery of heating furnace in steel industry. *XIV International Forum on Thermoelectricity (May 17-20, 2011, Russian Federation, Moscow).*
27. Kaibe H., Kaijihara T., Fujimoto S., Makino K., Hachiuma H. (2011) Recovery of plant waste heat by a thermoelectric generating system [S. Sano] *KOMATSU technical report*, 57(164), 26 – 30.
28. Kajikawa T. (2010). Thermoelectric application for power generation in Japan. *Advances in*

Science and Technology, 74, 83-92.
29. Kajikawa T. (2011). Advances In thermoelectric power generation technology in Japan. *J. of Thermoelectricity*, 3 (5 – 19).
30. Kaibe H., Fujimoto S., Mizukami H., Morimoto S. (2010). Field test of thermoelectric generating system at Komatsu Plant. *Proceedings of Automotive 2010, Berlin (2010.12).*
31. Kaibe H., Fujimoto S., Kajihara T., Makino K., Hachiuma H. (2011). Thermoelectric generating system attached to a carburizing furnace at Komatsu Ltd., Awazu Plant. *Proc of 9th European Conference on Thermoelectrics (Thessaloniki, Greece, September 2011, 201E_10_O.)*
32. Kaibe H., Makino K., Kajihara K., Fujimoto S. and Hachiuma H. (2012). Thermoelectric generating system attached to a carburizing furnace at Komatsu Ltd., Awazu Plant. *AIP Conf. Proc. 1449, 524*; http://dx.doi.org.sci-hub.org/10.1063/1.4731609.
33. Kaibe H., Makino K., Kajihara K., Lee Y.-H. and Hachiuma H. *Study of thermoelectric generation unit for radiant waste heat.*
34. Kaibe H., Kajihara T., Nagano K., Makino K., Hachiuma H., Natsuume D. (2014). Power delivery from an actual thermoelectric generation system. *Journal of Electronic Materials*.
35. Anatychuk L.I., Hwang Jenn-Dong, Lysko V.V., Prybyla A.V. (2013). Thermoelectric heat recuperators for cement kilns. *J.Thermoelectricity*, 5, 39-45.
36. Kuroki T., Kabeya K., Makino K., Kajihara T., Kaibe H., Hachiuma H., Matsuno H. (2014). Thermoelectric generation using heat in steal works. *Journal of Electronic Materials.*
37. Amaldi A., Tang F. (2014). *Proceedings of the 11th European conference on thermoelectrics : ECT 2013. Chapter 17. Waste heat recovery in steelworks using a thermoelectric generator.* Springer, 143-149.
38. Hendricks T. and Choate W.T. (2006). *Engineering Scoping Study of Thermoelectric Generator Systems for Industrial Waste Heat recovery* (Washington, D.C.: Industrial Technologies Program, U.S. Department of Energy, 2006), 1–76.
39. Waste heat recovery: Technology and opportunities in U.S. industry.– *U.S. department of energy: Industrial technologies program*, 2008, 112.
40. Waste heat to power systems.– Combined heat and power partnership. *U.S. environmental protection agency*, 2012, 9.
41. Villar A., Arribas J. (2012). Waste-to-energy thechnologies in continuous process industries. *Clean Techn Environ Policy*, 14, 29-39.
42. Joshi J., Patel N. (2012). Thermoelectric system to generate electricity from waste heat of the flue gases. *Advances in Applied Science Research*, 3(2), 1077-1084.
43. Amaldi A., Tang F. (2014). *Proceedings of the 11th European conference on thermoelectrics : ECT 2013. Chapter 26. Modeling and design of tubular thermoelectric generator used for waste heat recovery.* Springer.
44. Zhang Y., D'Angelo J., Wang X.,Yang J. (2012) Multi-physics modeling of thermoelectric generators for waste heat recovery applications. *(DEER Conference, Michigan).*
45. Faraji A., Singh R., Mochizuki M., Akbarzadeh A. (2013). Design and numerical simulation of a symbiotic thermoelectric generation system fed by a low-grade heat sorce. *Journal of Electronic Materials*.
46. Brazdil M., Pospisil J. (2012). A way tox use waste heat to generate thermoelectric power. *Acta Polytechnica*, 52(4), 21-25.
47. Qiu K., Hayden A. (2009). A natural-gas-fired thermoelectric power generation system. *Journal of Electronic Materials*, 38(7).

48. Ono K., Suzuki R. (1998). Thermoelectric power generation: Converting low-grade heat into electricity. *JOM*, 49-51.
49. Sasaki K., Horikawa D., Goto K. (2014). Consideration of thermoelectric power generation by using hot spring thermal energy or industrial waste heat. *Journal of Electronic Materials*.
50. Miller E., Hendricks T., Peterson R. (2009). Modeling energy recovery using thermoelectric conversion with an organic Rankine bottomig cycle. *Journal of Electronic Materials*, 38(7).
51. Miller E. (2010). Integrated dual cycle energy recovery using thermoelectric conversion with an organic Rankine bottomig cycle. *An abstract of the thesis for the degree of Master of Science in mechanical engineering.*
52. Fleurial J.-P., Gogna P., Li, B.C-Y., Firdosy S., Chen B.J., Huang C.-K., Ravi V., Caillat T., Star K.(2009). Waste heat recovery opportunities for thermoelectric generator. *Thermoelectric Applications Workshop.*
53. Energy Use, Loss and Oppor tunity Analysis: U. S. Manufacturing and Mining, December 2004, Energetics, Inc., E3M, Incorporated, page 10.
54. Hachiuma H. (2013). Thermoelectric energy harvesting for industrial waste heat recovery. *Energy Harvesting and Storage USA*.
55. Anatychuk L.I., Jenn-Dong Hwang, Prybyla A.V. (2010). Thermoelectric generator for conversion of heat from gas rolling furnaces. *29-th International Conference on Thermoelectrics* (China, Shanghai).
56. Saqr K.M., Mansour M.K., Musa M.N. (2008). Thermal design of automobile exhaust based thermoelectric generators: objectives and challenges. *J.Thermoelectricity*, 1, 64 – 73.
57. Anatychuk L.I., Kuz R.V. (2014). Effect of air cooling on the efficiency of sectional thermoelectric generator in a car with a diesel engine. *J.Thermoelectricity*, 4, 84 – 91.
58. Anatychuk L.I., Kuz R.V. (2014). Effect of air cooling on the efficiency of thermoelectric generator in a diesel-engined car. *J.Thermoelectricity*, 2, 61 – 69.
59. Anatychuk L.I., Kuz R.V. (2014). Effect of air cooling on the efficiency of a thermoelectric generator in a car with a petrol engine. *J. Thermoelectricity*, 3, 84 – 87.
60. Korzhuev M.A., Svechnikova T.E. (2013). Thermodynamic restrictions for the net power of automotive thermoelectric generators and prospects of their use in transport. *J.Thermoelectricity*, 3, 58 – 73.
61. Saqr K.M., Mansour M.K., and Musa M.N. (2008). Thermal design of automobile exhaust-based thermoelectric generators: objectivities and challenges. *International J. Automotive Technology*, 9(2), 155-160.
62. Rowe D.M., Smith J., Thomas G. and Min G. (2011). Weight penalty incurred in thermoelectric recovery of automobile exhaust heat. *J. Electronic Materials*, 40 (5), 784-788.
63. Lieb J., Neugebauer S., Eger A., Linde M., Masar B., Stűtz W. (2009). The thermoelectric generator from BMW is making use of waste heat. *MTZ*, 70 (4), 4-11.
64. Eger A., Linde M. (2011). The BMW Group. Roadmap for the application of thermoelectric generators (San Diego, 2011), 23 p.
65. Espinosa N., Lazard M., Aixala L., and Scherrer H. (2010). Modeling thermoelectric generator applied to diesel automotive heat recovery. *JEMS* 39 (9), 1446-1455.
66. Anatychuk L.I., Luste O.J., and Kuz R.V. (2011). Theoretical and experimental study of thermoelectric generators for vehicles. *JEMS* 40(5), 1326-1331.
67. Anatychuk L.I., Luste O.J., and Kuz R.V. (2011). Theoretical and experimental study of thermoelectric generators for vehicles. *JEMS* 40 (5), 1326-1331.
68. Fairbanks W. (2011). Development of automotive thermoelectric generators and air conditioner /

heaters. Proceedings of XIV International Forum on Thermoelectricity (Moscow 17-20.05.2011), [On line:http://forum.inst.cv.ua/].

69. Anatychuk L.I., Kuz R.V., Rozver Yu.Yu. (2012). Thermoelectric generator for petrol engine. *J.Thermoelectricity*, 2, 81 – 94.
70. Fainzilber E.M., Drabkin L.M. (1966). Ispolzovaniie tepla otrabotavshikh gazov dvigatelei v termoelektricheskom generatore dlia pitaniia elementov elektrooborudovaniia avtomobilei [Use of heat from exhaust gases of engines in a thermo-electric generator for powering elements of electrical equipment of cars]. *Avtomobilnaya promyshlennost*, 7, 9 – 10 [in Russian].
71. Korzhuev M.A., Granatkina Yu.V. (2012). Some bottlenecks of automobile thermoelectric generators and search for new materials to eliminate them. *J.Thermoelectricity*, 1, 81 – 94.
72. Korzhuev M.A. (2011). On the conflict of internal combustion engines and thermoelectric generators in the recovery of heat losses in cars. *Letters to JTP*, 37(4), 8 – 15.
73. Anatychuk L.I., Kuz R.V., Rozver Yu.Yu. (2011). Efficiency of thermoelectric recuperators of the exhaust gas heat of internal combustion engines. *J.Thermoelectricity*, 4, 80-85.
74. Anatychuk L.I., Rozver Yu.Yu., Misawa K., and Suzuki N. (1997). Thermal generators for waste heat utilization. *Proc. of 16th International Conference on Thermoelectrics* (Dresden, 1997), p. 586 – 587.
75. Zhang X., Chau K.T., and Chan C.C. (2008). Overview of thermoelectric generation for hybrid vehicles. *J. Asian Electric Vehicles,* 6 (2), 1119 – 1124.
76. Elsner N., Bass J., Ghamaty S., Krommenhoek D., Kushch A., and Snowden D. (2005). Diesel truck thermoelectric generator. Advanced combustion engine technologies. *FY 2005 Progress Report*, p. 301 – 305.
77. Yang Jihui, Seker F., Venkatasubramanian R., Nolas G.S., Uher C., and Wang H. (2006). Developing thermoelectric technology for automotive waste heat recovery. Advanced combustion engine technologies. *FY 2006 Progress Report*, p. 227 – 231.
78. Ikoma K., Munekiyo M., Furuya K., Kobayashi M., Izumi T., and Shinohara K. (1998). Thermoelectric module and generator for gasoline engine vehicles. *Proc. ICT'98. XVII International Conference on Thermoelectrics* (Nagoya, Japan, 1998), p. 464 – 467.
79. Takanose E., Tamakoshi H. (1993). The development of thermoelectric generator for passenger car. *Proc.12th International Conference on Thermoelectrics* (Yokohama, Japan, 1993), p. 467 – 470.
80. Stabler F. (2002). Automotive application of hight efficiency thermoelectrics. DARPA/ONR Program rewiew and DOE hight efficiency thermoelectric workshop. (San Diego (CA), March 24-27).
81. Bass J. et al. (1992). Thermoelectric generator development for heavy-duty truck applications. *Proceedings of Annual Automotive Technology Development Contractors Coordination Meeting* (Dearborn (USA). – P. 743-748.
82. Bass J. et al. (1995). Performance 1 kW thermoelectric generator for diesel engines. *Proc. AIP Conference*, P. 295-298.
83. Thacher E. F., Helenbrook B. T., Karri M. A. and Richter C. J. (2007). Testing an automobile thermoelectric exhaust based thermoelectric generator in a light truck. Proceedings of the I MECH E Part D. *Journal of Automobile Engineering*, 221(1), 95-107(13).
84. Kushch A., Karri M. A., Helenbrook B. T. and Richter C. J. (2004). The effects of an exhaust thermoelectric generator of a GM Sierra pickup truck. *Proceedings of Diesel Engine Emission Reduction (DEER) Conference* (Coronado, California, USA).

85. Jadhao J., Thombare D. (2013). Rewiew on exhaust gas heat recovery for I.C. engine. *International Journal of Engineering and Innovate Technology*, 2(12), 93-100.
86. Baker C., Vuppuluri P., Shi L., Hall M. (2012). Model of heat exchangers for waste heat recovery from diesel engine exhaust for thermoelectric power generation. *Journal of Electronic Materials*, 41(6).
87. Kim S., Won B., Rhi S., Kim S.H., Yoo J. (2011). Thermoelectric power generation system for future hybrid vehicles using hot exhaust gas. *Journal of Electronic Materials*, 40(5).
88. Su C., Ye B., Guo X., Hui P. (2012). Acoustic optimization of automotive exhaust heat thermoelectric generator. *Journal of Electronic Materials*, 41(6).
89. Deng Y., Zhang Y., Su C. (2014). Modular analysis of automotive exhaust thermoelectric power generation system. *Journal of Electronic Materials*.
90. Quan R., Tang X., Quan S., Huang L. (2013). A novel optimization method for the electric topology of thermoelectric modules used in an automobile exhaust thermoelectric generator. *Journal of Electronic Materials*, 42(7).
91. Fleurial G.-P. (2009). Thermoelectric power generation materials: technology and application opportunities. *JOM*, 61(4), 79-85.
92. Kumar C., Sonthalia A., Goel R. (2011). Experimental study on waste heat recovery from an IC Engine using thermoelectric technology. *Thermal Science*, 15(4), 1011-1022.
93. Vázquez, J., et al., State of the art of thermoelectric generators based on heat recovered from the exhaust gases of automobiles. *Proceedings of 7th European Workshop on Thermoelectrics*, Paper 17 (Pamplona, Spain, 2002).
94. Wojciechowski K.T., Zybala R., Leszczynski J., Nieroda P., Schmidt M., Merkisz J., Lijewski P., Fuc P. (2012). Analysis of possibilities of waste heat recovery in off-road vehicles. *AIP Conf. Proc*., 1449, 501 – 504.
95. Wojciechowski K. T., Zybala R., Tomankiewicz J., Fuc P., Lijewski P., Wojciechowski J., Merkisz J. (2012). Influence of back pressure on net efficiency of TEG generator mounted in the exhaust system of a diesel engine, published in book: *Thermoelectrics Goes Automotive II.* Daniel Jänsch (Ed.). Expert Verlag.
96. Baskar P., Seralathan S., Dipin D., Thangavel S. (2014). Experimental analysis of thermoelectric waste heat recovery system retrofitted to two stroke petrol engine. *International Journal of Advanced Mechanical Engineering,* 4(1), 9-14.
97. LaGrandeur J., Crane D., Hung S. (2006). Hight-efficiency thermoelectric waste energy recovery system for passenger vehicle application. *Advanced Combustion Engine Technologies*. *FY 2006 Progress Report,* p. 232 – 236.
98. Willigan R., Hautman D., Krommenhoek D., Martin P. (2006). Cost-effective fabrication routes for the production of quantun well structures and recovery of waste heat from heavy duty trucks. Advanced Combustion Engine Technologies. *FY 2006 Progress Report*.
99. Nelson C. (2006). Exhaust energy recovery. Advanced Combustion Engine Technologies. *FY 2006 Progress Report*, p. 247 – 250.
100. Schock H., Case E., Downey A. (2006)ю Thermoelectric conversion of waste heat to electricity in an IC engine powered vehicle. Advanced Combustion Engine Technologies. *FY 2006 Progress Report*, p. 242 – 246.
101. Shu G., Zhao J., Tian H., Liang X., Wei H. (2012). Parametric and exergetic analysis of waste heat recovery system based on thermoelectric generator and organic rankine cycle utilizing R123. *Energy*, 45, 806-816.
102. J. Merkisz, P. Fuc, P. Lijewski, A. Ziolkowski, K. Wojciechowski (2014). The analysis of

exhaust gas thermal energy recovery through a TEG generator in city traffic conditions reproduced on a dynamic engine test bed. *Journal of Electronic Materials*.

103. Nadaf S.L., Gangavat P.B. (2014). A review on waste heat recovery and utilization from diesel engines. *International Journal of Engineering and Innovate Technology*, 5(4), 31-39.
104. Noor A., Puteh R., Rajoo S. (2014). Waste heat recovery technologies in turbocharged automotive engine – A Review. Journal of Modern Science and Technology, 2(1), 108-119.
105. Anatychuk. L.I., Rozver. Yu.Yu., Misawa. K., Suzuki. N. (1997). Thermal generators for waste heat utilization. *Report on ICT'97*.
106. Anatychuk L.I., Razinkov V.V., Rozver Yu. Yu., Mikhailovsky V.Ya.(1997). Thermoelectric generator modules and blocks. *Report on ICT'97*.
107. Uemura K. (2002). History of thermoelectricity development in Japan. *J. of Thermoelectricity*, 3, 7 – 16.
108. Ohba R. and Nakamura S. (1986). Wind tunnel experiment of gas diffusion in thermally stratified flow. *Proc. 3rd Int. Workshop on Wind & Water Tunnel Modelling Atmospheric Flow & Dispersion* (Lausanne, YMG-1, 1986).
109. Brazdil M., Pospil J. (2013). Thermoelectric power generation utilizing the waste heat from a biomass boiler. *Journal of Electronic Materials*, 42(7).
110. *Characterization of the U.S. Industrial/Commercial boiler population.* Oak Ridge National Laboratory, May 2005. Prepared by Energy and Enviromental Analysis, Inc.
111. Anatychuk L.I., Morozov V.I., Mitin V.P., Prybyla A.V. (2012). Thermoelectric recupirator for gas turbines. *31-th International and 10-th European Conference on Thermoelectrics* (Aalborg, Denmark).
112. Date As., Date Ab., Dixon C., Akbarzadeh A. (2014). Progress of thermoelectric power generation systems: Prospect for small to medium scale power generation. *Renewable and Sustainable Energy Reviews*, 33, 371-381.
113. Champier D, Bedecarrats JP, Rivaletto M, Strub F. (2010). Thermoelectric power generation from biomass cook stoves. *Energy*, 35(2), 935–42.
114. Nuwayhid R.Y., Rowe D.M., Min G. (2003). Low cost stove-top thermoelectric generator for regions with unreliable electricity supply. *Renew Energy*, 28 (2), 205–22.
115. Nuwayhid RY, Shihadeh A, Ghaddar N. (2005). Development and testing of a domestic woodstove thermoelectric generator with natural convection cooling. *Energy Convers Manag*, 46(9–10), 1631–43.
116. Lertsatitthanakorn C. (2007). Electrical performance analysis and economic evaluation of combined biomass cook stove thermoelectric (BITE) generator. *Bioresour Technol*, 98(8), 1670–4.
117. Maneewan S., Chindaruksa S. (2009). Thermoelectric power generation using waste heat from a biomass drying. *Journal of Electronic Materials*, 38, 7.
118. Elefsiniotis A., Becker Th., Schmid U. (2013). Thermoelectric energy harvesting using phase change materials in high temperature enviroments in aircraft. *Journal of Electronic Materials*, 43 (6).
119. Elefsiniotis A., Kiziroglou M., Wright S., Becker Th., Yeatman E., Schmid U. (2013). Performance evaluation of a thermoelectric energy harvesting device using various change materials. *Journal of Physics: Conference Series*, 476.
120. Elefsiniotis A., Kokorakis N., Becker Th., Schmid U. (2014). A novel high-temperature aircraft-specific energy harvester using PCMs and state of the art TEGs. *12-th European*

Conference on Thermoelectrics.

121. Samson D, Kluge M., Fuss T., Becker Th., Schmid U. (2012). Flight test results of a thermoelectric energy harvester for aircraft. *Journal of Electronic Materials*, 41 (6).
122. Elefsiniotis A., Weiss M., Becker Th., Schmid U. (2013). Efficient power management for energy-autonomous wireless sensor nodes for aeronautical application. *Journal of Electronic Materials*, 42 (7).
123. Samson D, Kluge M., Otterpohl T., Becker Th., Schmid U. (2010). Aircraft-specific thermoelectric generator module. *Journal of Electronic Materials*, 39(9).
124. Shan Yeung (2010). Thermoelectricity: Experiments, Application and Modelling.– *An abstract of the Thesis for the Degree of Master of Science in materials engineering and nanotechnology.*
125. http://kryothermtec.com/ru/thermoelectric-generator-b25-12.html
126. Shostakovskii P. (2010). Termoelektricheskiie istochniki alternativnogo pitaniia [Thermoelectric sources of alternative power supply]. *Novyie Tekhnologii – Novel Technologies*, 12, 131-138- (2010) [in Russian].
127. Hendricks T., Yee Shannon, Leblanc S. (2016). Cost scaling of a real-world exhaust waste heat recovery thermoelectric generator: a deeper dive. *Journal of Electronic Materials*, 45(3).
128. Anatychuk L.I., Kuz R.V. (2011). Materials for vehicular thermoelectric generators. Proc. of ICT'2011 (Michigan, USA).
129. Anatychuk L.I., Kuz R.V., Hwang J.D. (2012). The energy and economic parameters of Bi-Te based thermoelectric generator modules for waste heat recovery. *J. of Thermoelectricity*, 4, 73 - 79.
130. Anatychuk L.I., Kuz R.V., Prybyla A.V. (2014). Efficiency improvement of sectional thermoelectric heat recuperators. *J.Thermoelectricity*, 6, 77-88.
131. https://ua.energy

Submitted 17.07.2020

ARTICLE SUBMISSION GUIDELINES

For publication in a specialized journal, scientific works are accepted that have never been printed before. The article should be written on an actual topic, contain the results of an in-depth scientific study, the novelty and justification of scientific conclusions for the purpose of the article (the task in view).

The materials published in the journal are subject to internal and external review which is carried out by members of the editorial board and international editorial board of the journal or experts of the relevant field. Reviewing is done on the basis of confidentiality. In the event of a negative review or substantial remarks, the article may be rejected or returned to the author(s) for revision. In the case when the author(s) disagrees with the opinion of the reviewer, an additional independent review may be done by the editorial board. After the author makes changes in accordance with the comments of the reviewer, the article is signed to print.

The editorial board has the right to refuse to publish manuscripts containing previously published data, as well as materials that do not fit the profile of the journal or materials of research pursued in violation of ethical norms (for instance, conflicts between authors or between authors and organization, plagiarism, etc.). The editorial board of the journal reserves the right to edit and reduce the manuscripts without violating the author's content. Rejected manuscripts are not returned to the authors.

Submission of manuscript to the journal

The manuscript is submitted to the editorial office of the journal in paper form in duplicate and in electronic form on an electronic medium (disc, memory stick). The electronic version of the article shall fully correspond to the paper version. The manuscript must be signed by all co-authors or a responsible representative.

In some cases it is allowed to send an article by e-mail instead of an electronic medium (disc, memory stick).

English-speaking authors submit their manuscripts in English. Russian-speaking and Ukrainian-speaking authors submit their manuscripts in English and in Russian or Ukrainian, respectively. Page format is A4. The number of pages shall not exceed 15 (together with References and extended abstracts). By agreement with the editorial board, the number of pages can be increased.

To the manuscript is added:

1. Official recommendation letter, signed by the head of the institution where the work was carried out.

2. License agreement on the transfer of copyright (the form of the agreement can be obtained from the editorial office of the journal or downloaded from the journal website – Dohovir.pdf). The license agreement comes into force after the acceptance of the article for publication. Signing of the license agreement by the author(s) means that they are acquainted and agree with the terms of the agreement.

3. Information about each of the authors – full name, position, place of work, academic title, academic degree, contact information (phone number, e-mail address), ORCID code (if available). Information about the authors is submitted as follows:

authors from Ukraine - in three languages, namely Ukrainian, Russian and English;

authors from the CIS countries - in two languages, namely Russian and English;

authors from foreign countries – in English.

4. Medium with the text of the article, figures, tables, information about the authors in electronic form.

5. Colored photo of the author(s). Black-and-white photos are not accepted by the editorial staff. With the number of authors more than two, their photos are not shown.

Requirements for article design

The article should be structured according to the following sections:

- *Introduction*. Contains the problem statement, relevance of the chosen topic, analysis of recent research and publications, purpose and objectives.
- *Presentation of the main research material* and the results obtained.
- *Conclusions* summing up the work and the prospects for further research in this direction.
- *References*.

The first page of the article contains information:

1) in the upper left corner – UDC identifier (for authors from Ukraine and the CIS countries);

2) surname(s) and initials, academic degree and scientific title of the author(s);

3) the name of the institution where the author(s) work, the postal address, telephone number, e-mail address of the author(s);

4) article title;

5) abstract to the article – not more than 1 800 characters. The abstract should reflect the consistent logic of describing the results and describe the main objectives of the study, summarize the most significant results;

6) key words – not more than 8 words.

The text of the article is printed in Times New Roman, font size 11 pt, line spacing 1.2 on A4 size paper, justified alignment. There should be no hyphenation in the article.

Page setup: "mirror margins" – top margin – 2.5 cm, bottom margin – 2.0 cm, inside – 2.0 cm, outside – 3.0 cm, from the edge to page header and page footer – 1.27 cm.

Graphic materials, pictures shall be submitted in color or, as an exception, black and white, in .opj or .cdr formats, .jpg or .tif formats being also permissible. According to author's choice, the tables and partially the text can be also in color.

Figures are printed on separate pages. The text in the figures must be in the font size 10 pt. On the charts, the units of measure are separated by commas. Figures are numbered in the order of their arrangement in the text, parts of the figures are numbered with letters – a, b, .. On the back of the figure, the title of the article, the author (authors) and the figure number are written in pencil. Scanned images and graphs are not allowed to be inserted.

Tables are provided on separate pages and must be executed using the MSWord table editor. Using pseudo-graph characters to design tables is inadmissible.

Formulae shall be typed in Equation or MatType formula editors. Articles with formulae written by hand are not accepted for printing. It is necessary to give definitions of quantities that are first used in the text, and then use the appropriate term.

Captions to figures and tables are printed in the manuscript after the references.

Reference list shall appear at the end of the article. References are numbered consecutively in the order in which they are quoted in the text of the article. References to unpublished and unfinished works are inadmissible.

Attention! In connection with the inclusion of the journal in the international bibliographic abstract database, the reference list should consist of two blocks: CITED LITERATURE and REFERENCES (this requirement also applies to English articles):

CITED LITERATURE – sources in the original language, executed in accordance with the

Ukrainian standard of bibliographic description DSTU 8302:2015. With the aid of VAK.in.ua (http://vak.in.ua) you can automatically, quickly and easily execute your "Cited literature" list in conformity with the requirements of State Certification Commission of Ukraine and prepare references to scientific sources in Ukraine in understandable and unified manner. This portal facilitates the processing of scientific sources when writing your publications, dissertations and other scientific papers.

REFERENCES – the same cited literature list transliterated in Roman alphabet (recommendations according to international bibliographic standard APA-2010, guidelines for drawing up a transliterated reference list "References" are on the site http//www.dse.org.ua, section for authors).

To speed up the publication of the article, please adhere to the following rules:

- in the upper left corner of the first page of the article – the UDC identifier;
- family name and initials of the author(s);
- academic degree, scientific title;

begin a new line, Times New Roman font, size 12 pt, line spacing 1.2, center alignment;

- name of organization, address (street, city, zip code, country), e-mail of the author(s);

begin a new line 1 cm below the name and initials of the author(s), Times New Roman font, size 11 pt, line spacing 1.2, center alignment;

- the title of the article is arranged 1 cm below the name of organization, in capital letters, semi-bold, font Times New Roman, size 12 pt, line spacing 1.2, center alignment. The title of the article shall be concrete and possibly concise;
- the abstract is arranged 1 cm below the title of the article, font Times New Roman, size 10 pt, in italics, line spacing 1.2, justified alignment in Ukrainian or Russian (for Ukrainian-speaking and Russian-speaking authors, respectively);
- key words are arranged below the abstract, font Times New Roman, size 10 pt, line spacing 1.2, justified alignment. The language of the key words corresponds to that of the abstract. Heading "Key words" - font Times New Roman, size 10 pt, semi-bold;
- the main text of the article is arranged 1 cm below the abstract, indent 1 cm, font Times New Roman, size 11 pt, line space spacing 1.2, justified alignment;
- formulae are typed in formula editor, fonts Symbol, Times New Roman. Font size is "normal" – 12 pt, "large index" – 7 pt, "small index" – 5 pt, "large symbol" – 18 pt, "small symbol" – 12 pt. The formula is arranged in the text, center aligned and shall not occupy more than 5/6 of the line width, formulae are numbered in parentheses on the right;
- dimensions of all quantities used in the article are represented in the International System of Units (SI) with the explication of the symbols employed;
- figures are arranged in the text. The figures and pictures shall be clear and contrast; the plot axes – parallel to sheet edges, thus eliminating possible displacement of angles in scaling; figures are submitted in color, black-and-white figures are not accepted by the editorial staff of the journal;
- tables are arranged in the text. The width of the table shall be 1 cm less than the line width. Above the table its ordinary number is indicated, right alignment. Continuous table numbering throughout the text. The title of the table is arranged below its number, center alignment;

• references should appear at the end of the article. References within the text should be enclosed in square brackets behind the text. References should be numbered in order of first appearance in the text. Examples of various reference types are given below.

Examples of LITERATURE CITED

Journal articles

Anatychuk L.I., Mykhailovsky V.Ya., Maksymuk M.V., Andrusiak I.S. Experimental research on thermoelectric automobile starting pre-heater operated with diesel fuel. *J.Thermoelectricity*. 2016. №4. P.84–94.

Books

Anatychuk L.I. *Thermoelements and thermoelectric devices. Handbook.* Kyiv, Naukova dumka, 1979. 768 p.

Patents

Patent of Ukraine № 85293. Anatychuk L.I., Luste O.J., Nitsovych O.V. Thermoelement.

Conference proceedings

Lysko V.V. *State of the art and expected progress in metrology of thermoelectric materials.* Proceedings of the XVII International Forum on Thermoelectricity (May 14-18, 2017, Belfast). Chernivtsi, 2017. 64 p.

Authors' abstracts

Kobylianskyi R.R. *Thermoelectric devices for treatment of skin diseases*: extended abstract of candidate's thesis. Chernivtsi, 2011. 20 p.

Examples of REFERENCES

Journal articles

Gorskiy P.V. (2015). Ob usloviakh vysokoi dobrotnosti i metodikakh poiska perspektivnykh sverhreshetochnykh termoelektricheskikh materialov [On the conditions of high figure of merit and methods of search for promising superlattice thermoelectric materials]. *Termoelektrichestvo - J.Thermoelectricity,* 3, 5 – 14 [in Russian].

Books

Anatychuk L.I. (2003). *Thermoelectricity. Vol.2. Thermoelectric power converters*. Kyiv, Chernivtsi: Institute of Thermoelectricity.

Patents

Patent of Ukraine № 85293. Anatychuk L. I., Luste O.Ya., Nitsovych O.V. Thermoelements [In Ukrainian].

Conference proceedings

Rifert V.G. Intensification of heat exchange at condensation and evaporation of liquid in 5 flowing-down films. In: *Proc. of the 9th International Conference Heat Transfer.* May 20-25, 1990, Israel.

Authors'abstracts

Mashukov A.O. *Efficiency hospital state of rehabilitation of patients with color carcer.* PhD (Med.) Odesa, 2011 [In Ukrainian].